Calhoun: The NPS Institutional Archive

DSpace Repository

Theses and Dissertations 1. Thesis and Dissertation Collection, all items

1951

An analysis of an electrohydraulic closed loop servomecha

Baeriswyl, Louis

Johns Hopkins University

http://hdl.handle.net/10945/13908

AN ANALYSIS OF AN ELECTROHYDRAULIC
CLOSED LOOP SERVOMECHANISM

Louis Baeriswyl

AN ANALYSIS OF AN ELECTROHYDRAULIC

CLOSED LOOP SERVOMECHANISM

By

Louis Baeriswyl, Jr.
First Lieutenant, U. S. Marine Corps.

ESSAY

SUBMITTED TO THE ADVISORY BOARD

OF THE

SCHOOL OF ENGINEERING

THE JOHNS HOPKINS UNIVERSITY

IN CONFORMITY WITH REQUIREMENTS

FOR THE DEGREE OF MASTER OF SCIENCE

IN ENGINEERING.

Baltimore

1 9 5 1

TABLE OF CONTENTS

I. INTRODUCTION

The object of this investigation was to conduct an experimental project designed to analyze the functioning of a closed loop electrohydraulic servomechanism by varying the frequency of the sinusoidal input signal, and studying the phase lag of the output signal and the amplitude ratio of output to input signal. The gain of the closed loop system was maintained constant while the time constant of the servo amplifier was adjusted to several selected values. For each time constant selected for the servo amplifier, the closed loop system response curves of phase lag and the ratio of the amplitude of output to input were obtained.

The above experimental results were correlated with the theoretical results as predicted from the calculated operation of a similar ideal closed loop system, based on certain assumptions as to the functioning of the various combined components of the system.

The investigation was carried out in three stages:

(a) Theoretical investigation of the operation of the closed loop system based on the assumed functioning of the various included components;

(b) Determination of the operating character-
istics of the various included components of the system
and correlation of the results with the theoretical
operation of the component;

(c) Determination of the operating character-
istics of the closed loop system and correlation of the
results with the theoretical operation of the assumed
closed loop system.

This experimental project was conducted at the
Applied Physics Laboratory, **Johns Hopkins University,**
8621 Georgia Avenue, Silver Spring, Maryland from July,
1950 until April, 1951 by Louis Baeriswyl, Jr.

II. THEORY

1. Basic Configuration.

The electrohydraulic servomechanism under investigation is composed of seven basic elements or components. These components are:

(a) Differential Transformer (electrical).

(b) Servo Amplifier (electrical).

(c) Torque Motor (electromechanical).

(d) Transfer Valve (mechanical-hydraulic).

(e) Actuator (hydromechanical).

(f) Mechanical Linkage (mechanical).

(g) Autosyn pair (mechanical-electrical).

These seven components are connected as indicated below in Figure 1.
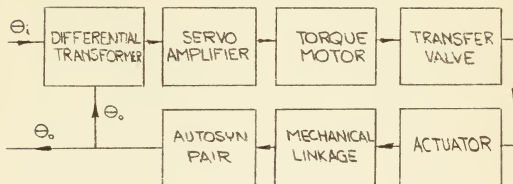
1/
Fig. 1. Block Diagram of the Theoretical Closed Loop System.

1. etc. refers to complete list of references in the bibliography.

2. Basic Assumptions.

In all work that follows, the Laplace
$\underline{2/}$
Transform will be employed, and "S" will be used to indicate the Laplace operator.

2.1. Differential Transformer.

The assumed operation of the differential transformer is linear with respect to the difference between the two input signals to the transformer $(\theta_i - \theta_o)$. and the output signal (e). It is further assumed that the differential transformer has no time delay. Thus, the transfer function is assumed to be

$$Y_1 = K_1$$

where K_1 is a constant.

2.2. Servo Amplifier.

The static characteristics of the servo amplifier are assumed to be linear, the differential output current being proportional to the input voltage. This characteristic is illustrated in Figure 22 by the assumed linear relation line.

Further, the servo amplifier is assumed to be a first order dynamic function with five time constants, Υ, which may be selected at will. The five time constants are $\Upsilon_1, \Upsilon_2, \Upsilon_3, \Upsilon_4$, and Υ_5, and have values of 13, 26 53, 105 and 157 milliseconds respectively. This dynamic

characteristic is exhibited by the phase lag between
the output and input signal as a function of the fre-
quency of the input signal. The assumed ideal first
order phase relations are shown on Figures 32, 33, 34,
35 and 36, for each assumed time constant selected for
the servo amplifier.

The transfer function for the servo amplifier
based on these assumptions is then given by

$$Y_2 = \frac{K_2}{Ts+1}$$

where T takes on the various selected values of the time
constant and K_2 is the element gain constant.

2.3. Torque Motor.

The operation of the torque motor
is assumed to be linear with respect to input differ-
ential current and the output displacement of the motor
rotor. This operating characteristic is illustrated
in Figure 38, by the line identified as the assumed
linear relation. It is further initially assumed that
the torque motor has no time delay. Thus, the transfer
function of the torque motor is assumed to be

$$Y_3 = K_3 ,$$

where K_3 is a constant.

2.4. Transfer Valve.

The operation of the transfer valve

is assumed to be linear with respect to the input de-
flection of the spool and the
output rate of oil flow from
the valve up to the point of
valve saturation. After the
saturation point has been
reached, no increased rate of
oil flow results from an in-
crease of the spool deflection.
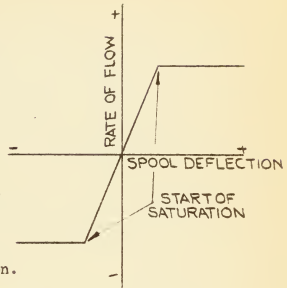
Fig. 2. Assumed Linear
Transfer Characteristic
of the Transfer Valve.

Further, theoretical considera-
tion will be given to the oc-
currence of this saturation. However, for the initial
examination, the transfer valve is assumed to be linear.
This characteristic is illustrated in Figure 2. It is
assumed that this element has no time delay. The trans-
fer function of the transfer valve is then assumed to be

$$Y_4 = \frac{K_4}{S} \text{ , where } K_4 \text{ is a constant.}$$

2.5. Actuator.

The assumed operation of the actuator
is linear with respect to the input rate of oil flow and
the output velocity of the actuator strut. The absence
of a time delay is also assumed in this component. The
assumed transfer function is $Y_5 = K_5$,where K_5 is a con-
stant.

2.6. Mechanical Linkage.

The output rotation of the mechanical linkage is assumed to be a linear function of the input horizonal displacement. The mechanical linkage is assumed to have no time delay related to its operation. The assumed linear characteristics of operation are illustrated in Figure 45. The transfer function of the assumed mechanical linkage is given by $Y_6 = K_6$, where K_6 is a constant.

2.7. Autosyn Pair.

The output voltage of the autosyn pair is assumed to be a linear function of the input rotation of the autosyn rotor, for the range of the input rotations applied to the rotor. This linear characteristic is illustrated in Figure 46. The assumption is made that the autosyn has zero time delay. The resulting assumed transfer function of this autosyn is then given as $Y_7 = K_7$, where K_7 is a constant.

3. Theoretical Development Leading to the Expression of Amplitude Ratio and Phase Shift for a Second Order System.

If the block diagram of Figure 1 is redrawn with the assumed transfer function of each component element, as given in Part 2, placed within the appropriate block, there results Figure 3.
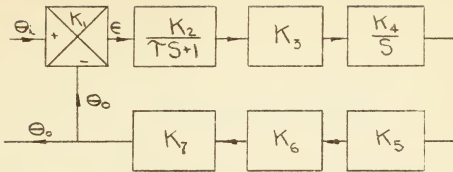
Fig. 3. Block Diagram of the Closed Loop System with the Associated Transfer Functions of Various Component Elements.

The various component elements of Figure 3 above may be combined and simplified, when

$$K_1 \ K_2 \ K_3 \ K_4 \ K_5 \ K_6 \ K_7 = K.$$

Thus, K is the closed loop gain constant, and the simplified block diagram as shown in Figure 4 results.
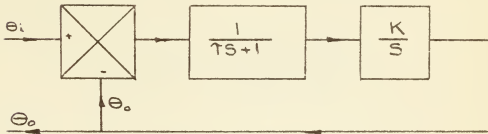
Fig. 4. Simplified Block Diagram of the Closed Loop System.

The open loop system transfer function may be written in terms of the product of the series connected

elements. If the open loop transfer function is denoted
as $KG(S)\big]_{op}$.

Then,

$$KG(S)\big]_{op} = \left[\frac{1}{TS+1}\right]\left[\frac{K}{S}\right]$$

The closed loop system transfer function may
be expressed in terms of the open loop system transfer
function as given below:[1]

$$KG(S) = \frac{KG(S)\big]_{op}}{1 + KG(S)\big]_{op}}$$

where KG(S) is the closed loop transfer function.

Thus,

$$KG(S) = \frac{\left(\frac{1}{TS+1}\right)\left(\frac{K}{S}\right)}{1 + \left(\frac{1}{TS+1}\right)\left(\frac{K}{S}\right)}$$

$$KG(S) = \frac{K\left(\frac{1}{TS+1}\right)\left(\frac{1}{S}\right)}{\frac{S(TS+1)+K}{(TS+1)(S)}}$$

$$KG(S) = \frac{K}{TS^2 + S + K}$$

$$KG(S) = \frac{1}{\left(\frac{T}{K}\right)S^2 + \left(\frac{1}{K}\right)S + 1}$$

1. Page 141.

And since θ_i and θ_o are sinusoidally varying quantities the Laplace operator "S" may be replaced by $j\omega$ [1], where j is the complex operator and ω is the angular sinusoidal input variation.

Thus,

$$KG(j\omega) = \frac{1}{\frac{T}{K}(j\omega)^2 + \frac{1}{K}(j\omega) + 1}$$

$$KG(j\omega) = \frac{1}{\left(1 - \frac{\omega^2 T}{K}\right) + j\left(\frac{\omega}{K}\right)}$$

But

$$KG(j\omega) = \frac{\theta_o}{\theta_i}(j\omega)$$

Therefore,

$$\left|\frac{\theta_o}{\theta_i}(j\omega)\right| = \frac{1}{\sqrt{\left(1 - \frac{\omega^2 T}{K}\right)^2 + \left(\frac{\omega}{K}\right)^2}}$$

and if the phase between the output and input signal is $\emptyset$, there is obtained,

$$\emptyset = -\arctan\left(\frac{\frac{\omega}{K}}{1 - \frac{\omega^2 T}{K}}\right)$$

There,

$$\emptyset = -\arctan\left(\frac{\omega}{K - \omega^2 T}\right)$$

The above two expressions provide a means for theoretically predicting the amplitude ratio of output to input signal and the phase angle by which the output lags the input signal.

1. Page 96.

It is desirable to be able to obtain the phase lag, ϕ, and the amplitude ratio, A, as a function of the input frequency in radians per second, for each particular time constant assigned to the servo amplifier, for this particular closed loop servomechanism configuration.

When the servo amplifier time constant, τ, is expressed as some multiple of the reciprocal of the loop gain, e.g., $\frac{4}{K}$, $\frac{1}{K}$ or $\frac{1}{4K}$; and when the frequency, ω, is expressed as some other multiple of the loop gain, e.g., 0.2K, K or 2K, there are obtained numerical solutions for the phase shift in degrees and the amplitude ratio. The selection of τ and ω as a function of K enables the characteristic response curves of this system to be determined by substitution of the selected τ and ω into the equations for the phase lag and amplitude ratio. As an example,

Let $\tau = \frac{1}{4K}$

And $\omega = 5K$,

then substituting these values into the previously developed equations, there is obtained,

$$\left| \frac{\Theta_o}{\Theta_i}(j\omega) \right| = \frac{1}{\sqrt{\left[1 - \frac{(5K)^2(1/4K)}{K}\right]^2 + \left[\frac{(5K)}{K}\right]^2}}$$

$$\left|\frac{\Theta_o}{\Theta_i}(j\omega)\right| = \frac{1}{\sqrt{\left(1 - \frac{25K^2}{4K^2}\right)^2 + (5)^2}}$$

$$\left|\frac{\Theta_o}{\Theta_i}(j\omega)\right| = \frac{1}{\sqrt{(-5.25)^2 + 25}}$$

$$\left|\frac{\Theta_o}{\Theta_i}(j\omega)\right| = 0.138$$

And

$$\phi = -\arctan\frac{(5K)}{\left[K - (25K^2)\left(\frac{1}{4K}\right)\right]}$$

$$\phi = -\arctan\left(\frac{5}{-5.25}\right) = \arctan(0.952)$$

$$\phi = -(180.^\circ - 43.6^\circ)$$

$$\phi = -136.4^\circ$$

Nine values of the amplifier time constant ranging from 4/K to 1/50K seconds and for τ = 0 seconds were selected and characteristic curves were calculated for angular frequencies ranging from 0.1K to 100K radians per second. The calculated phase lag data are tabulated in Table I and Table II. The amplitude ratio calculations are tabulated in Table III.

The tabulated calculations are plotted in Figures 5 and 6 for the phase lag and amplitude ratio respectively.

TABLE I . THEORETICAL PHASE LAG CALCULATION DATA FOR A SECOND ORDER SYSTEM.

Phase Lag Ø in Degrees	Frequency -ω- in Radians per Second							
	$T=1/20K$	$T=1/10K$	$T=1/5K$	$T=1/4K$	$T=1/2K$	$T=1/K$	$T=2/K$	$T=4/K$
1								.025K
2								.033K
3								.049K
4								.078K
5							.09K	.083K
10	0.00K		0.18K		.17K	.17K	.17K	.16K
15	0.35K	0.35K	.35K		.26K	.26K	.24K	.22K
20				.35K	.35K	.33K	.30K	.26K
30	.55K	.56K	.54K	.53K	.51K	.46K	.40K	.33K
45	.96K	.91K	.85K	.82K	.73K	.62K	.50K	.39K
60	1.54K	1.40K	1.22K	1.16K	.96K	.76K	.58K	.43K
75	2.53K	2.10K	1.66K	1.53K	1.17K	.87K	.64K	.47K
90	4.47K	3.16K	2.24K	2.00K	1.41K	1.00K	.71K	.50K
97.6	6.00K							
105	7.87K	4.78K	3.00K	2.62K	1.71K	1.14K	.78K	.54K
120	13.08K	7.12K	4.08K	3.45K	2.10K	1.33K	.86K	.58K
135	20.96K	10.91K	5.85K	4.83K	2.73K	1.62K	1.00K	.64K
150	35.20K	17.91K	9.22K	7.47K	3.99K	2.19K	1.26K	.76K
160	55.35K	27.71K	14.07K	11.36K	5.84K	3.08K	1.67K	.95K
165		37.50K			7.73K	3.98K	2.10K	1.15K
170	113.30K	56.20K	28.53K	22.88K	11.50K	5.84K	3.00K	1.58K
174		95.50K	47.96K	38.21K	18.94K			
175						11.56K	5.82K	2.95K
176			70.57K					3.67K
177					42.21K	18.92K	9.60K	4.83K
178							14.35K	7.21K
179								14.40K
180	∞	∞	∞	∞	∞	∞	∞	∞

TABLE II. THEORETICAL PHASE LAG CALCULATION DATA FOR
A SECOND ORDER SYSTEM (CONTINUED).

Frequency In Radians Per Second	Phase Lag — ϕ In Degrees $\tau = \frac{1}{50K}$	$\tau = 0$
0.1K	5.74	
0.2K	11.32	
0.25K		14.06
0.4K	21.87	
0.5K		26.56
0.7K	35.23	
1.0K	45.56	45.0
1.5K	57.68	56.34
2. K	65.29	63.44
3. K		71.58
4. K	80.35	75.96
5. K		78.70
6. K		80.55
7. K		81.87
7.07K	90.00	
8. K		82.88
9. K		83.65
10. K	95.74	84.30
11. K		84.78
12. K		85.22
13. K		85.85
14. K		85.90
20. K	109.30	
40. K	127.80	
70. K	145.00	
100. K	153.32	

TABLE III. THEORETICAL AMPLITUDE RATIO CALCULATION DATA FOR A SECOND ORDER SYSTEM.

Amplitude Ratio for Various Servo Amplifier Time Constants.

Frequency in Radians Per Second	$\tau = 0$	$\tau = 1/20K$	$\tau = 1/10K$	$\tau = 1/5K$	$\tau = 1/4K$	$\tau = 1/2K$	$\tau = 1/K$	$\tau = 2/K$	$\tau = 4/K$
0.1K	0.995	0.999	.999	.996	.9975	.999	1.005	1.0154	1.0361
.2K	.932	.984	.985	.990	.9901		1.0303	1.06216	1.1582
.25K							1.0414	1.145	
.30K								1.2676	1.4148
.40K									
.4675K									2.07*
.50K	.895	.904	.912	.933	.942	.992	1.1074	1.414	2.00
.60K					.912			1.5103	1.3441
.612K								1.513*	
.70K					.991			1.429	
.707K						.942	1.155*	1.415	
.80K							1.12	1.18	
.85K								.915	
.90K								.707	.571
1.0K	.707	.725	.745	.781	.800	.895	1.00		.3182
1.5K							.5125		
2.0K	.448	.467	.480	.498	.500	.448	.2855	.1375	.0661
2.5K							.173		.0445
3.0K							.117		.02846
4.0K					.200				
5.0K	.196	.2(-)	.1916	.1562	.138	.0798	.04075	.0703	.01019
6.0K					.138				
8.0K					.100				
10.0K	.0995	.121	.0743	.0466	.0385	.020	.0101	.005018	.00251
14.0K		.0929							
15.0K		.0605							
20.0K	.0499	.0362	.0228	.0123	.010	.005(-)	.0025	.002262	.00111
30.0K		.0187						.001251	.000625
50.0K	.02(-)	.00748	.00392	.00199	.001597	.0008(-)			
100.0K	.01(-)	.00197	.000993	.000473					

* Indicates Max Value

PHASE LAG IN DEGREES VS
FREQUENCY IN RADIAN PER SECOND
FOR A CLOSED LOOP SYSTEM

WHERE: θ_i = INPUT
θ_o = OUTPUT
$\varepsilon = \theta_i - \theta_o$ = ERROR
$1/\omega_n = T = \sqrt{\gamma/K}$
$\gamma = \dfrac{1}{2\sqrt{TK}}$

$$\frac{\theta_o}{\theta_i} = \frac{1}{\left(\frac{\gamma}{K}\right)S^2 + \left(\frac{1}{K}\right)S + 1} = \frac{1}{T^2(S)^2 + 2T\gamma(S) + 1}$$

$$\phi = Ang\left|\frac{\theta_o}{\theta_i}\right| = Tan^{-1}\left(\frac{1}{\frac{\gamma}{K}(j\omega)^2 + \frac{1}{K}(j\omega) + 1}\right)$$

$$-\phi = Tan^{-1}\left(\frac{\omega}{K - \gamma\omega^2}\right)$$

FIG. 5.

1ST Lt Louis BAERISWYL
U.S. MARINE CORPS.
6 JULY, 1950
APL/JHU

-16-

LAG ANGLE ($-\phi$) IN DEGREES

FREQUENCY (ω) IN RADIANS/SEC.
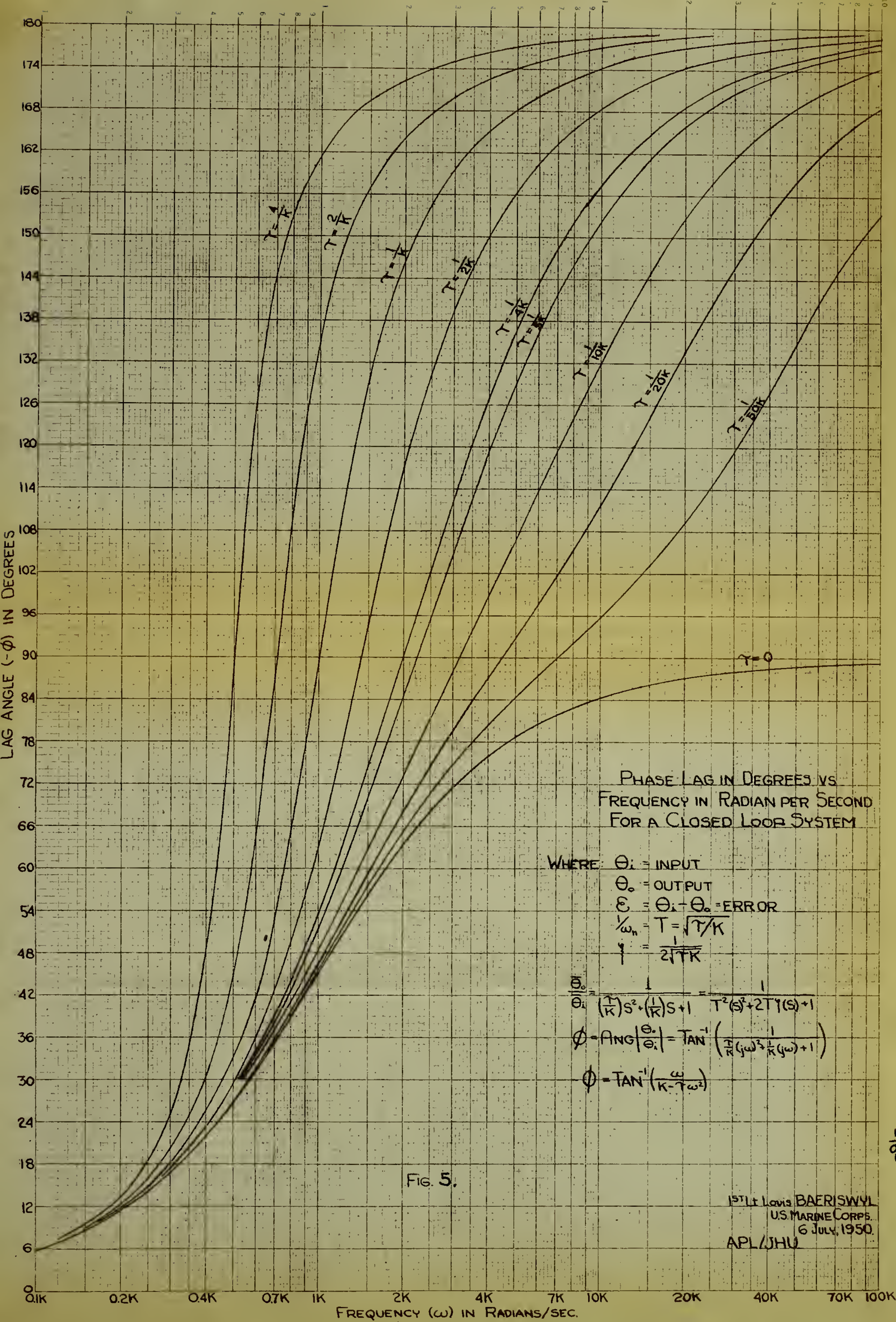
THE AMPLITUDE RATIO VS THE FREQUENCY IN RADIANS PER SECOND FOR A CLOSED LOOP SYSTEM

WHERE: θ_i = INPUT
θ_o = OUTPUT
$\varepsilon = \theta_i - \theta_o$ = ERROR
ω = IMPRESSED FREQUENCY
$M = |\theta_o/\theta_i|$ AMPLITUDE RATIO

$$\frac{\theta_o}{\theta_i} = \frac{1}{\left(\frac{T}{K}\right)S^2 + \left(\frac{1}{K}\right)S + 1}$$

$$\frac{\theta_o}{\theta_i} = \frac{1}{\left(\frac{T}{K}\right)(j\omega)^2 + \left(\frac{1}{K}\right)(j\omega) + 1}$$

$$M = \left|\frac{\theta_o}{\theta_i}\right| = \frac{1}{\sqrt{\left(1 - \frac{T\omega^2}{K}\right)^2 + \left(\frac{\omega}{K}\right)^2}}$$
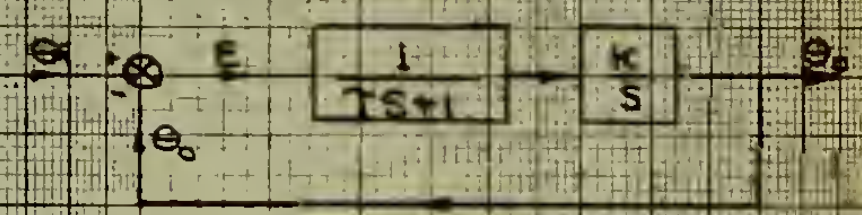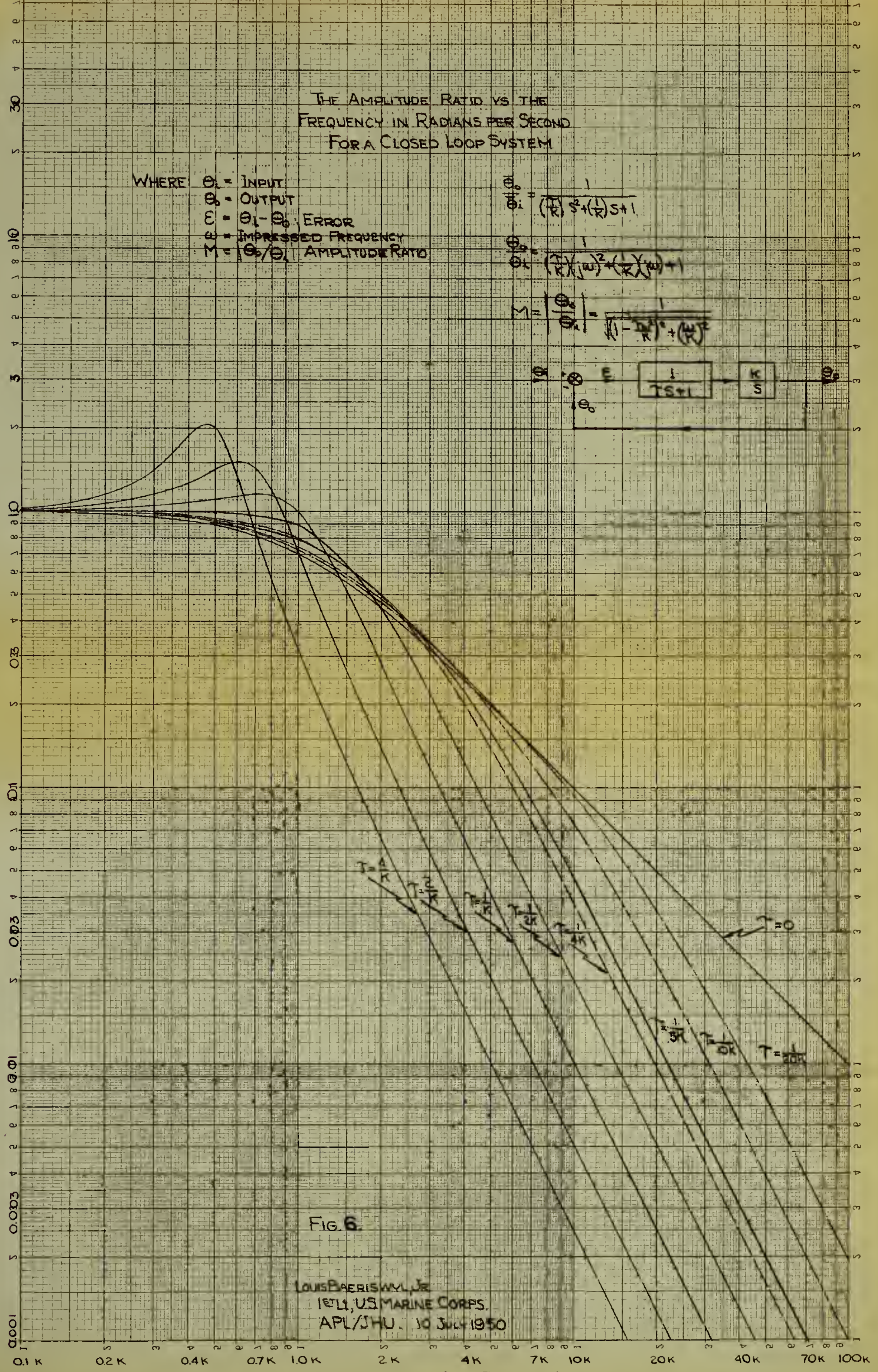
FIG. 6.

LOUIS BREISWYL, JR.
1ST LT, U.S. MARINE CORPS.
APL/JHU. 10 JUL 1950

M — THE AMPLITUDE OF θ_o/θ_i

FREQUENCY (ω) IN RADIANS/SEC.

$T = \frac{4}{K}$ $T = \frac{2}{K}$ $T = \frac{1}{K}$ $T = \frac{1}{2K}$ $T = \frac{1}{4K}$ $T = 0$

$T = \frac{1}{5K}$ $T = \frac{1}{10K}$ $T = \frac{1}{20K}$

-17-

4. Development of the Phase Lag and
Amplitude Ratio for a Third Order System.

Let a closed loop system similar to
the previous system be considered, which has, in addition,
a second component with a time delay. This system will
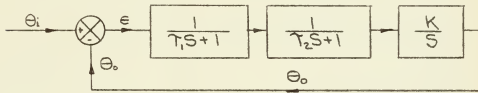be represented in the block diagram of Figure 7, shown
below:

Fig. 7. Block Diagram of a Closed Loop Servo System
Containing Two Time Delay Components and Inte-
grating Component.

The open loop transfer function for this sys-
tem is given by the equation.

$$KG(S)\Big|_{op} = \frac{K}{(T_1S+1)(T_2S+1)(S)}$$

The closed loop transfer function for this
servo system is given by

$$KG(S) = \frac{KG(S)\big|_{op}}{1+KG(S)\big|_{op}}$$

$$KG(S) = \frac{\frac{K}{(T_1S+1)(T_2S+1)(S)}}{1+\frac{K}{(T_1S+1)(T_2S+1)(S)}}$$

$$KG(S) = \frac{K}{(T_1S+1)(T_2S+1)(S)+K}$$

$$KG(S) = \frac{1}{\left(\frac{T_1 T_2}{K}\right)S^3 + \left(\frac{T_1 + T_2}{K}\right)S^2 + \left(\frac{1}{K}\right)S + 1}$$

Further, if the input signal is sinusoidal, there is
obtained:

$$KG(j\omega) = \frac{1}{\left(\frac{T_1 T_2}{K}\right)(-j\omega^3) + \left(\frac{T_1 + T_2}{K}\right)(-\omega^2) + \left(\frac{j\omega}{K}\right) + 1}$$

$$KG(j\omega) = \frac{1}{\left[1 - \frac{\omega^2}{K}(T_1 + T_2)\right] + j\left[\frac{\omega}{K} - \frac{\omega^3}{K}(T_1 T_2)\right]}$$

$$KG(j\omega) = \frac{K}{\left[K - \omega^2(T_1 + T_2)\right] + j\left[\omega - \omega^3(T_1 T_2)\right]}$$

but

$$KG(j\omega) = \frac{\theta_0}{\theta_1}(j\omega)$$

and therefore,

$$\frac{\theta_0}{\theta_1}(j\omega) = \frac{K}{\left[K - \omega^2(T_1 + T_2)\right] + j\left[\omega - \omega^3 T_1 T_2\right]}$$

Thus,

$$\left|\frac{\theta_0}{\theta_1}(j\omega)\right| = \frac{K}{\sqrt{\left[K - \omega^2(T_1 + T_2)\right]^2 + \left[\omega - \omega^3 T_1 T_2\right]^2}}$$

If the phase angle between output and input signals
is $\emptyset$, then

$$\emptyset = -\arctan\left(\frac{\left[\omega - \omega^3 T_1 T_2\right]}{\left[K - \omega^2(T_1 + T_2)\right]}\right)$$

$$\emptyset = -\arctan\left(\frac{\left[1 - \omega^2 T_1 T_2\right]}{\left[\frac{K}{\omega} - \omega(T_1 + T_2)\right]}\right)$$

These equations for the amplitude ratio and
the phase shift may be applied to a system similar to
the system developed in Part 3, Section II, except that
the torque motor transfer function is here taken as

$$Y_3 = \left(\frac{K_3}{T_2 S + 1} \right)$$

where K_3 is the component gain constant,

and T_2 is the component time constant in

seconds.

5. Simplified Linear and Saturation
Limiting Theory.

Consider a closed loop system composed of

the following series connected components:

1) Linear Amplifier

2) Linear Torque Motor

3) Integrating Transfer Valve

4) Linear Actuator

5) Linear Mechanical Linkage

6) Autosyn pair operated in linear region.

These components are connected from left to

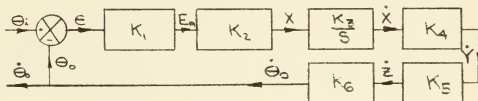right in series, as given above, and as shown below in

Figure 8:

Fig. 8. Block Diagram of Components Used in Development
of Simplified Linear and Saturation Limiting
Theory.

The operation of the above components may be

expressed more simply if the last four components are

combined into a single component with transfer function (K_7/S). Thus, the system is reduced to one as shown in Figure 9:
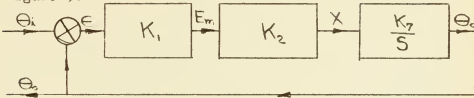

Fig. 9. Block Diagram of the Simplified Closed Loop Servo System for the Development of Linear and Saturation Limiting Theory.

The operation of the system is governed by the following equations:

$$\epsilon = \theta_i - \theta_o \quad ; \text{ for the differential}$$

$$E_m = K_1\epsilon \quad ; \text{ for the servo amplifier}$$

$$X = K_2E_m \quad ; \text{ for the torque motor}$$

$$\dot{\theta}_o = K_7X \quad ; \text{ for the transfer valve, actuator mechanical linkage, and feedback autosyn pair.}$$

And by substituting,

$$\dot{\theta}_o = K_7(K_2E_m) = K_7K_2K_1\epsilon$$

Let $K_7K_2K_1 = K$

Then, $\dot{\theta}_o = K (\theta_i - \theta_o)$

$$\dot{\theta}_o + K\theta_o = K\theta_i$$

The case wherein saturation is just beginning to appear in the transfer valve, will be examined next.

For this case, the input sinusoidal signal is of such magnitude as to barely cause the transfer valve to saturate at the input signal peaks. The signal between various components, as a function of time, is indicated below in Figure 10, for the above mentioned linear limiting condition.
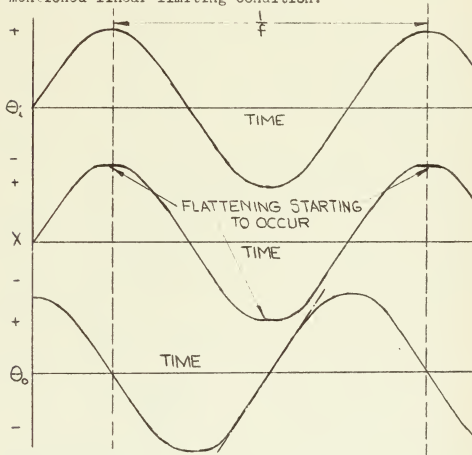

Fig. 10.   Signals between Various Components as a Function of Time under Valve Linear Limiting Conditions.

The output signal as a function of time in Figure 10 was obtained from the following:

$$\dot{\theta}_o = K_7 X$$

$$\int \dot{\theta}_o dt = \int K_7 X dt$$

$$\theta_o = K_7 \int X dt + C$$

The output signal of Figure 10 may be expressed

as,

$$\theta_o = a \, \mathrm{Sin}\, \omega t = a \, \mathrm{Sin}\, (2\pi f) t$$

where,

a is 1/2 the peak to peak output signal
amplitude,

and,

f is the input signal frequency,

$$\dot{\theta}_o = a(2\pi f) \, \mathrm{Cos}\, (2\pi f) t$$

but, $\dot{\theta}_o$ max occurs when

$$\mathrm{Cos}\, (2\pi f) t = 1.0$$

and therefore,

$$\dot{\theta}_o \, \mathrm{max} = a(2\pi f).$$

Thus,

$$af = \frac{\dot{\theta}_o \, \mathrm{max}}{2\pi}$$

is an expression for transfer valve linear limiting condi-

tion.

With a sinusoidal input and with the transfer

valve driven far past the saturation point by an input

signal of large magnitude, transfer valve saturation

limiting occurs.

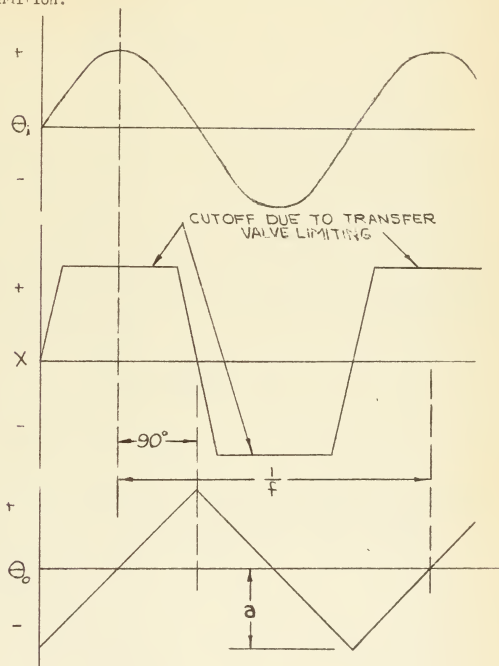The signal between various components is indicated below in Figure 11, for the above mentioned condition.

Fig. 11. Signals between Various Components as a Function of Time under Valve Saturation Limiting Conditions.

The output curve, i.e., θ_o, as a function of time, is obtained from:

$$\dot{\theta}_o = K_7 X$$

$$\int \dot{\theta}_o dt = \int K_7 X dt$$

$$\theta_o = K_7 \int X dt + C$$

The symbol "a" is defined as one half the peak-to-peak value of the output signal and "f" is defined as the frequency of the input signal in cycles per second.

During 1/2 cycle, i.e., $\frac{1}{2}(\frac{1}{f})$ seconds, the valve goes through 2 amplitudes, i.e., through 2a, and hence the maximum output rate, $\dot{\theta}_{o\ max}$, is found from the slope of the output curve to be:

$$\dot{\theta}_{o\ max} = \frac{2a}{(\frac{1}{2})(\frac{1}{f})} = 4af$$

and therefore,

$$af = \frac{1}{4}\dot{\theta}_{o\ max}$$

The above expresses the condition of transfer valve saturation limiting in terms of the output signal amplitude and the input signal frequency.

III. EXPERIMENTAL.

1. Description of Various Components.

1.1. The Servo Amplifier and Differential Transformer.

The servo amplifier and differential transformer circuit are interconnected, as shown in Figure 12. These two components are mounted in a single case, with the filter element, feeding the 6AQ5 tubes, external to the case so that the condensers may be altered to vary the servo amplifier time constant. Cornell Decade Condenser boxes were used for the various values needed in the filter network.

This unit is shown in the center of Figure 27 as indicated by the overlay to this figure. This unit was designed and built at the Applied Physics Laboratory.

1.2. The Torque Motor.

The torque motor used in this servo system was manufactured by the Curtiss Wright Aviation Corporation. The photograph of Figure 13 shows the torque motor connected to the transfer valve.

3/

The construction of the motor is similar to an enlarged version of the balanced armature type of loud speaker unit or the magnetic phonograph cutting head which employ permanent magnets for polarizing purposes.

An operational illustration of the motor may be seen in Figure 14.

The vane or armature (D), Figure 14, is supported by a torsion spring (K) between two sets of magnetic poles (C,C,B,B). These poles are polarized either by permanent magnets (A) or by D.C. coils. About the vane are two control coils (H and I) which can polarize the vane in the desired manner to cause it to be attracted to one pair of the poles. Because of the torsion spring, which restrains the vane motion and the design of the magnetic circuit, the physical displacement of the vane is very nearly a linear function of the current in the coils. By reversing the current in the vane coils, the direction of motion is reversed. The motor is normally operated with a steady idling current in each control coil. Torque is produced by simultaneously raising the current in one coil and lowering it in the other. Thus, the motor is D.C. powered and operates, in principle, similar to a Class A amplifier. Figures 15 and 16 show flux path in motor for various positions of the vane.

1.3. The Transfer Valve.

The transfer valve used in this servo system was designed and manufactured by the
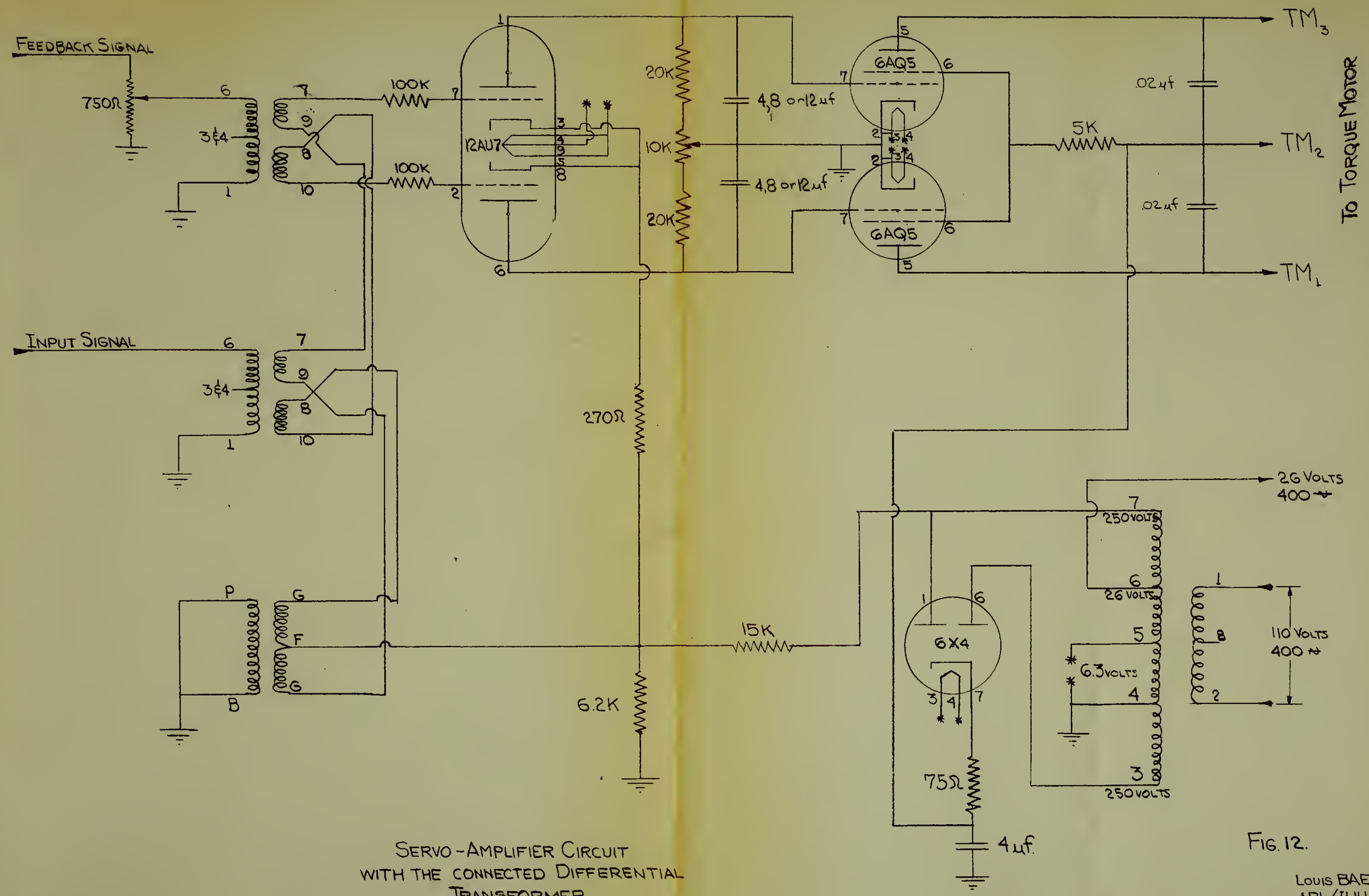
SERVO-AMPLIFIER CIRCUIT
WITH THE CONNECTED DIFFERENTIAL
TRANSFORMER
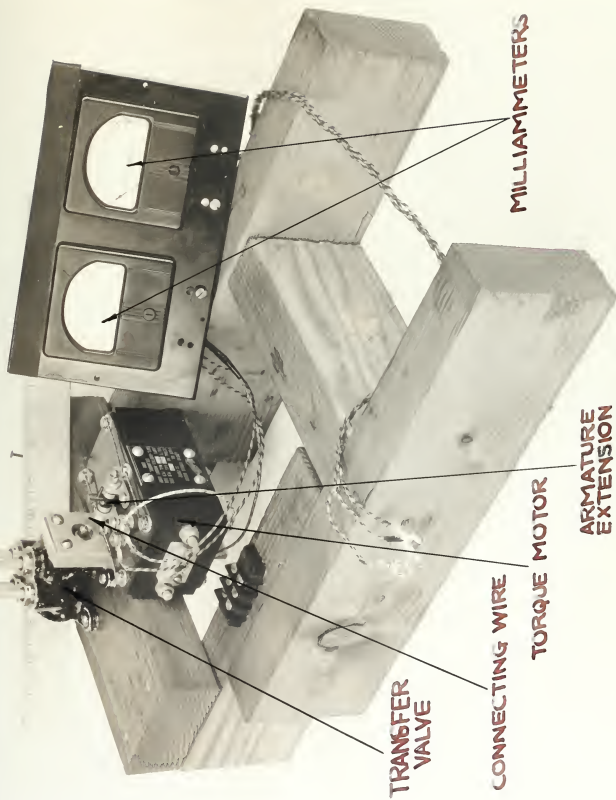
FIG. 12.

Louis BAERISWYL, Jr
APL/JHU 8 MARCH 51

MILLIAMMETERS

ARMATURE
EXTENSION

CONNECTING WIRE

TORQUE MOTOR

TRANSFER
VALVE

FIG. 13. CONNECTED TORQUE MOTOR AND TRANSFER VALVE.
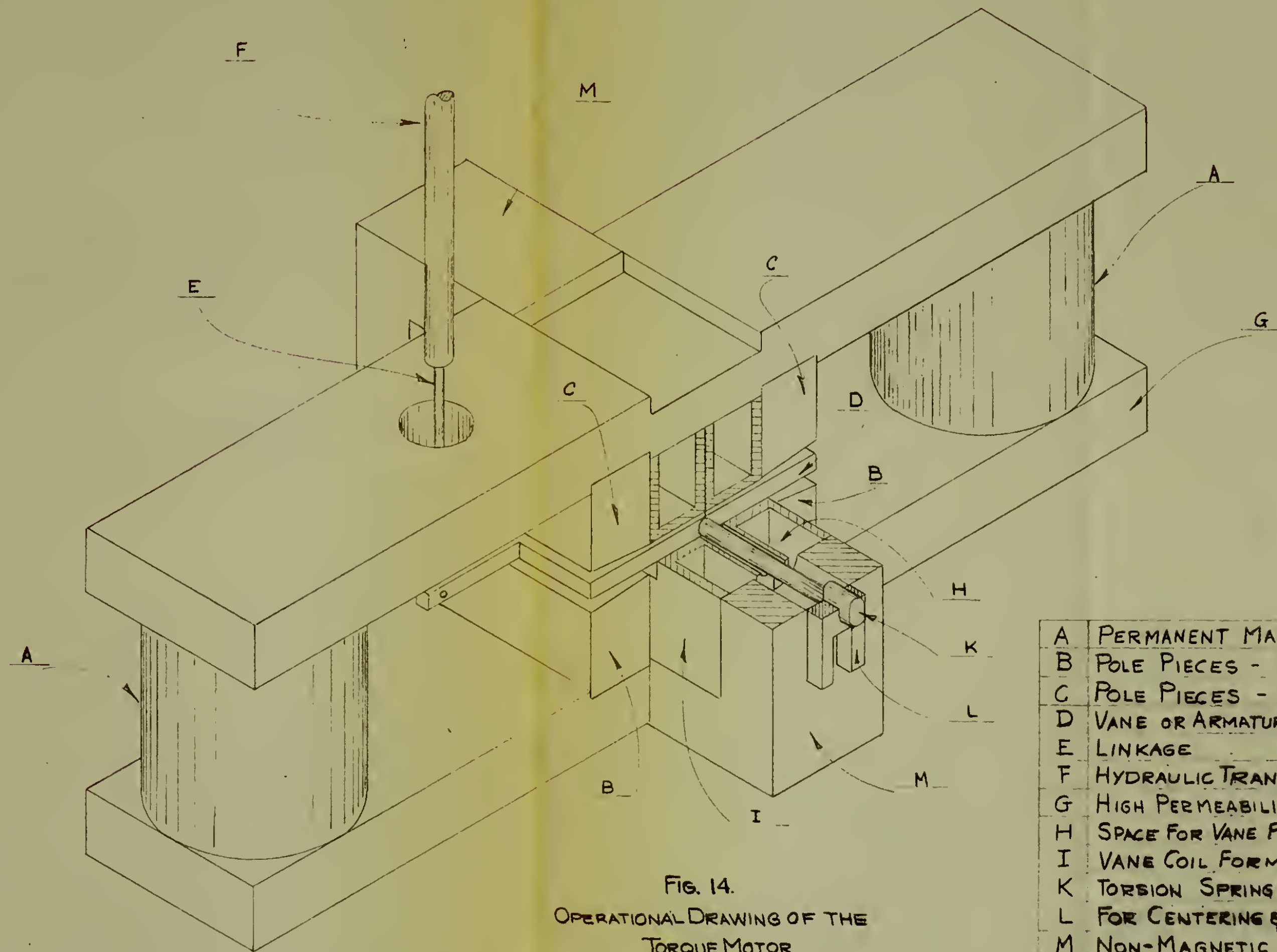
Fig. 14.
Operational Drawing of the
Torque Motor

A	Permanent Magnets Alnico V
B	Pole Pieces - South Polarity
C	Pole Pieces - North Polarity
D	Vane or Armature
E	Linkage
F	Hydraulic Transfer Valve Spool
G	High Permeability Iron
H	Space for Vane Polarizing Coils
I	Vane Coil Forms
K	Torsion Spring
L	For Centering & Locking Torsion Spring
M	Non-Magnetic Material

REVISION	DATE	BY	SCALE Full
MATERIAL		DRAWN Paddison, F.C.	
FINISH	REQUIRED	CHECKED 11 June 1947	B-11900 - 0
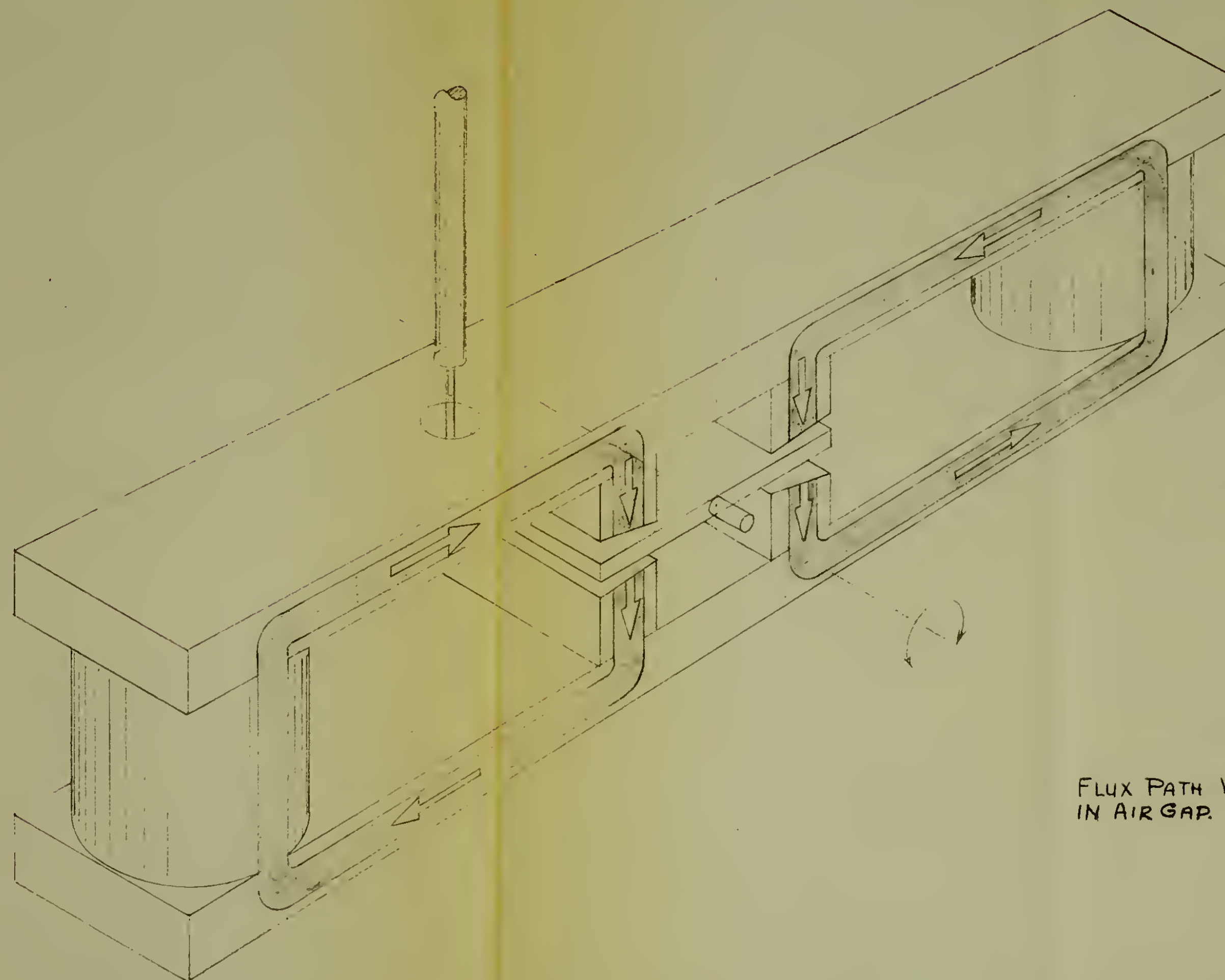
Fig. 15.

FLUX PATH WHEN VANE IS CENTERED
IN AIR GAP.

CENTERED

	REVISION	DATE	BY	SCALE Full
MATERIAL	DRAWN PADDISON, F.C			B-11
FINISH	REQUIRED	CHECKED		

NORTH

NORTH

SOUTH

AXIS OF ROTATION
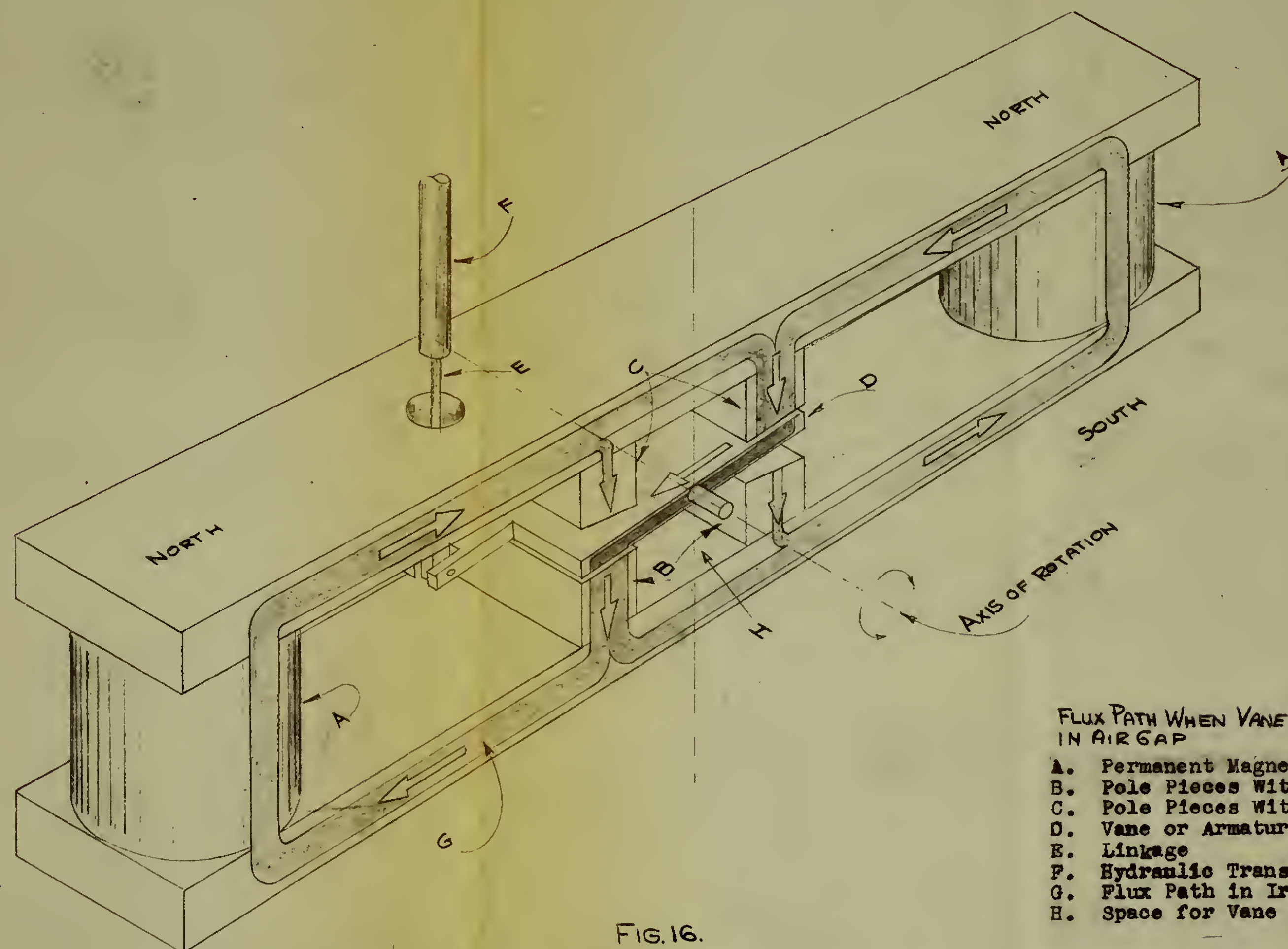
FLUX PATH WHEN VANE IS NOT CENTERED
IN AIR GAP

A. Permanent Magnets
B. Pole Pieces With South Polarity
C. Pole Pieces With North Polarity
D. Vane or Armature
E. Linkage
F. Hydraulic Transfer Valve Spool
G. Flux Path in Iron
H. Space for Vane Polarizing Coils

FIG. 16.

JOHNS HOPKINS UNIVERSITY - HIGH SPEED LINEAR TORQUE MOTOR

MATERIAL		REVISION	DATE	BY	SCALE FULL
		DRAWN PADDISON, E.C.			
FINISH	REQUIRED	CHECKED 11 JUNE 1947			B-11899-0

Products Division, Bendix Aviation Corporation,
South Bend, Ind. The transfer valve is illustrated
in the photograph of Figure 13 and in the schematic
drawing of Figure 17.

The transfer valve was designed to have a
rate of flow that was a linear function of the spool
displacement. The deadspace was to be a minimum,
while the maximum flow rate, under an accumulator
pressure of 1500 pounds per square inch, was to be
5 cubic inches per second.

The transfer valve has four ports. Ports
1 and 2 are connected to the actuator; port 3 is
connected to the high pressure accumulators; and port
4 is connected to the surge tank. Movement of the
valvespool to the left (See Figure 17), enables oil
to flow from the valve through port 1 and into the
valve through port 2. Movement of the valvespool to
the right reverses the direction of oil flow through
valve ports 1 and 2.

1.4. The Actuator.

The actuator is schematically
illustrated in Figure 17 and shown in the photograph
of Figure 18. The actuator consists of a hollow
metal cylinder having two ports, one at each end.

These ports allow oil to flow to and from the cylinder,
driving the enclosed piston in alternate directions.
The high pressure oil entering port 1 drives the pis-
ton to the left and discharges the oil to the left of the
piston through port 2. The reverse motion of the pis-
ton is obtained when the high pressure oil enters
through port 2 while exhaust oil leaves through port 1.

The actuator has a volume of 12 cubic inches
with a maximum piston stroke of slightly larger than
4 inches.

1.5.   The Mechanical Linkage.

The mechanical linkage is shown
in the photograph of Figure 18. A schematic of this
linkage is illustrated in Figure 17.

The mechanical linkage consists of two pivot-
ed arms, the ends of which are connected to the feed-
back autosyn, and the actuator strut. The purpose of
the linkage is to transfer the linear motion of the
actuator strut into rotation of the feedback autosyn
rotors. This is readily accomplished by the designed
linkage.

1.6.   The Feedback Autosyn Pair.

The feedback autosyn pair are of
conventional design. High precision autosyns manu-
factured by the Eclipse-Pioneer Division, Bendix
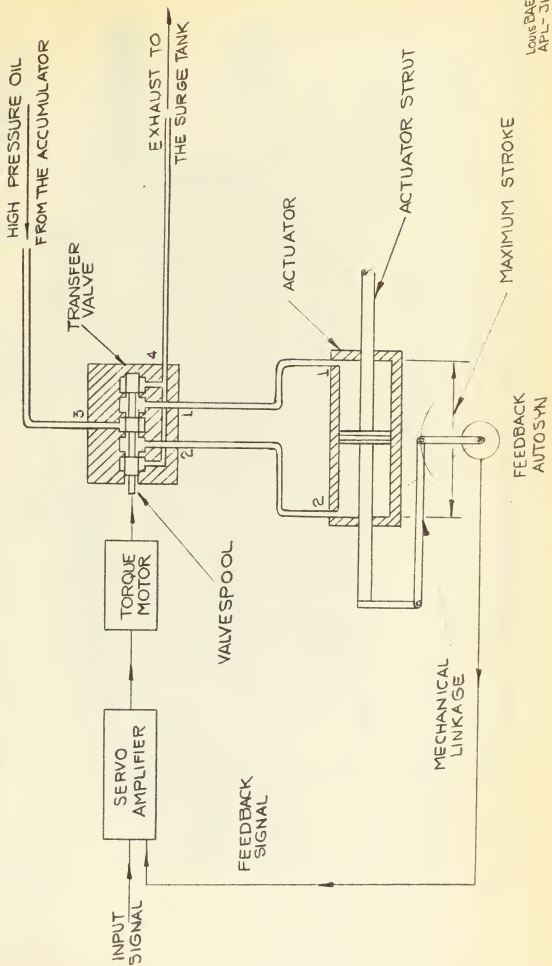
FIG. 17. SCHEMATIC OF THE CONNECTED SERVO SYSTEM COMPONENTS

COUPLED FEEDBACK AUTOSYNS

ACTUATOR PORT

ACTUATOR PORT

PICKOFF CONTACT

PICKOFF POTENTIOMETER

MECHANICAL LINKAGE

ACTUATOR STRUT

UNMOUNTED AUTOSYN
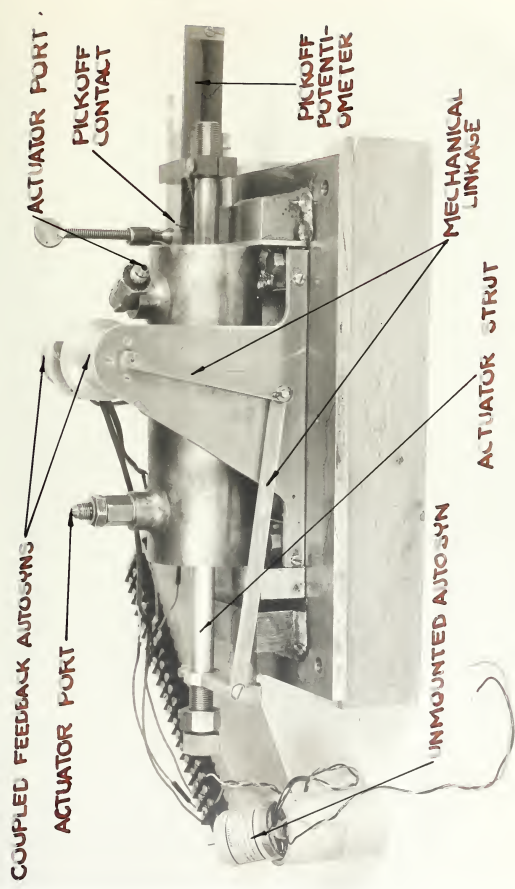
Fig. 13. ACTUATOR, MECHANICAL LINKAGE AND FEEDBACK AUTOSYN ASSEMBLY.

Aviation Corporation, were used in all cases.

Autosyn pairs were connected in the pre-
scribed manner 485/, with the rotors of the first auto-
syns in each pair locked in a fixed position. The
rotors of the second autosyns of each pair were con-
nected to the mechanical linkage output. The auto-
syns were excited with 26 volts at 400 cycles per
second, and with 25 volts at 3000 cycles per second.

As the autosyn rotors were moved by the
mechanical linkage, the output carrier signal was
modulated. The feedback autosyns are illustrated in
the photograph of Figure 18.

1.7. The Hydraulic Loop.

The hydraulic loop is shown in the
schematic drawing of Figure 19 and in part in the
photograph of Figure 20.
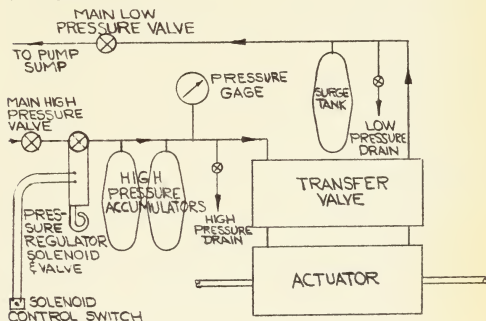
Fig. 19. Schematic Drawing of the Hydraulic Loop.

The hydraulic pump used to supply oil to the system was manufactured by Denison Equipment Company and is capable of supplying oil at a pressure of 5000 pounds per square inch.

The main high and low pressure valves are used to connect and disconnect the loop from the pump, to prevent the loss of oil in the event a break occurs in the loop and to enable the hydraulic loop to be opened at any point without shutting down the pump. High and low pressure drains are provided so that the oil may be drained from the loop after the main valves have been closed, when it is necessary that the loop be opened. The drains also provide a means of bleeding air from the loop. When the loop is first placed in operation, air will be trapped in various parts of the loop. To remove this air, the high pressure drain is partly opened and the undesirable air and oil are drained from the loop. This same process is also repeated on the low pressure side of the transfer valve. Here it is necessary to move the transfer valvespool from side to side to enable oil to discharge through the hydraulic loop.

If the loop is once bled and then not opened, the loop may retain its air-free condition by allowing
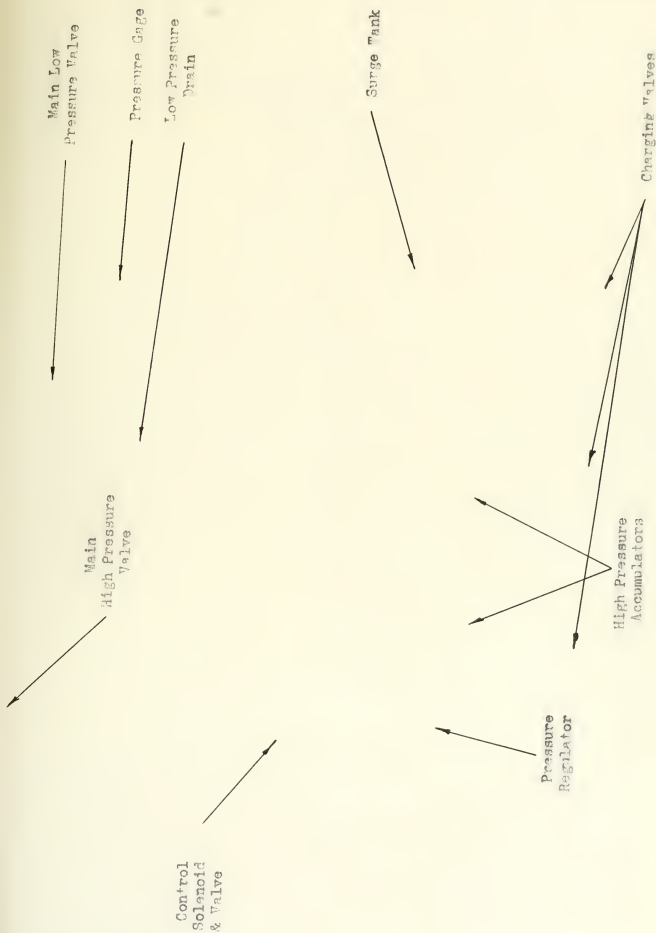
Fig. 20. Overlay to the Photograph of the Accumulators, Surge Tank, and Control and Regulator Components.

Cylinders

Instrument High Pressure

Pressure Regulator

Surge Gage

Pressure Gage

Main Gate Valve

Main Line Pressure Valve

Main Line Pressure High Pressure Valve

Control Pioneer & Valve

Fig. 30. Overlay of the Photograph of the Accumulators, Surge Tank, and Control and Switching Components.
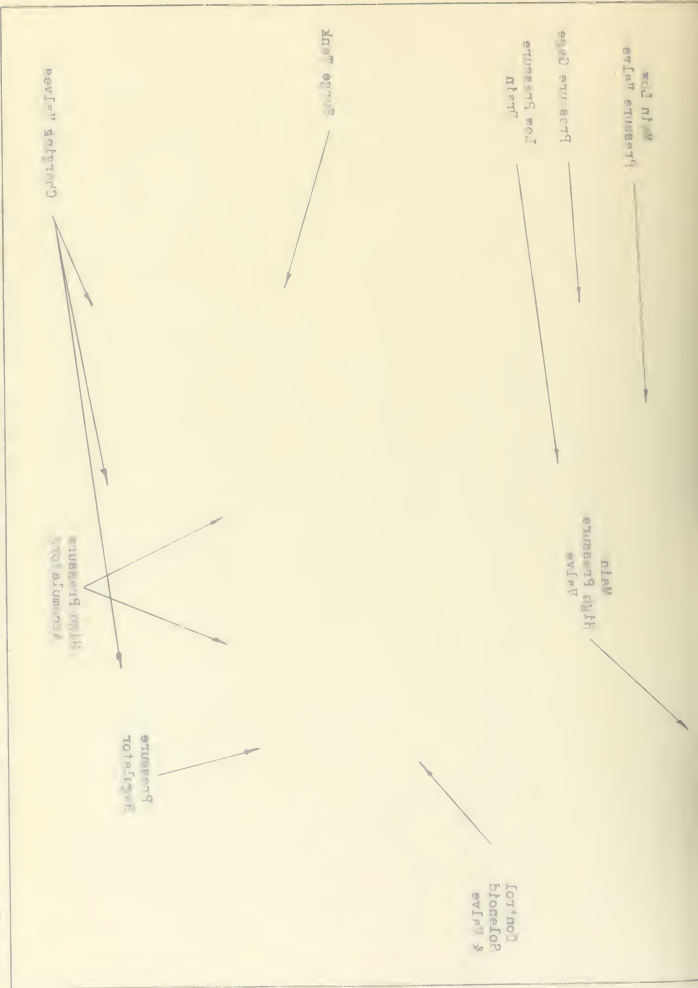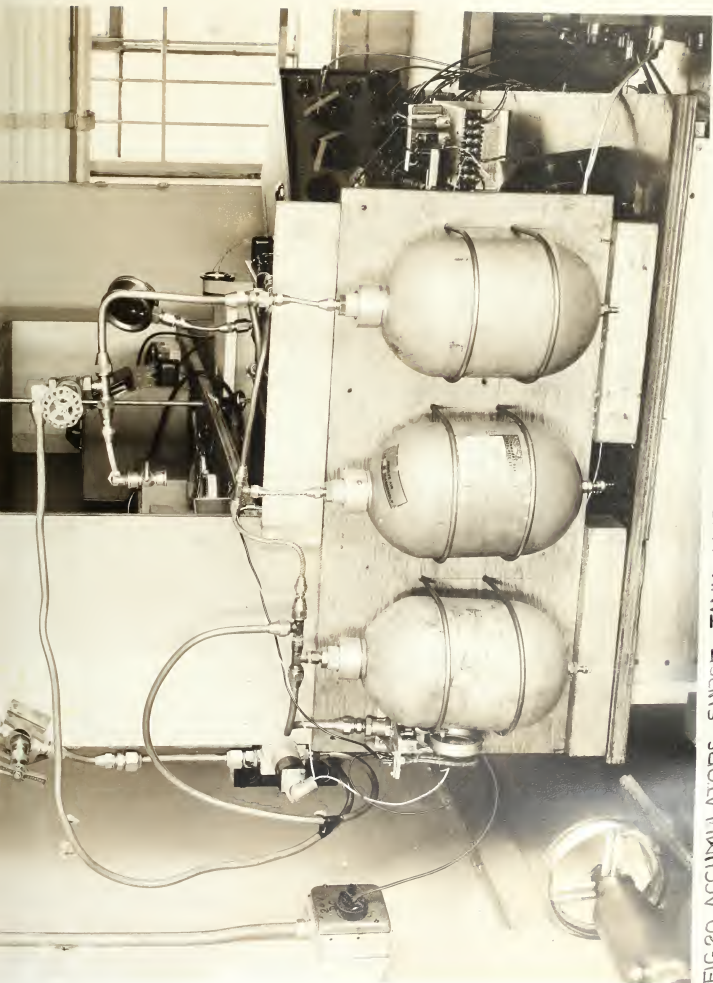
FIG. 20. ACCUMULATORS, SURGE TANK, HYDRAULIC CONTROLS AND REGULATOR COMPONENTS.

the hydraulic system to be charged to 1000 pounds per square inch before closing the main valves, when securing the pump. This pressure bias seems to prevent air from leaking into the hydraulic system.

The two accumulator tanks and a surge tank are of the same construction. They were manufactured by Simmonds Aerocessories, Inc., as part No. H-105B of the Simmonds Olaer Hydraulic System. The accumulators each have a volume of 220 cubic inches with a design operating pressure of 1500 psi., and maximum test pressure of 3000 psi. The high pressure accumulators are different from the surge tank only in that the bladder of the latter is at atmospheric pressure, while the former is charged to 800 psi. when no oil is in the accumulator tank. Commercial nitrogen was used to charge these accumulators. The bladders were charged through a charging valve shown at the bottom of the tanks in Figure 20.

A hydraulic pressure regulator is connected in the high pressure side of the loop. With the solenoid control switch open, the pressure regulator valve is closed and the only oil delivered to the transfer valve will be supplied by the oil stored in the high pressure accumulator. If the solenoid

control switch is left open, the accumulator will
be charged to approximately 1600 psi. which is the
pump discharge pressure. As oil is used by the sys-
tem, the pressure will drop until the pressure is
1000 psi. At this point the pressure regulator con-
trol valve again opens and the accumulators are again
recharged with oil at a pressure of 1600 psi. The
solenoid of the pressure regulator operates from 24
volt D.C. supply.

The various hydraulic components are con-
nected by means of copper and aluminum seamless tub-
ing which is easily bent due to its flexibility.

2. Correlation of Experimental Results
and Assumptions for Various Components.

2.1. Servo Amplifier.

i. Static Test.

The static test was conducted
on the servo amplifier in order to verify the assump-
tion that the output differential current was a linear
function of the input voltage signal. The test was
further conducted to determine the range of linearity
of the output signal with respect to the input signal
and to determine the gain of the amplifier from the
slope of the static amplifier test curve.

The servo amplifier was connected to its
normal load, the Curtiss high speed torque motor, with
two milliammeters connected into the polarizing coils

of the motor. All input terminals to the amplifier
were shorted. The servo amplifier power transformer
was connected to the line power supply of 110 volts at
400 cycles per second through a switch. The switch was
closed and the amplifier was allowed to warm up. After
the warm-up, the amplifier balance was adjusted to give
a zero differential output current as indicated by the
two milliammeters connected to the torque motor polar-
izing coils. This balanced condition usually occurred
with each polarizing coil carrying approximately 26
milliamperes. After the balancing was completed, the
shorted input was disconnected.

The input signal to the servo amplifier was
supplied by an autosyn pair terminated in a 750 ohm
variable resistance, the resistor being adjusted to
give varied input voltage to the amplifier. The auto-
syn pair was excited by a 26 volt 400 cycle per second
input which was tapped from the servo amplifier power
transformer.

The input signal to the servo amplifier was
fed into the input differential transformer which is
constructed as an integral part of the servo amplifier.
See Figure 12 for the servo amplifier circuit with the
connected differential transformer.

An electronic voltmeter was connected between the output of the 750 ohm resistor and the input terminal to the amplifier unit.

A schematic of the test set-up employed is shown in Figure 21.
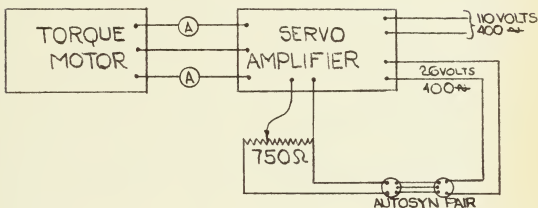
Fig. 21. Schematic Diagram of Test Set-up for Determining the Static Characteristics of the Servo Amplifier.

The autosyn pair were adjusted to an output null. At the null point one rotor was blocked, i.e., locked in position, while the other could be rotated manually. The voltage signal into the servo amplifier was increased by rotating the movable autosyn rotor to various fixed positions. At each such position, the voltage input to the servo amplifier and the differential current output were recorded. These values are tabulated in Table IV. This test was conducted using each of the three condenser pairs, later used to alter the amplifier time constant in the closed loop test. Using

the three different condensers in the filter feeding
the 6AQ5 tubes of the amplifier, in no way altered the
recorded static characteristics. From the recorded
data of Table IV, Figure 22, was drawn. This static
characteristic curve indicates that for a differential
current range of ± 30 milliamperes, the output is a
linear function of the input. Thus, for a limited
range, the assumption of linearity is proved as the
assumed and experimental results correspond with one
another. The slope of this curve in the linear region
is 160 milliamperes per volt and represents the servo
amplifier gain.

As the input signal increases, saturation
finally occurs at approximately ±80 milliamperes.

ii. Dynamic Test.

The dynamic test was conducted on
the servo amplifier to verify the assumption that the
servo amplifier was a first order delay system and
further, to determine the time constant of the servo
amplifier when various condensers were used in the
filter circuit feeding the 6AQ5 tubes. See Figure 12.
The phase lag of the amplifier was selected as the
basis for determining the order of the amplifier as
the phase measuring system has a higher degree of
accuracy and is also more readily interpreted in terms

TABLE IV.   STATIC CHARACTERISTIC DATA FOR THE SERVO
AMPLIFIER WITH 4 μf. CONDENSERS IN THE FILTER FEEDING
THE 6AQ5 TUBES OF THE SERVO AMPLIFIER.

INPUT SIGNAL IN RMS VOLTS	OUTPUT SIGNAL IN MILLIAMPERES		
	i_1	i_2	Δi
0.0	25.8	25.8	0.0
.056	20.2	30.5	10.3
.110	17.8	35.0	17.2
.163	12.0	38.2	26.2
.211	9.0	41.3	32.3
.268	6.5	44.4	37.9
.302	5.4	46.2	40.8
.400	3.2	50.2	47.0
.500	2.5	54.0	51.5
.600	2.0	57.5	55.5
.807	1.5	64.0	62.5
1.0	1.2	68.5	67.3
1.2	1.0	72.0	71.0
1.4	.4	74.4	74.0
1.6	.2	75.5	75.3
1.8	0.0	76.5	76.5
2.0	0.0	77.0	77.0
2.5	0.0	78.0	78.0
3.0	0.0	78.3	78.3
4.0	0.0	79.0	79.0
5.0	0.0	79.2	79.2
6.0	0.0	79.2	79.2

Louis Baeriswyl, Jr.
23 Feb. '51, APL/JHU

SERVO AMPLIFIER
VOLTAGE INPUT (400 CYCLES PER SECOND)
VS. DIFFERENTIAL CURRENT OUTPUT

DIFFERENTIAL CURRENT OUTPUT IN MILLIAMPERES

$K_2 = 160$ MILLIAMPERES/VOLT

VOLTAGE INPUT - VOLTS (RMS)

ASSUMED LINEAR
RELATION

FIG. 22.

Louis BAERISWYL, JR.
APL/JHU - 24 FEB, 51.
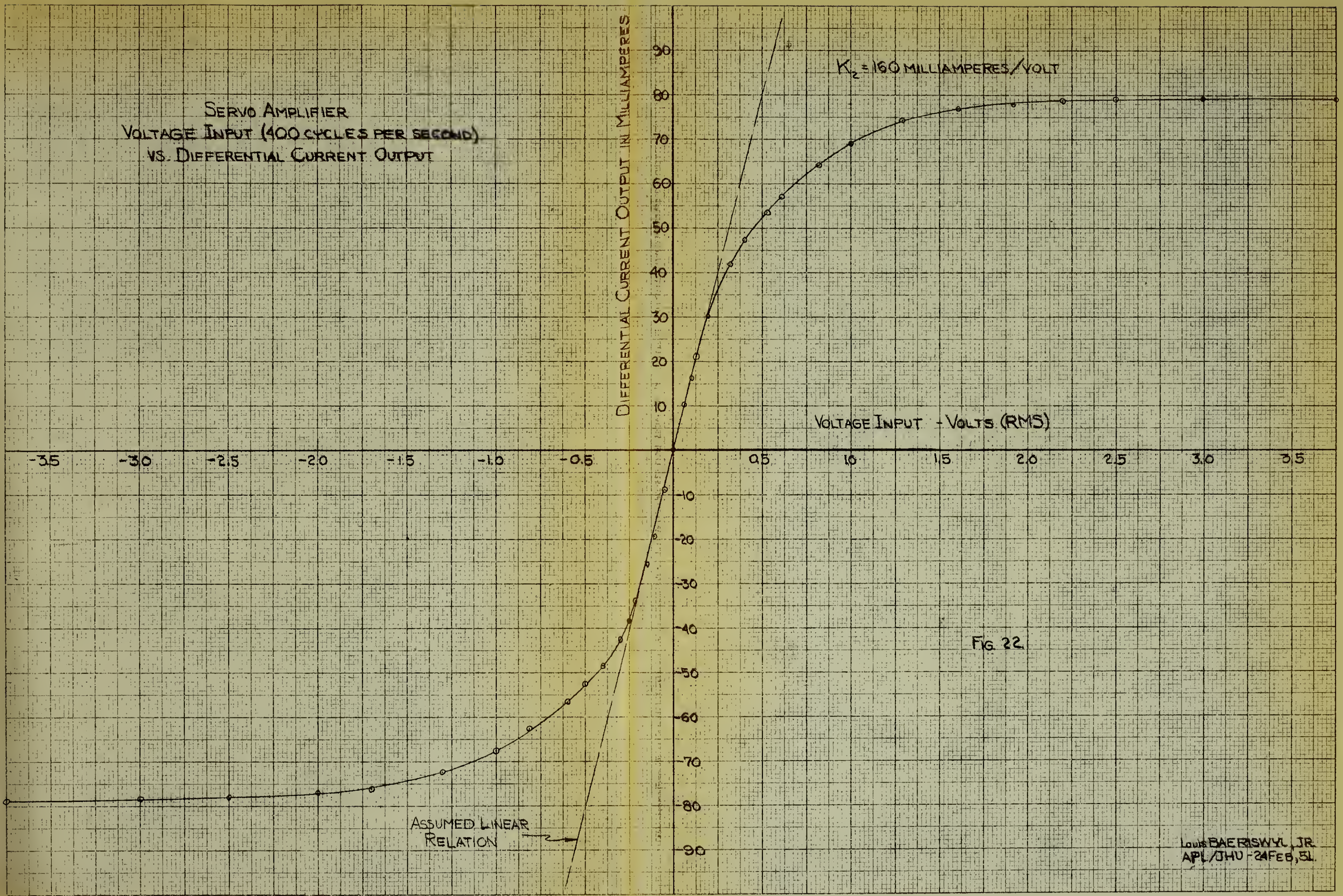
of the amplifier time constant than the results of the
amplitude measuring system. The phase lag was to be
determined by observing the Lissajou figure produced
by the output and input signals to the servo amplifier.
Since the input signal to the servo amplifier was the
output of an autosyn pair, which was a modulated 400
cycle per second signal, it was not suitable to use
this signal, as the input to the cathode ray oscillo-
scope to produce a useable Lissajou figure.

A possible solution to this difficulty, and
the one used, is to develop another signal that is always
in phase with the autosyn signal feeding the amplifier
and to use this latter signal as an input to the cathode
ray oscilloscope. A Bendix Eclipse Pioneer Resolver
was used to produce the desired signal.

The resolver stator consisted of two coils,
but only one of these was excited in order to avoid any
unnecessary harmonics in the resolver output. One
stator coil was left open, while the other was excited
from a 1½ volt battery through a variable resistance,
to limit the current to an allowable value of 60 milli-
amperes. If the resolver is excited in this manner,
and its rotor is rotated uniformly, there results an
output voltage signal from the rotor circuit that is

sinusoidal. The signal developed by the resolver must be inphase with the signal developed by the autosyn. This is accomplished by the use of the test set-up shown in Figure 23 below.
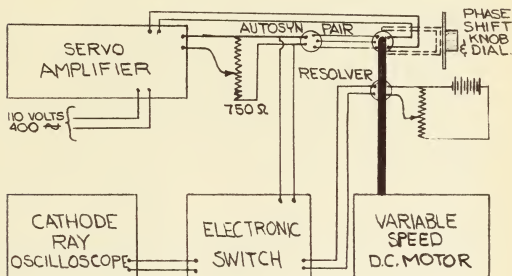
Fig. 23. Schematic of Test Set-up Required to Zero the Resolver and Autosyn Signal.

The resolver and one autosyn have their rotor shafts coupled together. These two shafts are in turn coupled to a variable speed D.C. motor, the speed of which controls the angular frequency of the modulated input signal from the autosyn to the servo amplifier and of the signal from the resolver to the electronic switch. The phase of the resolver output is related to the relative position of its rotor and field coil, while the phase of the output signal of the autosyn pair is related to the combined position of the two rotors and

their field coils. The body of the autosyn, whose rotor
is coupled to the resolver, is so arranged that it may
be rotated relative to the rotor, even while the latter is
rotating. This body rotation is accomplished by turning
a knob with a connected dial calibrated in 1/2 degrees
for a total of 360 degrees. This dial is set to read
zero. The second autosyn of this pair, the rotor of
which is not driven, is so arranged that it may be rotated
to any position relative to its stator coils and there
locked in position.

The output of this second autosyn is terminat-
ed in a 750 ohm potentiometer. The amplitude of the
signal fed to the servo amplifier is then varied by ad-
justing this potentiometer. The first autosyn is supplied
with 26 volts at 400 cycles per second, tapped from the
power transformer of the servo amplifier. The output
signal from the autosyn pair is connected to one pair of
input terminals of the electronic switch $\frac{7/}{}$, while the
resolver output signal is connected to the other pair of
input terminals of the electronic switch. The output
terminals of electronic switch are connected to a
cathode ray oscilloscope modified for D.C. signals. All
test elements and equipment were turned on and allowed to
warm up. Then the variable speed motor was driven at 5
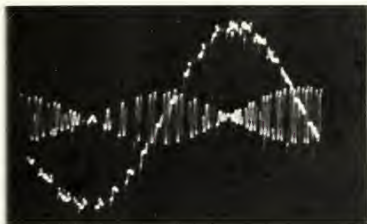
Fig. 24. Superimposed Autosyn and Resolver Signals -
Out of Phase Condition.

Fig. 25. Superimposed Autosyn and Resolver Signals -
Inphase Condition.

cycles per second. There will be observed on the cathode
ray tube two superimposed traces, one a modulated sinu-
soidal signal with a 400 cycle carrier, from the autosyn,
and a second sinusoidal signal from the resolver. Ini-
tially these will not be inphase. This condition is
illustrated in the photograph of Figure 24.

To zero these two signals, the rotor of the
second autosyn is unlocked and rotated until the signals
on the cathode ray tube are inphase. This condition is
illustrated in the photograph of Figure 25. After the
rotor of the second autosyn has been moved to give the
desired inphase signal, it is again locked in place
relative to its stator coils. Thus, the two signals
are inphase, as required. This is true for all signal
frequencies used in this test.

The test set-up of Figure 23 is altered to that
of Figure 26 without changing the zero condition of the
autosyn pair and the resolver.
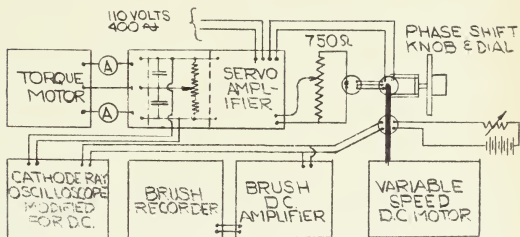
Fig. 26. Test Set-up for Determining the Amplifier Time
Constant.

The servo amplifier, as in the previous set-up, Figure 23, is connected to the autosyn pair through a 850 ohm potentiometer. The servo amplifier output is connected to a Curtiss high speed torque motor through two milliammeters, one in each polarizing coil circuit.

The resolver feeds into the cathode ray oscilloscope and a D. C. amplifier made by the Brush Development Company [3]. This D.C. amplifier, in turn, feeds a Brush Recorder [2].

The output signal of the servo amplifier was taken from the filter circuit feeding the 6AQ5 tubes, as shown in Figure 26. (See Figure 12). The output was taken at this point as there is little effective delay encountered between this point and the output to the torque motor coils, and, as normal amplifier loading is possible, i.e., the servo amplifier output is terminated in the torque motor polarizing coils. The amplifier output to the cathode ray tube should have a sinusoidal wave shape to obtain the desired Lissajou figure. The wave shape obtained at the filters feeding the 6AQ5 tubes is sinusoidal at a frequency of the input signal, with a small 400 cycle component added. The wave shape, as measured across the servo amplifier output when feeding into the torque motor, is greatly distorted, due to such effects as the inductance of the torque motor polarizing coil windings. Thus, in determining the time constant

of the servo amplifier, the output phase was measured
across the filter feeding the 6AQ5 tubes.

The measuring equipment and elements under
test are connected as shown in the schematic diagram
of Figure 26, and the test set-up photograph and over-
lay of Figure 27. The elements are supplied with the
required power and are allowed to warm up. All signal
inputs to the servo amplifier are short circuited and
the current output to the torque motor is observed
on the two milliammeters in the circuit of the torque
motor polarizing coils. If the differential reading
is not zero, the servo amplifier balance is adjusted
to give this desired condition. See Figure 12 for the
location of the servo amplifier balance.

After balancing the output of the servo
amplifier, the short across the servo amplifier input
terminals is disconnected and the output from the
potentiometer is reconnected to the servo amplifier.
The balance of the servo amplifier should be checked
from time to time to avoid the effect of drift that
may be encountered.

The variable speed D.C. motor used to drive
the autosyn and resolver is varied in speed from about
0.5 to 25.0 cycles per second. A rough indication of
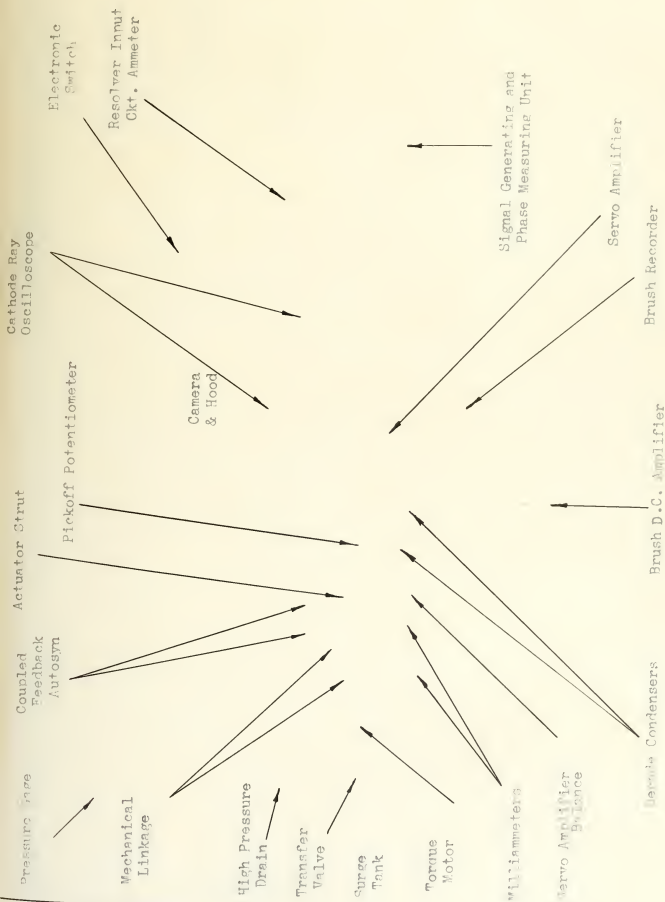
Fig. 20. Overlay to the Photograph of the Test Set-Up for the Servo Amplifier Dynamic Test.

Pressure Gage

Mechanical Linkage

High Pressure Drain

Transfer Valve

Surge Tank

Torque Motor

Milliammeters

Servo Amplifier Balance

Sample Condensers

Coupled Feedback Autosyn

Actuator Strut

Pickoff Potentiometer

Electronic Switch

Resolver Input Ckt. Ammeter

Cathode Ray Oscilloscope

Camera & Hood

Signal Generating and Phase Measuring Unit

Servo Amplifier

Brush Recorder

Brush D.C. Amplifier
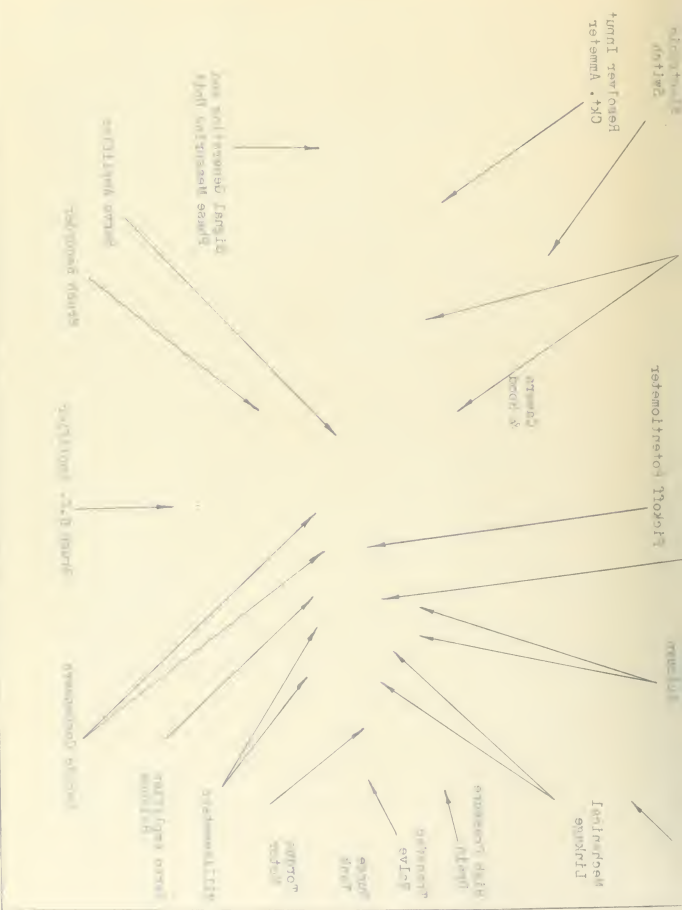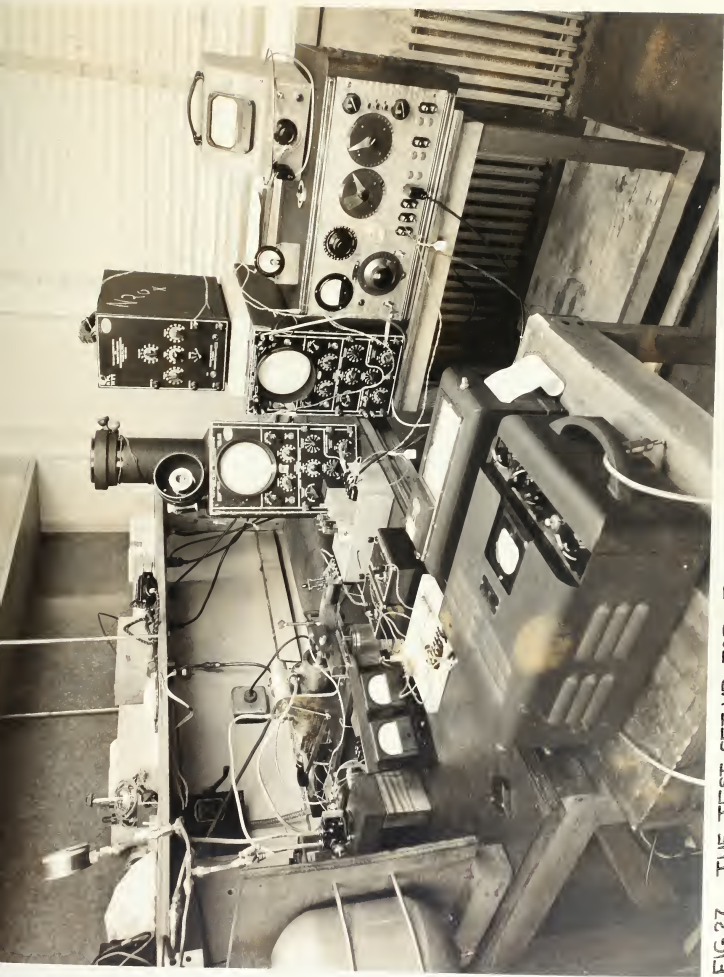
FIG. 27. THE TEST SET-UP FOR THE DYNAMIC TEST OF THE SERVO AMPLIFIER.

the speed setting is given by a tachometer, which
is built into the signal generating unit. The more
accurate input signal frequency is obtained from the
Brush recorder record as shown in Figure 28. The
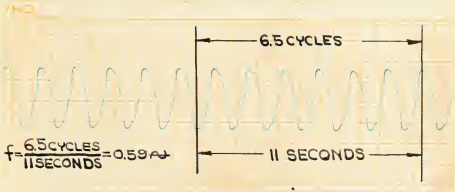
Fig. 28. Brush Recorder Record of Input Signal Frequency.

number of cycles and the elapsed time are measured from
the recorder tape to obtain the signal input frequency
in cycles per second. At each selected frequency of
input signal, the Lissajou figure on the cathode ray
tube was observed. The output signal lags the input
signal of the amplifier by a greater and greater angle
as the frequency of the input signal is increased.

When the two signals are 90 degrees out of
phase, the Lissajou figure $\underline{10/}$ becomes a circle, while,
when the signals are inphase, the circle closes to a
straight line. These conditions are indicated in the
photographs of Figure 29, 30 and 31. In all Lissajou
figure photographs, the output signal was applied to

the "y" axis, and the input signal was applied to the
"x" axis.

Fig. 29. Lissajou Figure with Input and Output 90
Degrees Out of Phase at a Signal Frequency of 20
Cycles per Second and with Low Gain on the "x" Axis.

With the movable body and attached dial, the
input signal of the autosyn pair may be advanced any
number of degrees to lead the resolver signal by a
known fixed phase, as read from the autosyn phase
dial. Thus, the autosyn output signal to the servo
amplifier is caused to lead the resolver signal. If

Fig. 30. Lissajou Figure with Input and Output 90 Degrees Out of Phase at a Signal Frequency of 20 Cycles per Second and with High Gain on the "x" axis.

Fig. 31. Lissajou Figure with Input and Output Signals in Phase at a Signal Frequency of 20 Cycles per Second and a High Gain of the "x" axis.

the autosyn signal is advanced by an amount equal to the phase lag in the servo amplifier, the servo amplifier output signal will be inphase with the resolver signal. The resulting Lissajou figure will be a straight line under these conditions.

Now there is at hand a system for determining the servo amplifier phase lag. At each selected frequency (ranging from 0.5 to 25 cycles per second), of the input signal, the phase dial is adjusted to give a Lissajou figure which is a straight line. The phase lag is thus read directly from the phase dial in degrees. Therewith, the necessary data for the phase lag in degrees and the frequency of the input signal in cycles per second, is obtained.

The previously described test procedure was repeated for the servo amplifier with five different values of the condenser pairs in the filter feeding the 6AQ5 tubes. See Figure 12, for the location of these condensers. The condenser values selected were 1,2,4, 8, and 12 μ f.

The phase lag data collected from the five runs is given in Table V and the experimental results are illustrated in Figures 32,33,34,35 and 36.

The experimental points fall along the smooth theoretical curve. The frequency at which the 45 degree

TABLE V.   PHASE LAG DATA FOR THE SERVO AMPLIFIER AT VARIOUS
FREQUENCIES WITH VARIOUS CONDENSERS IN THE FILTER FEEDING
THE 6AQ5 TUBES.

| INPUT SIGNAL FREQUENCY | | PHASE LAG IN DEGREES | | | | |
| | | CONDENSER IN FILTER FEEDING 6AQ5 | | | | |
CYCLE/SECOND	RADIANS/SECOND	1μf.	2μf.	4μf.	8μf.	12μf.
23.8	149.5	61.9	75.9	83.0	86.0	87.5
22.95	144.0	60.2	75.2	82.6	86.0	87.0
22.0	138.0	60.7	74.5	82.2	86.0	87.0
21.2	133.0	60.2	73.7	81.9	85.5	87.0
20.25	127.0	58.4	73.0	81.3	85.5	87.0
19.45	122.0	57.3	72.3	80.9	85.0	87.0
18.35	115.2	56.7	71.6	80.4	85.0	86.5
17.5	110.0	55.1	70.8	80.4	84.5	86.0
16.5	103.6	52.9	69.5	79.3	84.0	86.0
15.6	98.0	50.9	68.7	79.1	84.0	85.5
14.5	91.0	49.4	66.9	77.9	84.0	85.0
13.55	82.2	47.6	65.5	77.2	83.5	85.0
12.67	79.6	46.0	63.7	76.3	82.5	84.5
11.7	73.5	43.9	62.2	75.2	82.0	84.0
10.7	67.2	41.0	60.3	74.0	81.5	84.0
9.9	62.2	38.2	57.7	72.3	81.0	83.0
8.73	54.8	34.8	54.7	71.0	80.0	82.0
7.9	49.6	31.3	52.4	68.6	78.5	82.0
6.86	45.1	29.2	48.	65.9	77.5	81.0
5.92	37.2	24.9	43.5	63.9	76.0	80.0
4.97	31.2	21.7	40.5	58.7	73.0	78.5
4.52	28.4	19.4		55.2		
4.06	25.5	18.5	34.3	53.3	70.5	75.5
3.06	22.6	16.3	30.4	49.5		
3.01	18.9	14.6	25.3	45.3	64.0	71.0
2.70	17.0	13.6	23.8	41.3	59.5	69.5
2.17	13.6	8.7	15.0	34.7	54.5	65.0
2.08	13.1				53.0	64.0
1.68	10.5				48.5	59.0
1.53	9.6			26.1	43.5	56.5
1.31	8.2			17.5	40.0	52.0
1.04	6.5				35.0	45.5
.57	3.9				20.0	30.5
.45	3.1					25.0

COMPARISON OF THE PHASE LAG OF AN IDEAL FIRST ORDER TIME DELAY (THEORETICAL) HAVING A TIME CONSTANT OF 12.94 MILLISECONDS AND THE SERVO AMPLIFIER USING A 1 MICROFARAD CONDENSER IN THE FILTER SYSTEM

FIG. 32.

THEORETICAL ————
EXPERIMENTAL o o o o

Louis BAERISWYL JR.
APL/JHU -23FEB,51

PHASE LAG IN DEGREES φ

FREQUENCY IN RADIANS PER SECOND -ω

Comparison of the Phase Lag of an Ideal First Order Time Delay (Theoretical) having a Time Constant of 26.3 Milliseconds and the Servo-Amplifier using a 2 Microfarad Condenser in the Filter System
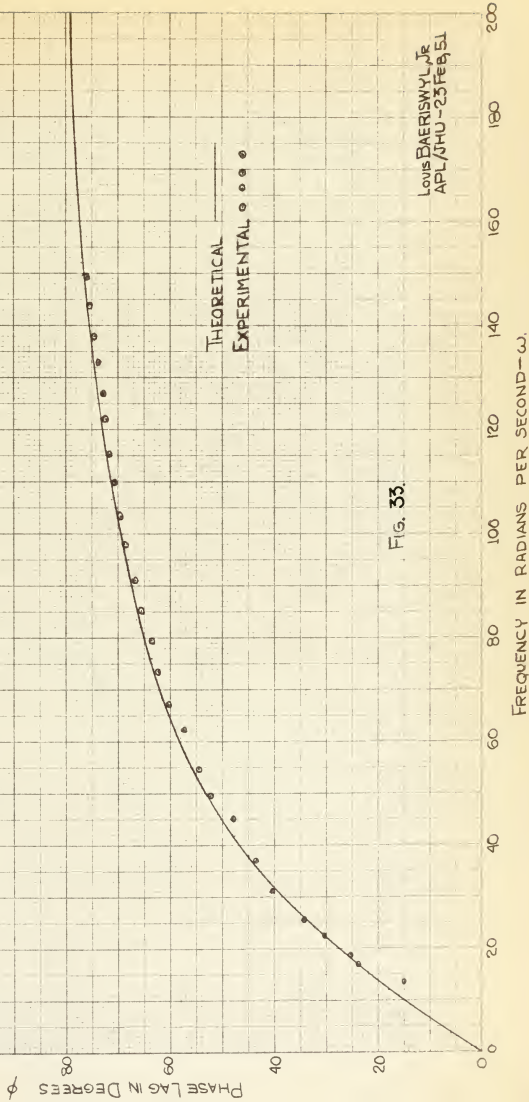
Fig. 33.

THEORETICAL ————
EXPERIMENTAL ⊙ ⊙ ⊙ ⊙

Louis Baeriswyl Jr
APL/JHU—23 Feb, 51

FREQUENCY IN RADIANS PER SECOND—ω.

PHASE LAG IN DEGREES φ

COMPARISON OF THE PHASE LAG OF AN IDEAL FIRST ORDER TIME DELAY (THEORETICAL) HAVING A TIME CONSTANT OF 52.6 MILLISECOND AND THE SERVO-AMPLIFIER USING A 4 MICROFARAD CONDENSER IN THE FILTER SYSTEM
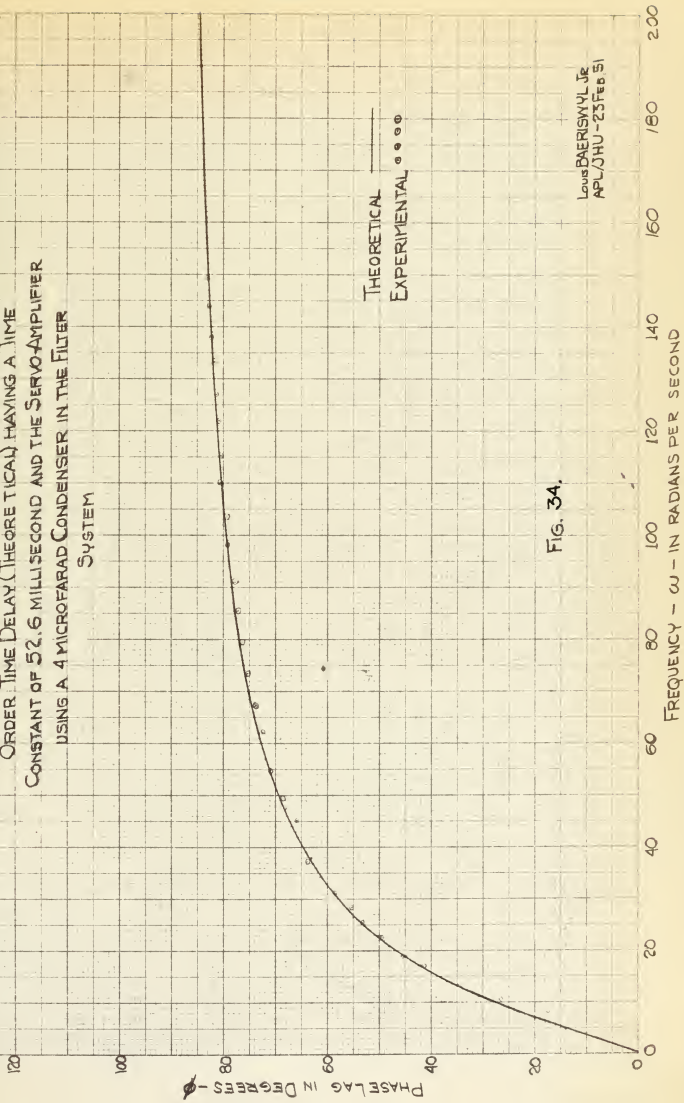
THEORETICAL ———
EXPERIMENTAL o o o o

FIG. 34.

Louis BAERISWYL JR
APL/JHU-25 FEB 51

FREQUENCY - ω - IN RADIANS PER SECOND

PHASE LAG IN DEGREES - φ

COMPARISON OF THE PHASE LAG OF AN IDEAL FIRST ORDER TIME DELAY (THEORETICAL) HAVING A TIME CONSTANT OF 104.5 MILLISECONDS AND THE SERVO AMPLIFIER USING AN 8 MICROFARAD CONDENSER IN THE FILTER SYSTEM
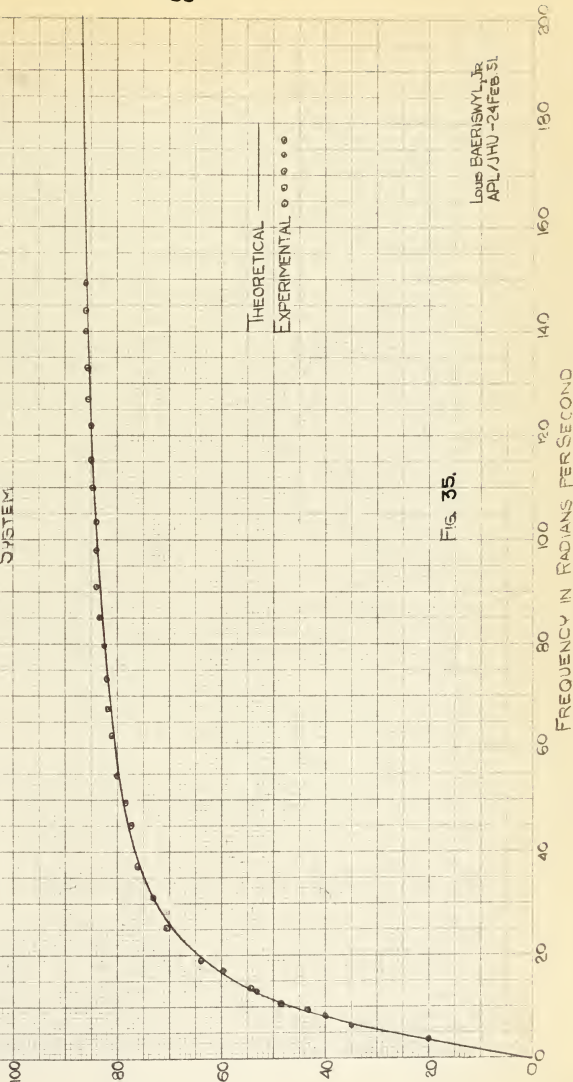
FIG. 35.

THEORETICAL ———
EXPERIMENTAL ∘∘∘∘∘

LOUIS BAERISWYL JR
APL/JHU – 24 FEB 51

FREQUENCY IN RADIANS PER SECOND

ϕ – PHASE LAG IN DEGREES

COMPARISON OF THE PHASE LAG OF AN IDEAL FIRST ORDER TIME DELAY (THEORETICAL) HAVING A TIME CONSTANT OF 15.3 MILLISECONDS AND THE SERVO AMPLIFIER USING A 12 MICROFARAD CONDENSER IN THE FILTER SYSTEM.

FIG. 36.

Louis BAERISWYL JR
APL/JHU—24 FEB. 51

THEORETICAL
EXPERIMENTAL

PHASE LAG IN DEGREES φ

FREQUENCY IN RADIANS PER SECOND
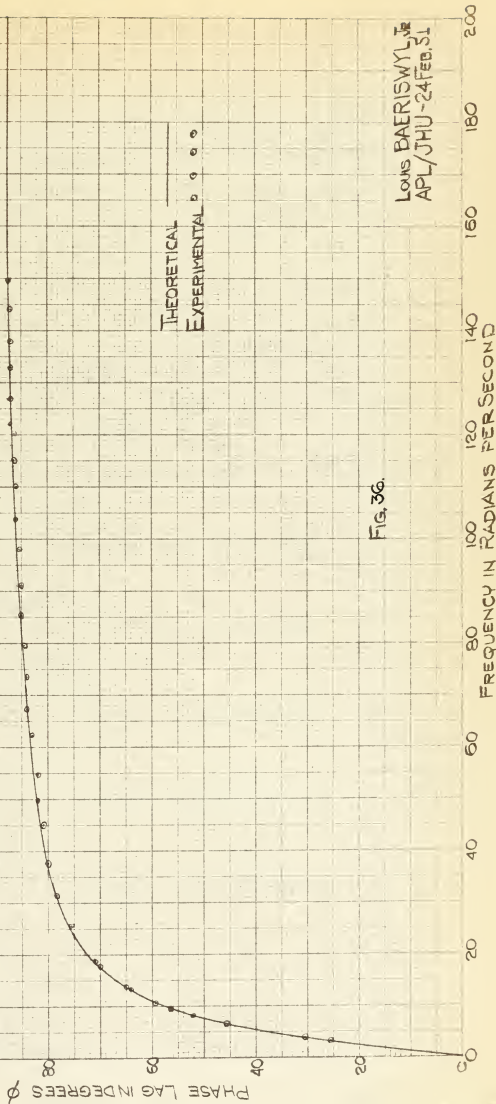
phase lag occurred was noted for each of the five runs.
The reciprocal of the corresponding angular frequency
at each 45 degree phase lag was determined and used as
a basis for establishing the time constant of the servo
amplifier[1] under the five filter conditions.

$$\omega_c = 2\pi f_c$$

$$\tau = \frac{1}{\omega_c}$$

where: f_c = the frequency at which the 45° phase lag
occurred.

ω_c = the angular frequency at which the 45° phase
lag occurred.

τ = the amplifier time constant in seconds.

Using $1 \mu f$ condenser,

$$\tau_1 = \frac{1}{2\pi(12.3)} = 12.94 \text{ milliseconds.}$$

$2 \mu f$ condenser,

$$\tau_2 = \frac{1}{2\pi(6.06)} = 26.3 \text{ milliseconds.}$$

$4 \mu f$ condenser,

$$\tau_3 = \frac{1}{2\pi(3.03)} = 52.6 \text{ milliseconds.}$$

$8 \mu f$ condenser,

$$\tau_4 = \frac{1}{2\pi(1.525)} = 104.5 \text{ milliseconds.}$$

$12 \mu f$ condenser,

$$\tau_5 = \frac{1}{2\pi(1.012)} = 157.3 \text{ milliseconds.}$$

Based on the five experimental time constants, theoretical first order systems curves were superimposed on the experimental characteristic phase points, (Figures 32, 33, 34, 35 and 36). These theoretical curves are based on a transfer function of:

$$KG(j\omega) = \frac{1}{\Upsilon(j\omega) + 1}$$

The theoretical first order phase lag was computed directly from a normalized curve prepared at the Massachusetts Institute of Technology and shown in Appendix B.

It is to be noted that the agreement between the experimental and theoretical curves is extremely good, indicating that the assumed first order condition of the servo amplifier is valid for the frequency range considered.

Further, note might well be made that the amplifier time constant is a linear function of the condenser capacity used in the filter circuit feeding the 6AQ5 tubes. This follows from simple time delay theory [11/] for an RC filter network, where Υ = RC. Thus, doubling the condenser capacity of the filter doubles the time constant of the servo amplifier. Only the 4, 8 and 12 μf condensers are used in the final system analysis.

2.2. Torque Motor.
i. Static Test.

The static test was conducted

on the Curtiss Wright linear high speed polarized torque motor in order to verify the assumption that the output displacement of the motor armature was a linear function of the input differential current to the motor armature polarizing coils. The test was also conducted to determine the range of linearity of the output displacement with respect to the input differential current signal and to determine the gain of the torque motor from the slope of the static torque motor test curve.

The torque motor was connected to the amplifier and coupled to the transfer valve, the transfer valve and torque motor being connected through a coupling wire. The torque motor coupled to the transfer valve is shown in the photograph of Figure 13. The schematic drawing of the static test set-up for the torque motor is shown in Figure 37.
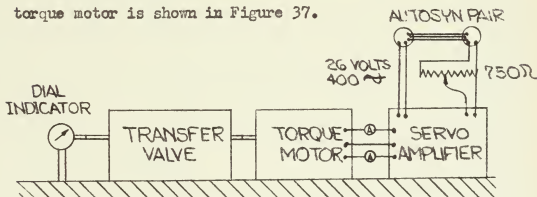
Fig. 37. Schematic Drawing of the Static Test Set-Up for the Torque Motor.

The servo amplifier was connected to the torque motor through two milliammeters. The torque motor armature was coupled to the transfer valve. No hydraulic pressure was applied to the transfer valve. A dial indicator was placed against the valvespool of the transfer valve. Thus, the torque motor armature motion was transmitted to the dial indicator through the valvespool. The transfer valve body and torque motor body are firmly connected. So that there would be no motion between the dial indicator and the torque motor, the dial indicator was also firmly attached to the motor and valve.

The signal input terminals to the servo amplifier were shorted. After the amplifier had sufficient time to warm up, the servo amplifier balance was adjusted so that both milliammeter readings were equal. Next the input terminals to the amplifier were connected to an autosyn pair through a 750 ohm resistor. The autosyns $\frac{4 \& 5}{}$ were connected in the prescribed manner and were excited by a 26 volt, 400 cycle per second signal.

For each data collecting setting, one autosyn rotor was rotated to give the desired differential current. The differential current was progressively

increased with the differential current and the arma-
ture displacement being recorded at each particular
setting, until a differential current of about +80
milliamperes was obtained. From this value, the
differential current was progressively decreased to
about -80 milliamperes and finally increased to the
original balanced condition. The data collected is
given in Table VI and plotted in Figure 38.

The curve obtained is in the form of a
hysteresis loop. The slope of this curve is nearly
linear over a range of ±30 milliamperes, while a
saturation value is approached near ±80 milliamperes.
If the mean of the two sides of the experimental curve
were drawn, it would fall on top of the assumed linear
relation for the range over which the hysteresis loop
is linear. Thus, for a limited range of differential
current, the mean value of the experimental data gives
good agreement with the assumed linear relation. The
slope of the mean experimental data in the range of
linearity is 0.00065 inches/milliampere which value is
the gain constant for the torque motor. The dead space
at zero differential current is 0.0033 inches. This is
a relatively small value which was obtained by conducting
the above procedure on four torque motors, Serials 12,
14, 15 and 18, and selecting the torque motor with the
smallest dead space, i.e., Serial 15.

TABLE VI. STATIC CHARACTERISTIC OF THE CURTISS LINEAR
HIGH SPEED TORQUE MOTOR SERIAL NO. 15.

i_1	i_2	Δi	Displace-ment	i_1	i_2	Δi	Displace-ment
Milliamperes			In Inches	Milliamperes			In Inches
31.5	31.5	0.	0				
1.0	77.	76.	0				
2.	70.	68.	.0007	1.	78.	77.	-.0007
4.	63.5	59.5	.0018	2.	71.	69.	+.0007
6.	59.5	53.5	.0028	4.	64.5	60.5	.0022
8.	56.0	48.	.0040	6.	60.5	53.5	.0037
10.	53.	43.	.0055	8.	57.	49.	.0061
12.	50.5	38.5	.0072	10.	53.	43.	.0082
14.	48.	34.	.0101	12.	51.	39.	.0096
16.	46.5	30.5	.0113	14.	49.	35.	.0117
18.	45.	27.	.0138	16.	46.	30.	.0147
20.	42.5	22.5	.0158	18.	44.	26.	.0174
22.	41.	19.	.0183	20.	42.5	22.5	.0194
24.	39.	15.	.0215	22.	40.	18.	.0222
26.	37.	11.	.0233	24.	37.5	13.5	.0248
28.	35.	7.	.0260	26.	37.	11.	.0262
30.	34.	4.	.0283	28.	35.	7.	.0297
32.	32.	0.	.0307	30.	33.	3.	.0323
34.5	30.	- 4.5	.0338	34.	30.	- 4.	.0373
37.5	28.	- 9.5	.0377	37.	28.	- 9.	.0404
39.5	26.	-13.5	.0402	39.	26.	- 13.	.0432
42.5	24.	-18.5	.0426	42.	24.	- 18.	.0457
45.	22.	-23.	.0452	44.5	22.	- 22.5	.0489
48.	20.	-28.	.0482	47.	20.	- 27.	.0511
51.	18.	-33.	.0510	50.	18.	- 32.	.0540
53.5	16.	-37.5	.0534	53.	16.	- 37.	.0561
56.5	14.	-42.5	.0560	55.5	14.	- 41.5	.0580
60.	12.	-48.	.0585	58.	12.	- 46.	.0596
64.	10.	-54.	.0607	62.5	10.	- 52.5	.0625
68.	8.	-60.	.0625	67.	8.	- 59.	.0633
75.	6.	-69.	.0638	74.	4.	- 70.	.0647
83.	4.	-79.	.0660				

CALIBRATION CURVE OF THE
CURTISS LINEAR TORQUE MOTOR FOR
Serial #15

SLOPE = $\frac{0.0065 \text{ in}}{100 \text{ ma}}$

$K_3 = 0.000065$ inches/milliampere

DEAD SPACE = 0.0035 inches

FIG. 38

Louis BAERISWYL, Jr.
APL/JHU
16 AUGUST, 1950

DIFFERENTIAL CURRENT IN MILLIAMPERES

DEFLECTION IN HUNDREDTHS OF AN INCH

- 74 -
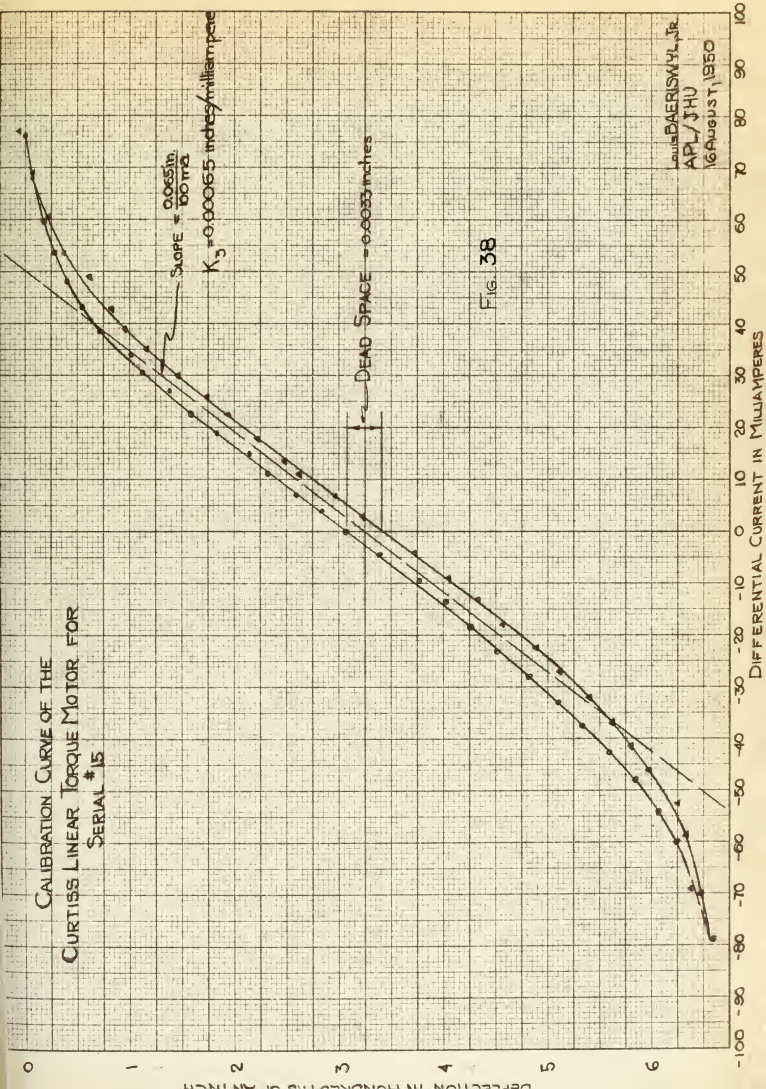
ii. Dynamic Characteristics.

No dynamic tests were conducted
on the torque motor by this author. However, the
Curtiss Wright Aviation Corporation supplied the
dynamic test data shown in Table VII with Serial No.
15. This data is plotted in Figure 39. The 45 degree
phase lag for the torque motor occurs at a frequency
46.7 cycles per second. It is to be particularly
noted that this is a relatively high corner frequency.
For a first order time delay this corner frequency
would correspond to a time delay of 3.42 milliseconds.
A theoretical first order time delay phase curve with
a time constant 3.42 is also drawn on Figure 39 from
Appendix B.

The Curtiss Wright data does not lend itself
well to the drawing of a uniform curve through the
experimental points. The phase lag seems to be a
linear function of frequency up to about 140 cycles
per second. At this frequency a leveling that might
be expected from a second order system occurs, followed
at still higher frequencies by phase lags that increase
beyond 180°.

The assumed condition of Part 3, Section II
was that the motor had zero time delay. While this
assumption is not experimentally valid, certain approxi-
mation may prove interesting. Since the time constant

of the motor is 3.42 milliseconds, while the time
constant of the amplifier used in the closed loop
test is 52.6, 104.5 and 157.3 milliseconds, the
motor time constant will have only a small effect on
the closed loop phase lag at low frequencies. Thus,
on the basis of the relatively small torque motor
time constant, it may be assumed that there is no
effective time delay due to the torque motor for low
frequency signals.

The assumed condition, as given in Part 4,
Section II, is found to be in closer agreement with
the experimental results than that of Part 3. A
comparison of the theoretical first order delay phase
lag curve of time constant 3.42 milliseconds and the experi-
mental curve as shown in Figure 39, indicate that for
frequencies up to 50 cycles per second, there is not
more than 3 degrees of phase lag difference between the
experimental and theoretical curves.

Thus, the assumptions that the torque motor
is a first order delay phase lag as given in Part 4,
Section II is supported over a limited frequency range.
In regard to certain work to follow where the torque
motor is assumed to have a first order time delay, a time
constant of 3.4 milliseconds will be applied to the
torque motor. This assumption would appear to be parti-
cularly valid as the frequencies in the closed loop test

TABLE VII. DYNAMIC CHARACTERISTICS OF THE CURTISS
LINEAR HIGH SPEED MOTOR FOR A CONSTANT CURRENT INPUT ·
TO MOTOR OF .029 AMPS.

FREQUENCY (CPS)	AMPLITUDE (INCHES) PEAK TO PEAK	PHASE SHIFT DEGREES
20	.032	21
40	.034	39
60	.034	54
80	.035	86
100	.035	98
120	.034	119
140	.034	136
160	.032	154
180	.027	160
200	.031	163
220	.032	171
230	.035	176
240	.034	215
260	.016	225

PHASE LAG CHARACTERISTICS OF THE CURTISS WRIGHT HIGH SPEED LINEAR TORQUE MOTOR

FIG. 39.

Louis BAERSWYL, Jr.
APL-JHU. 3 APR 51

EXPERIMENTAL

FOR A FIRST ORDER TIME DELAY OF 3.42 MILLISECONDS.

$f_c = 46.1 \sim$

FREQUENCY IN CYCLES PER SECOND

PHASE LAG IN DEGREES
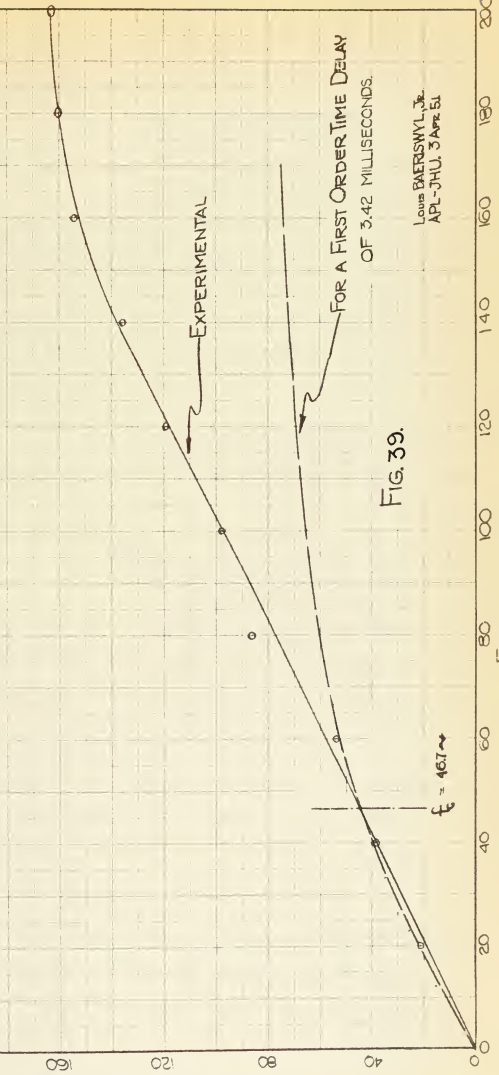
do not exceed 25 cycles per second.

2.3. Transfer Valve and Actuator.

i. Static Test.

The transfer valve and actuator
are considered together, as by so handling the static
characteristic, the need of measuring the rate of oil
flow from the transfer valve to the actuator is avoided.
This quantity would be difficult to measure with the
same degree of accuracy which other inputs and outputs
are measured.

For the static condition the output velocity
of the actuator may be mathematically expressed as:

$$V = \frac{R}{A}$$

where

V = actuator velocity in inches
per second,

R = rate of oil flow in cubic
inches per second,

A = piston area in inches.

If the given formula is assumed to be correct,
it follows directly that the actuator velocity is a
linear function of the oil flow rate into the actuator.
Since the piston area is 3 square inches, the assumed
gain will be,

$$K = \frac{V}{R} = \frac{V}{AV} = \frac{1}{3in.^2}$$

To determine the desired static characteristic,
the components are connected, as shown in Figure 40.
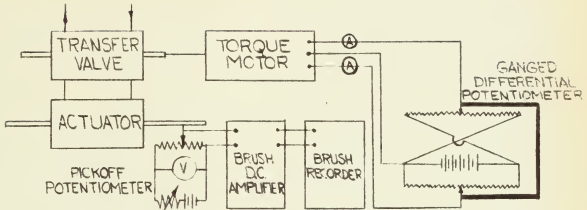
Fig. 40. Static Test Set-Up for the Transfer Valve and the Actuator.

A differentially ganged potentiometer was excited by means of several series connected dry cells and this was used to supply a differential current to the torque motor polarizing coil windings. Two milliammeters are connected in the polarizing coil circuits to measure the differential current to the torque motor. The motor armature, in turn, was connected to the transfer valvespool through a connecting wire or linkage. The end of this connecting wire was threaded and screwed into an extension on the torque motor armature where it could be locked in place by a locking screw. These interconnecting parts are clearly shown in the photograph of Figure 13.

It is necessary to zero to the transfer valve with respect to the torque motor. This is

accomplished by screwing connecting wire into the
armature extension to such an extent that a differ-
ential current of equal magnitude and opposite sign
cause the actuator to move at the same velocity, but
in opposite directions. Screwing the connecting wire
into the armature simply relocates the valvespool
zero position with respect to the internal valve
faces. The measuring of the velocity of the actuator
output velocity is described in another paragraph in
this part of this section.

While the above described method is simple
to understand, it is difficult to perform as it is
a "cut and try" system of zeroing. The difficulty is
increased by the fact that a very small angle of rota-
tion of the connecting wire greatly alters the transfer
valve flow rate. After considerable time, the transfer
valve and torque motors were zeroed to within $1\frac{1}{4}$
milliamperes of differential current.

The pickoff potentiometer was fed through
a variable resistor that was excited by two $4\frac{1}{2}$ volt
dry cells connected in series. The variable resistor
is adjusted to give a five volt drop across the pickoff
potentiometer as measured by the connected voltmeter.
As the actuator strut moves through a full stroke, the

pickoff voltage varies uniformly. The pickoff
voltage signal used as an input to the Brush re-
corder is fed through the Brush D.C. amplifier.

The recording tape records the varying
voltage signal as a function of time and enables the
velocity of the actuator to be calculated in volts
per second. A sample of such a tape recording is
shown in Figure 41.
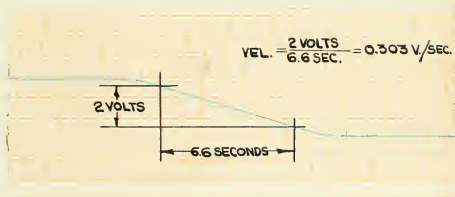
Fig. 41. Sample Brush Recorder Tape Record of the
Actuator Velocity.

So that the velocity of the actuator could
be expressed in inches per second, the linear potentio-
meter pickoff was calibrated. 12 volts were applied
across the 8000 ohm potentiometer, and at 0.25 inch
intervals along the potentiometer, the pickoff voltage
was recorded. These collected data are shown in Table
VIII and are plotted in Figure 42. Figure 42 indicates
that the potentiometer has linear characteristics.
The voltage to displacement ratio is 1.785 volts per

inch when there is a 12 volt drop though the potentio-
meter. As only 5 volts were impressed across the
potentiometer to determine the actuator velocity, the
voltage-to-displacement ratio is (1.785)(5/12) volts/
inch = 0.743 volts/inch. Thus, the actuator velocity
expressed as 0.743 volts/sec is equivalent to 1.0 inches/
second.

　　　　The actuator was connected to the transfer
valve in the normal manner and for each test run per-
formed the initial accumulator pressure was 1000 psi.
The ganged potentiometer was moved from its balanced
position causing a differential current to flow. This
current was determined from the readings of the two
milliammeters in the torque motor polarizing coil cir-
cuit. The actuator velocity was determined from the
voltage change that occurred in a measured time interval
as recorded by the Brush recorder. The above collected
data are recorded in Table IX and plotted in Figure 43.
The static torque motor characteristic having been shown
to be approximately linear over a limited input signal
range and the actuator static characteristic based on
$V = \dot{H}_A$ having been assumed to be linear, it may be con-
cluded that the shape of the experimental curve of
Figure 43 is due to the transfer valve. The experi-
mental curve shape may be explained on the bases of
the design of the transfer valve.

TABLE VIII.   CALIBRATION DATA FOR THE PICKOFF
POTENTIOMETER.

RELATIVE POSITION IN INCHES	ELECTRICAL OUTPUT IN VOLTS	
10.50	0.	
10.25	.45	
10.00	.92	
9.75	1.34	
9.50	1.80	
9.25	2.20	
9.00	2.67	
8.75	3.15	3.10
8.50	3.55	3.55
8.25	4.00	4.00
8.00	4.42	4.50
7.75	4.90	4.92
7.50	5.33	5.40
7.25	5.80	
7.00		6.27
6.75	6.70	

Fig. 42.

POTENTIOMETER
Voltage vs. Displacement
for output amplitude pickoff

SLOPE = 1.785 VOLTS/INCH

Louis BAERISWYL JR.
APL/JHU-7 MARCH 51

LINEAR POTENTIOMETER DISPLACEMENT IN INCHES

POTENTIOMETER PICKOFF VOLTAGE - D.C. VOLTS

TABLE IX.   COMBINED STATIC CHARACTERISTIC DATA FOR
THE TORQUE MOTOR, TRANSFER VALVE AND ACTUATOR.

i_1	i_2	Δi	Actuator Velocity
Current in Milliamperes			in Volts per Second
6.	60.	54.	1.89
8.	56.	48.	1.75
11.	53.	42.	1.63
12.	50.	38.	1.36
14.	48.	34.	1.25
16.	46.	30.	1.06
17.	44.	27.	.94
19.	42.	23.	.77
21.	40.	19.	.56
23.5	38.	14.5	.32
25.5	36.	10.5	.091
28.	34.	6.	.012
30.	32.	2.	.015
32.	30.	- 2.	- .019
34.	28.	- 6.	- .085
37.	27.	-10.	- .32
38.	24.5	-13.5	- .44
40.	23.	-17.	- .64
42.	21.	-21.	- .81
44.	20.	-24.	- .97
46.	18.	-28.	- 1.11
48.	16.	-32.	- 1.28
50.	14.	-36.	- 1.41
53.	12.	-41.	- 1.60
56.	10.	-46.	- 1.80
60.	8.	-52.	- 1.97

COMBINED STATIC CHARACTERISTICS
OF THE TORQUE MOTOR,
TRANSFER VALVE, AND
ACTUATOR.

ASSUMED LINEAR CONDITION
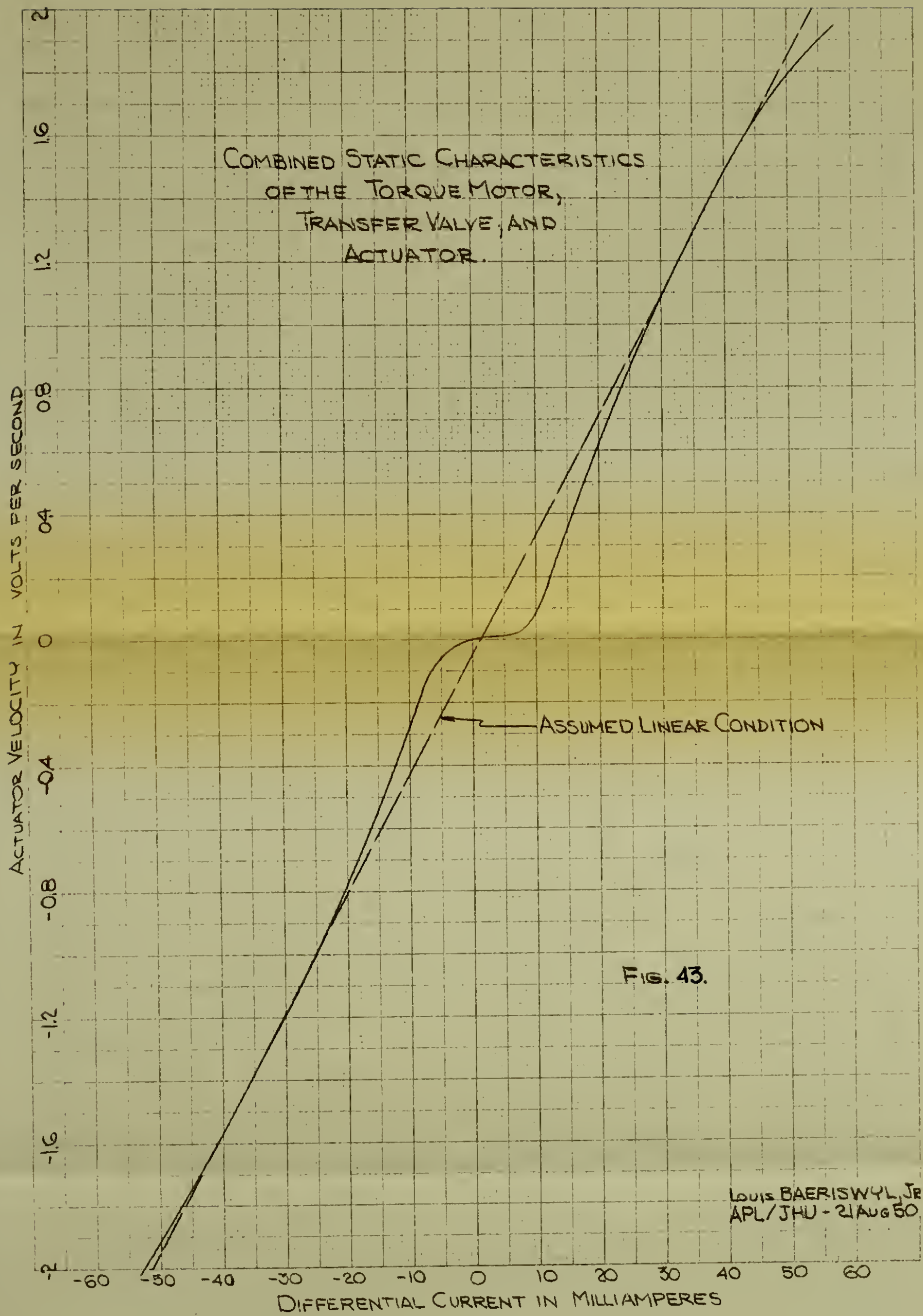
FIG. 43.

LOUIS BAERISWYL, JR
APL/JHU - 21 AUG 50.

ACTUATOR VELOCITY IN VOLTS PER SECOND

DIFFERENTIAL CURRENT IN MILLIAMPERES

In the region of ± 5 milliamperes of differential current the curve has a small positive slope. This condition occurs due to the fact that the valvespool must extend a small amount beyond the internal valvefaces to prevent oil from leaking from the accumulator when the valve is in the zero position. The slight movement of the valvespool, when at the zero position, that is possible before oil flow occurs, is commonly termed as "dead space". Two transfer valves were checked with regard to minimum dead space and the one here employed, Serial 3, was found to be markedly superior.

Further, it is to be noted that the experimental curve is symmetrical with respect to the straight line labeled "Assumed Linear Condition". This is another feature of good transfer valve design. The straight line, however, falls to the right of the zero differential current position, indicating the torque motor and transfer valve are not perfectly zeroed. The results indicate the zeroing adjustment is within $1\frac{1}{4}$ milliamperes of differential current, which may be regarded as an excellent zeroing.

From Figure 43 it is seen that for the range of ± 50 milliamperes, the assumed and experimental results correspond closely except in the limited dead

space region. Beyond ±50 milliamperes of differential
current, saturation effects appear to start.

ii.Dynamic Characteristics.

No dynamic characteristics
were obtained on the transfer valve or actuator. It
is felt that a small delay may occur in these compon-
ents due to the slight compressibility of the oil under
operating pressures. It is believed that any time
delays here encountered will be so small as to have
little effect on the closed loop response for the
frequency range employed in this experiment.

24. Mechanical Linkage.

i. Static Characteristics.

The mechanical linkage is shown in the
photograph of Figure 13. A schematic operating
drawing of the linkage is shown in Figure 44. This
figure was used as the basis for determining the
static linkage characteristics. The mechanical link-
age schematic is drawn to full scale. The position
directly under the arm pivot is taken as the zero rota-
tion position. The rotating arm of the schematic is
calibrated to ±40 degrees at 5 degree intervals.
With the arm of the rotating member in the zero posi-
tion, the end of the linear displacement arm is taken
as being in the zero displacement position. The end
position of the linear displacement arm for each

rotation position of the rotating member is indicated
by the linearized rotation scale on Figure 44. The
displacement scale is located below the linearized
rotation scale.

The displacement in inches for each angular
position taken at 5 degree intervals to ±35 degrees
is shown in the table on the graph of Figure 45. The
curve that results is linear between ± 15 degrees.
The graphically determined data of the linear region
is contined beyond the linear region and is indicated
as the assumed linear relation. The slope of this
curve is 15 degrees per inch and indicates the value
of the mechanical linkage gain. Here again for a
limited region, the assumed and determined characteris-
tics are linear.

2.5. Autosyn Pair.

An autosyn pair similar to
those shown in Figure 18 were connected in the pre-
scribed manner 9 & 10/ with one autosyn terminated in
a 750 ohm potentiometer, which is the most desirable
terminating resistance and the values used in the
closed loop system. The autosyn pair was excited
from a 26 volt, 400 cycle per second source. The
rotor of one autosyn was secured in position while
the other could be rotated, with the degrees of rota-
tion being read from the rotating dial connected to
the autosyn rotor.

Schematic of the
Mechanical Linkage Connecting the
Actuator and the Feedback Autosyn with
the Zero Rotation Position Taken as Down
and the Zero Linear Position Taken
as Shown.

Linearized Rotation Scale

-40° -35° -30° -25° -20° -15° -10° -5° 0° 5° 10° 15° 20° 25° 30° 35° 40°

Actuator Displacement in Inches

4"

7.375"

Louis BAERISWYL, Jr
APL/JHU-24 FEB, 51

Fig. 44.
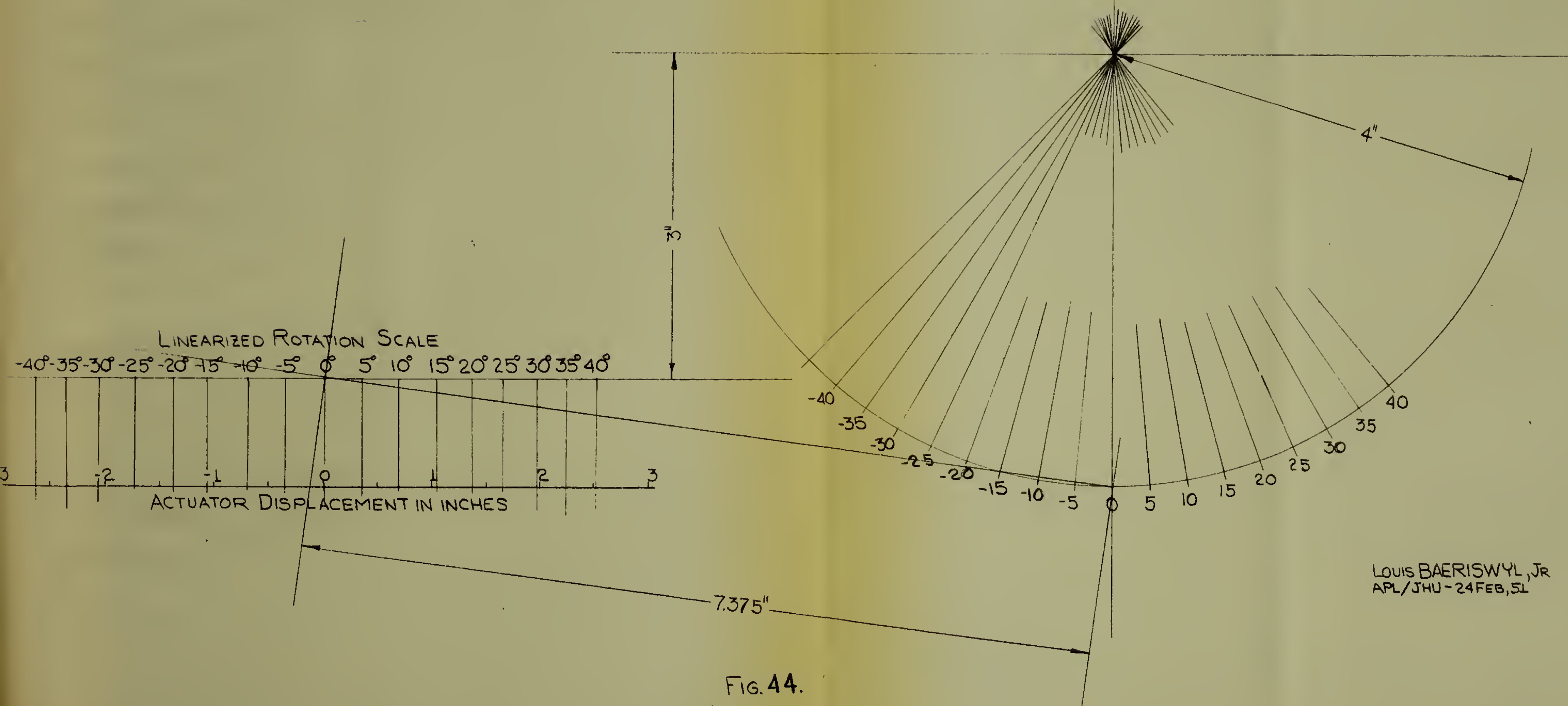
MECHANICAL LINKAGE INPUT
IN INCHES OF ACTUATOR
MOTION VS THE OUTPUT IN DEGREES
OF AUTOSYN ROTATION

SEE MECHANICAL LINKAGE SCHEMATIC
FOR DETAILS AND REFERENCE POSI-
TION. DATA FOR THIS CURVE TAKEN
FROM THE SCHEMATIC

ASSUMED
LINEAR RELATION

K_6 = 15 DEGREES/INCH

AUTOSYN ROTATION IN DEGREES

ACTUATOR DISPLACEMENT IN INCHES

ROTATION IN DEGREES	DISPLACEMENT IN INCHES
35	2.25
30	1.96
25	1.64
20	1.36
15	1.03
10	.68
5	.34
0	.00
-5	.36
-10	.71
-15	1.08
-20	1.40
-25	1.75
-30	2.08
-35	2.37

FIG. 45.

Louis BAERISWYL JR.
APL/JHU-23 Feb,54
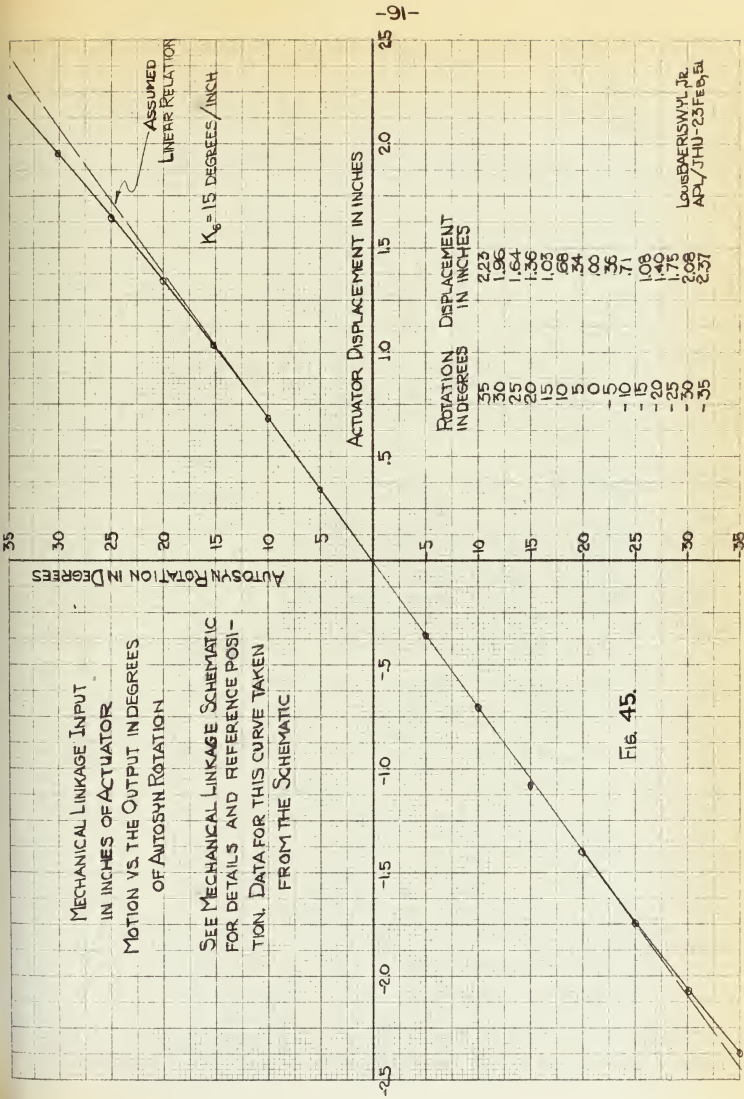
The rotor of the autosyn that was adjustable was varied over 180 degrees with the output voltage being read from the voltmeter at each autosyn rotor position. These values are tabulated in Table X and are plotted for rotor rotation over a range of ± 30 degrees in Figure 46.

From Figure 46 it is noted that the experimental results are linear over a range of ± 15 degrees and thus correspond with the assumed condition. The slope of the experimental curve in the linear region is equal to 0.242 volts per degree.

3. The Connected Closed Loop Servomechanism and Measuring Equipment.

The closed loop servomechanism with the necessary measuring components for determining the system output signal amplitude ratio and phase lag is shown schematically in Figure 47, and is shown by the photograph of Figure 48. The complete schematic drawing of Figure 47 will be examined in three parts: 1. Closed loop servomechanism; 2. Amplitude measuring system; and 3. Phase Lag measuring system.

3.1. The Closed Loop Servomechanism.

The servo amplifier is connected to a 110 volt 400 cycle per second power supply. The servo amplifier output signal is fed to the torque motor polarizing coils through two milliamperes which is used to check the balance of the servo amplifier output. The armature of the

TABLE X.   DATA FROM THE STATIC TEST OF AUTOSYN PAIR
TERMINATED IN A 750 OHM POTENTIOMETER WHEN EXCITED BY
26 VOLTS AT 400 CYCLES PER SECOND.

ROTOR ROTATION IN DEGREES	VOLTAGE OUTPUT IN VOLTS
- 90.	13.50
- 30.	6.70
- 25.	5.75
- 20.	4.67
- 15.	3.55
- 10.	2.36
- 7.5	1.79
- 5.	1.20
- 4.	.94
- 3.	.71
- 2.	.48
- 1.	.22
0.	.04
1.	.28
2.	.55
3.	.72
4.	.93
5.	1.22
7.5	1.75
10.	2.30
15.	3.50
20.	4.55
25.	5.70
30.	6.65
90.	13.50

AUTOSYN ROTATION
in Degrees vs. A.C. Voltage
Output when Input is 26 volts
at 400 cycles per second and where
the Output is terminated
in a 750 OHM Resistor

ASSUMED LINEAR RELATION

$K_7 = 0.242$ volts/degree

OUTPUT VOLTAGE – RMS VOLTS

AUTOSYN ROTATION IN DEGREES
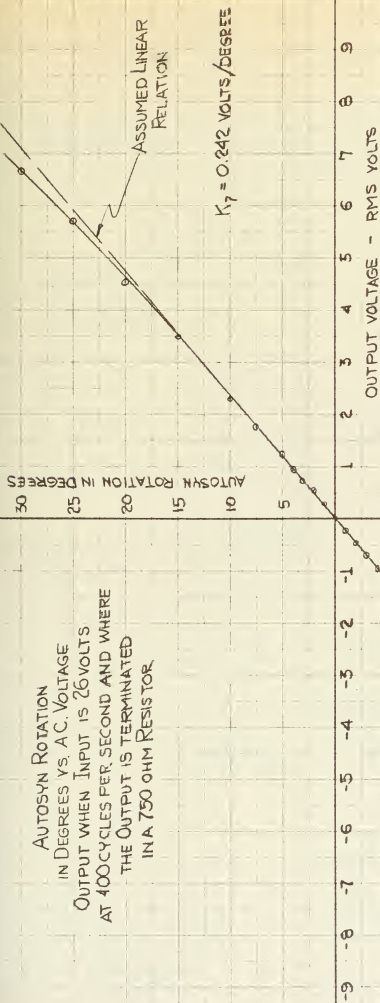
Fig. 46.
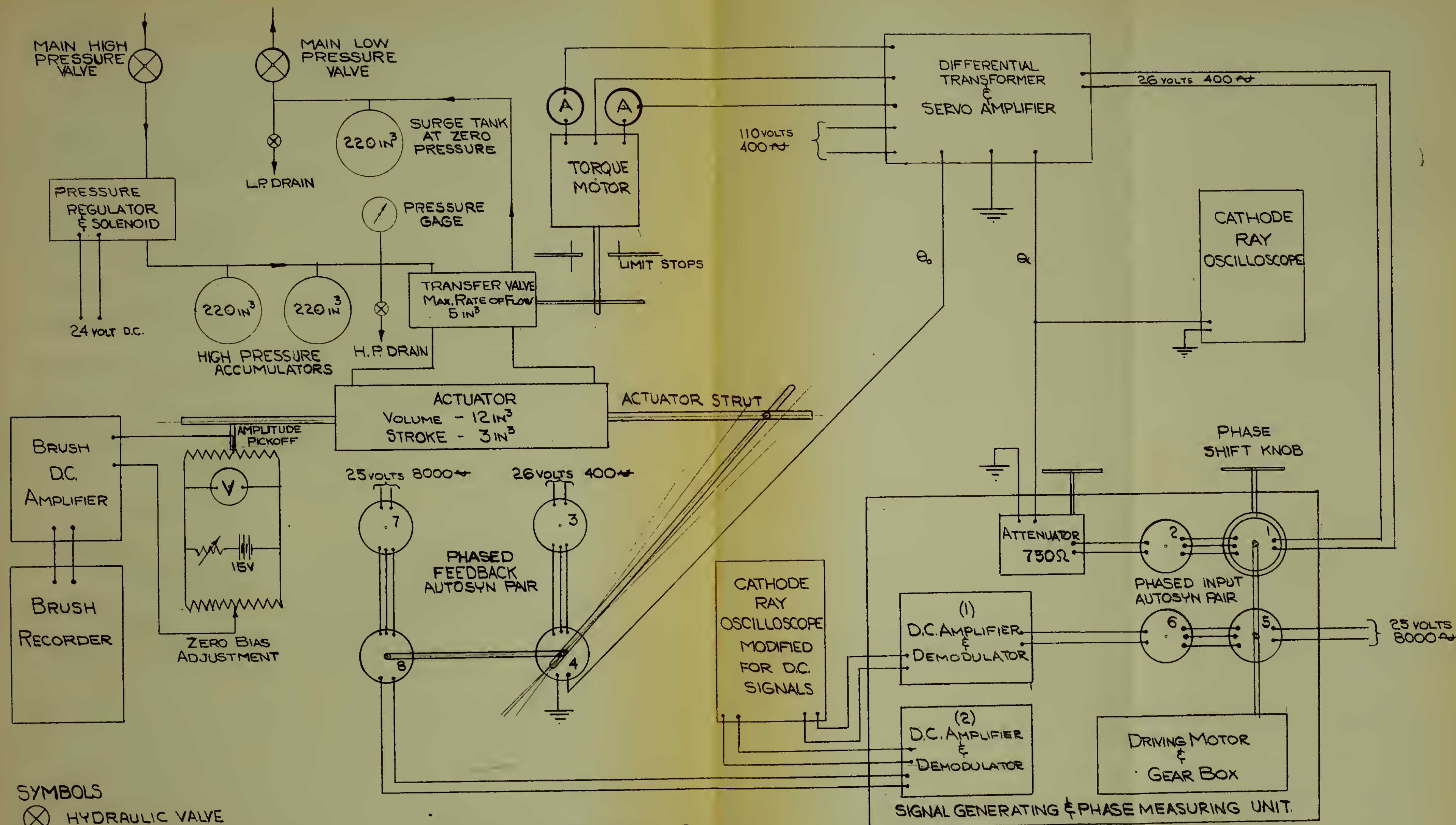
Louis Babriswyl, Jr.
APL/JHU – 7 MARCH 51

EXPERIMENTAL TEST SET-UP SCHEMATIC
FOR DETERMINATION OF THE PHASE LAG
AND AMPLITUDE RATIO OF THE SERVO
SYSTEM

LOUIS BAERISWYL, JR.
APL-JHU —27 MARCH 51

FIG. 47.
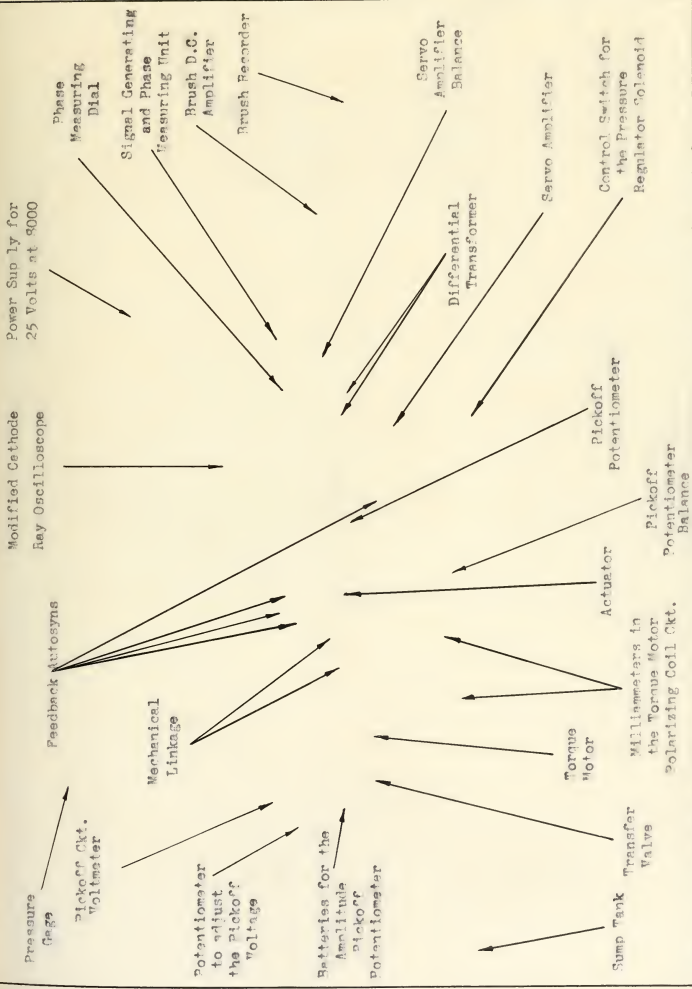
Fig. 43. Overlay to the photograph of the Closed-Loop Servo System with the Measuring Equipment to Determine the Amplitude Ratio and Phase Lag of the Servo System.
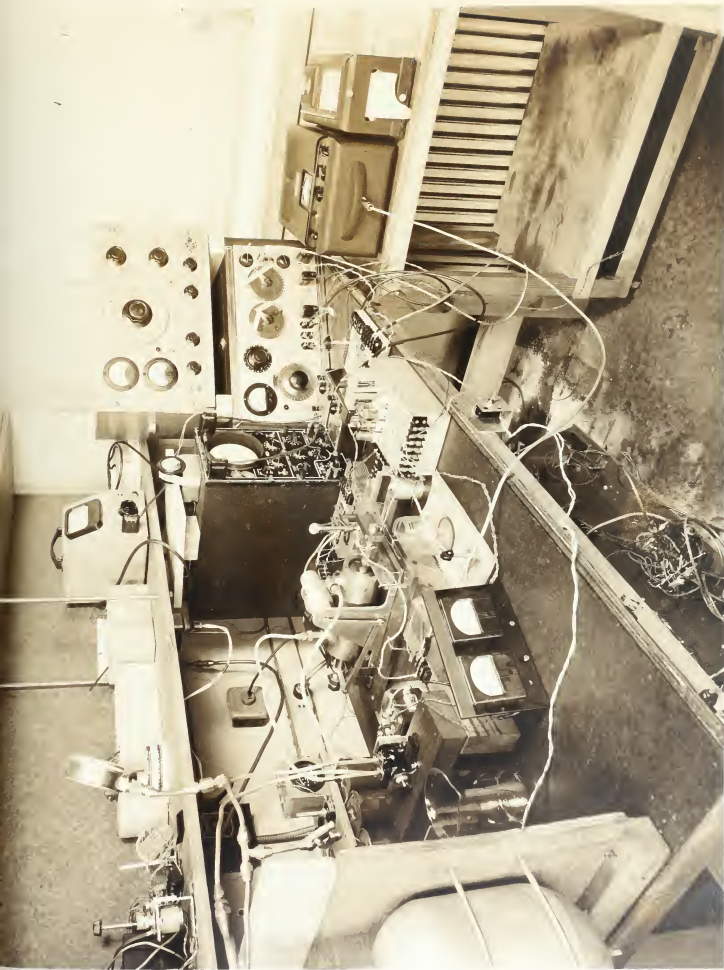
FIG. 48. TEST SET-UP FOR DETERMINING THE SYSTEM AMPLITUDE RATIO & PHASE LAG.

torque motor is connected to the transfer valvespool by
means of a connecting wire which enabled the components
to be balanced, as described in Part 2.3 of Section III.
Thus, displacement of the torque motor armature causes
the valvespool to be moved. The movement of the transfer
valvespool allows oil to flow from the high pressure side
of the hydraulic loop through the transfer valve and into
the actuator. This high pressure oil acts on the actuator
piston, causing it to move and displace the actuator strut
and forcing the oil on the low pressure side of the
actuator to discharge through the transfer valve into the
low pressure side of the hydraulic loop. The hydraulic
loop was fully explained in Part 1.7 of Section III.

The motion of the actuator strut displaces one
arm of the mechanical linkage and causes a second arm to
rotate the rotor of feedback autosyn 4. Feedback autosyn
3 is excited by 26 volts at 400 cycles per second, tapped
from the servo amplifier power transformer. The rotor of
autosyn 3 is rotated and locked in a position such that a
minimum output signal is developed by autosyn 4 when the
actuator strut is at the mid-point of its stroke. Rotation
of the rotor of feedback autosyn 4 caused a modulated 400
cycle per second signal to be fed to the feedback terminals
of the servo amplifier. The feedback signal to the servo
amplifier may be attenuated by means of a 750 ohm potentio-
meter located within the servo amplifier and shown in

Figure 12. Adjustment of this feedback attenuator varies
the gain of the closed loop and is discussed fully in a
later paragraph.

3.2. The Amplitude Measuring System.

The amplitude measuring system is shown
in the lower left hand corner of Figure 47. It consists of
an amplitude pickoff, a linear pickoff potentiometer, a
voltmeter. several dry cells, an attenuating potentiometer,
a bias potentiometer, a D.C. Brush amplifier and a Brush
recorder.

The series connected batteries were connected to
a potentiometer which was adjusted to cause the output
voltage across the combination to be 12 volts. This 12 volt
potential difference was applied to the parallel connected
linear pickoff potentiometer, voltmeter and biasing potentio-
meter. The voltmeter was required to indicate that the
voltage across the linear pickoff potentiometer remained
constant at the selected value. The calibration of this
linear potentiometer was explained in Part 2.3 of Section
III. The biasing potentiometer was employed so that the
potential at the center point about which the pickoff moved
would be zero. This enables the D.C. Brush amplifier to
operate with a higher sensitivity for small displacements of
the amplitude pickoff. The D. C. Brush amplifier may be used
to amplify the pickoff signal when the latter is small. Finally,
the Brush recorder records the amplitude of the pickoff signal
as a function of time on a paper tape.

The amplitude system provides a means for measuring the output amplitude and also an actual measure of the input signal frequency. The frequency data is obtained in the same manner as described and illustrated in Part 2.1 (ii) of Section III.

At low input signal frequencies, the gain of the Brush D.C. amplifier is so adjusted that the Brush recorder pen swings a peak to peak distance of 30 millimeters. As the frequency increases, a small amplitude output increase may initially occur, but this condition soon changes and the output amplitude of the servomechanism decreases with the increasing frequency of the input signal. When the amplitude has decreased to where the recorder pen swings a peak to peak distance on the tape of 3 millimeters, the gain of the Brush D.C. amplifier is increased ten times causing the recorder pen to again swing a peak to peak distance of 30 millimeters on the recording tape. The recorded sinusoidal wave of output amplitude starts to degenerate after it falls below 5 percent of the low frequency amplitude.

At low frequencies, theory predicts that the amplitude ratio will be unity. This was assumed to be the case and thus the amplitude ratio was taken to be the peak to peak distance recorded by the pen in millimeters, divided by thirty or three hundred depending on which gain setting the Brush D.C. amplifier was operating.

The assumed condition of unity amplitude ratio at low frequencies is supported by experimental results

to be introduced later. For a considerable low frequency range, the amplitude signal remains at the assumed unity value as predicted by theory.

3.3. The Phase Lag Measuring System.

The phase lag measuring system consists of three pairs of autosyns, two similar D. C. amplifiers, two similar demodulators and a cathode ray oscilloscope modified for D.C. signals.

Autosyns 5 and 7 are excited by 25 volts at 3000 cycles per second from an audio signal generator. Autosyn 1 is excited by 26 volts at 400 cycles per second, tapped from the servo amplifier power transformer. The rotors of autosyns 1 and 5 are mechanically coupled and can be driven by a variable speed D.C. motor. Autosyn 1 is so constructed that the body of the autosyn may be rotated 360 degrees while its rotor is driven by the variable speed motor. The body of autosyn 1 is rotated by means of a phase shift knob, to which there is connected a dial calibrated in degrees. Initially the phase shift dial is set at zero.

It is next necessary to phase autosyn pairs 1-2 and 5-6. Autosyns 1 and 5 are excited with their respective 400 and 3000 cycle per second signals. The output of autosyns 2 and 6 are connected to an electronic switch 12/ set at a high switching rate. The electronic switch is connected to a cathode ray oscilloscope using a time sweep. If the rotors of 1 and 5 are not driven, there will appear on the cathode

ray tube two traces, with frequencies of 400 and 8000
cycles per second. The rotors of autosyns 2 and 6 are
adjusted so that the amplitude of the traces on the
cathode ray tube are both reduced to a minimum. When
this condition is obtained, the rotors are locked in
place. Then if the rotors of autosyns 1 and 5 are driven
by the variable speed D.C. motor at a constant speed, the
modulated signal traces on the cathode ray tube will be in
phase. The outputs of autosyns 2 and 6 are disconnected
from the electronic switch and connected to the attenuator,
and D.C. amplifier and demodulator (1) respectively, as
shown in Figure 47. The two feedback autosyn pairs 3-4
and 7-8 are phased in the same manner as described above.
Autosyns 4 and 8 have their rotors mechanically coupled.
This is clearly shown in photograph, Figure 48.

The modulated output signal of feedback autosyn
8 is fed to the D.C. amplifier and demodulator (2). The
two amplified and demodulated output signals of the two
D.C. amplifiers and demodulators are applied to the cathode
ray oscilloscope modified for D.C. signals. When these
two signals are sinusoidal, a single loop Lissajou figure
appears on the cathode ray tube. Further, if the two
sinusoidally modulated signals are in phase, the single
loop Lissajou figure closes to a single straight line.[15]

The manner in which the servomechanism phase lag

is determined will now be examined. When the phase
shift knob is set to zero, the modulated signals from
autosyns 2 and 6 are in phase for all dirving speeds.
A phase lag will occur through the closed loop servo-
mechanism and the output modulated signals from autosyns
4 and 8 will lag the input signals by equal angles. If
the phase shift knob of autosyn 1 is rotated so as to
cause the input signal of autosyn 2 to lead the input
signal of autosyn 6 by an amount equal to the phase lag
that occurred in this servomechanism, there results
modulated signals from autosyns 6 and 8 which are inphase.
This inphase condition is easily identified when the
single loop of the Lissajou figure on the cathode ray
tube becomes a straight line. Thus, to determine the
servomechanism phase lag, it is only necessary to turn
the phase shift dial until the Lissajou figure on the
cathode ray tube becomes a straight line. The measured
phase lag is then read directly from the dial face.

To check if there was a difference in phase
lag between the two D.C. amplifiers and demodulators,
these units were fed from autosyns 2 and 6 when both
autosyns 1 and 5 were excited with 25 volts at 8000
cycles per second. The D.C. amplifier - demodulator
outputs as before were connected to the cathode ray
oscilloscope. The rotors of autosyns 1 and 5 were

driven at speeds up to 20 cycles per second and the phase
lag difference between the two D.C. amplifier-demodulator
units was determined for several frequencies by the method
as described above. The collected data is tabulated and
plotted on Figure 49. This difference in phase lag
through the two D.C. amplifier-demodulator units must be
applied to the servomechanism measured phase lag readings,
as read from the phase shift dial, as a correction which
decreases the measured servomechanism phase lag.

    4. Considerations Affecting Selection of
the Magnitude of the Input Signal.

    The simple linear limiting theory of Part 5
of Section II is applied to determine the magnitude of
the maximum input signal to the closed loop system. At
low frequencies the ratio of output to input signal is
unity. The stroke of the actuator, being an easily
measured quantity, will be used at a low frequency input
signal to determine the measurable magnitude of the
input signal.

    It is desirable that the input signal be as
large as possible at all input signal frequencies and yet
at all times be within the linear limited region to avoid
non-linear operation of the servomechanism. A large input
signal is desirable as a correspondingly large output signal
results. With an increase of the input signal frequency,
the magnitude of the output signal decreases, finally to

a magnitude so small that it cannot be measured by the
equipment used in this experimental work. Thus, a
larger initial output signal enables the experimental
data to be determined to higher frequencies than might
otherwise be possible.

If the linear and saturation limiting condition
is plotted on log-log graph paper, they will be straight
lines as shown in Figure 52. The areas of operation are
divided into three parts: 1. Linear region; 2. Non-linear
region; and 3. Saturated region. So that the theory of
Section II may be applied, it is necessary to cause the
closed loop servomechanism to operate in the linear
region. If the coordinates of Figure 6 and Figure 52 were
the same, it would be required that all of the curve under
consideration in Figure 6, be within the linear region
if the previously developed theory is to apply. The maxi-
mum input signal for which linear operation occurs is
thus obtained by adjusting the curves in Figure 6 so that
they are just tangent to the linear limit line. The
maximum input signal for which linear operation occurs is
thus obtained by adjusting the curves in Figure 6 so that
they are just tangent to the linear limit line. The
maximum allowable input signal may then be read directly
from the input amplitude scale at the lowest frequency
reading. It should be recalled that in deriving the
linear limiting equation, "a" was defined as equal to
one half the amplitude of the output signal.

Phase Lag Between the D.C. Amplifier - Demodulator Unit 2 and Unit 1

For Various Input Signal Frequencies

Frequency in Cycle 4/Sec	Phase Lag in Degrees
20.25	7.
19.45	6.75
19.25	6.25
17.55	6.
16.6	5.5
16.5	5.5
15.4	5.
14.75	4.5
13.9	4.75
13.2	4.
11.25	3.25
11.2	3.
11.1	2.5
10.6	2.25
9.3	2.
8.75	1.5
7.85	1.25
7.86	.5
5.95	.5
4.27	.0

FIG. 49.

Louis Baeriswyl, Jr.
APL/JHU - 4 Apr. 51.

Again, referring to the curves of Figure 6, it
will be noted that low amplifier time constant curves
would become tangent to the linear limiting line at
higher frequencies with a resultant small allowable
maximum input signal. As higher amplifier time constant
curves are used, the point of tangency occurs at lower
frequencies and results in larger allowable maximum input
signals. Unfortunately, this condition does not continue
as the time constants become greater for the curves at
higher amplifier time constants change shape, developing
an over-shoot hump. While the point of tangency con-
tinues to occur at lower frequencies, the allowable
maximum input signal amplitude becomes less due to the
curve shape.

The closed loop gain may also be altered to
obtain a larger allowable maximum input signal. Note
that the frequency scale of Figure 6 is given in terms
of K. For a fixed frequency scale, reducing K effectively
moves the amplitude ratio curves to the left which, when
used in conjunction with the linear limit line, results
in a larger allowable maximum input signal. In this
experimental work, a larger input signal was obtained
by reducing the gain from its maximum value of 14 to a
value of approximately 5. Higher amplifier time constants
were finally used, with two earlier selected values being
discarded.

5. Determination of the Maximum Output Velocity and Closed Loop Gain.

The maximum output velocity, $\dot{\Theta}_{o\ max}$, and the closed loop gain K are determined by using the test set-up shown in the schematic drawing of Figure 50.
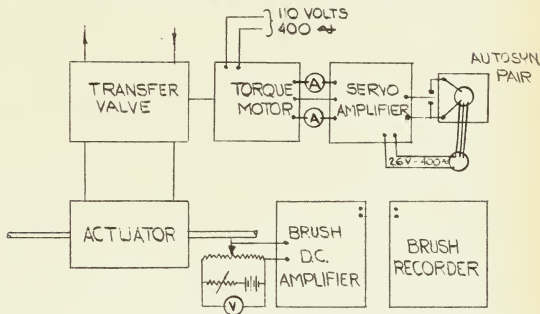
Fig. 50. Schematic of Test Set-up for Determining $\dot{\Theta}_{o\ max}$ and K.

The components are connected as shown. Initially the feedback and input terminals of the servo amplifier are shorted and the servo amplifier output is balanced as indicated by the two milliammeters. After balancing the output, the feedback terminals are opened and an autosyn pair is connected. The autosyn pair operates from 26 volts at 400 cycles tapped from the power transformer of the servo amplifier. The servo amplifier input terminals remain shorted. One autosyn of the autosyn pair is so mounted that

its rotor may be rotated by means of a dial knob. The dial has a vernier scale which enables it to be read to a tenth of a degree. This autosyn pair was zeroed so that a minimum signal occurred at the zero dial reading.

The gain of the closed loop system is adjusted by varying the setting of the 750 ohm feedback potentiometer in the servo amplifier. Test runs were made at several settings until the desired K was obtained.

The test consisted of setting the autosyn to a particular dial reading in degrees and opening the short of the feedback terminal and connecting the autosyn output to these terminals. The above switching action was accomplished by one switch. At the beginning of each run the actuator strut was moved to one end of the stroke and the initial pressure at the start of the run was 1000 psi. When the above mentioned switch was closed, the actuator strut moved through its full stroke and the pickoff potentiometer fed the pickoff voltage to the Brush D.C. amplifier and in turn to the Brush recorder. The velocity in volts per second was obtained in the same manner as fully described in Part 2.3 of Section III. Since 12 volts were applied across the pickoff potentiometer, the voltage to displacement ratio was 1.735 volts per inch.

The recorded autosyn rotor setting in degrees and the determined actuator velocity in volts per second

is tabulated in Table XI. The negative values of the autosyn rotor settings are taken counter clockwise and the negative velocities are velocities measured in the opposite direction of actuator motion to that arbitrarily assigned as positive. The magnitude of velocities due to signals of equal magnitude and opposite sign were averaged and these averages are also tabulated. The above test was repeated for all three selected amplifier time constants and within experimental error, the same results were obtained for each condition.

Increasing the autosyn signal beyond 10 degrees results in no greater actuator velocity. Thus, using the average maximum velocity output, there is obtained:

$$\dot{\ominus}_{o\ max} = 2.446 \text{ v./sec.} = \frac{(2.446 \text{ v/sec.})}{(1.785 \text{ v./in.})}$$

$$\dot{\ominus}_{o\ max} = 1.37 \text{ in./sec.}$$

The closed loop gain is equal to the output velocity divided by the input signal. These values are also tabulated in Table XI.

The input signal used in determining the phase lag and amplitude ratio of the closed loop servomechanism was equal to $\pm 3/16$ inches. The mechanical linkage gain is 15 degrees/inch and thus the input signal corresponds to an autosyn rotation of ± 2.82 degrees. From Table XI it will be noted that the gain increases with the magnitude

TABLE XI. MAXIMUM ACTUATOR VELOCITY DATA AND THE CLOSED
LOOP GAIN DATA FOR VARIOUS INPUT SIGNAL MAGNITUDES, USING
THREE AMPLIFIER TIME CONSTANTS.

AMPLIFIER TIME CONSTANT = 0.0526 SECONDS.

Autosyn Input in Deg.	Actuator Velocity v./sec.	Autosyn Input in Deg.	Actuator Velocity v./sec.	Avg.Actuator Velocity v./sec.	Avg. System Gain deg./sec./deg.
0.3	0.177	- 0.3	- 0.192	0.185	5.18
0.7	0.385	- 0.7	- 0.595	0.490	5.87
1.0	0.835	- 1.0	- 0.863	0.849	7.14
1.5	1.175	- 1.5	- 1.220	1.198	6.72
2.	1.505	- 2.	- 1.580	1.543	6.48
3.	1.905	- 3.	- 1.935	1.920	5.38
4.	2.06	- 4.	- 2.15	2.105	4.42
5.	2.24	- 5.	- 2.29	2.265	3.81
10.	2.44	-10.	- 2.45	2.445	2.05

AMPLIFIER TIME CONSTANT = 0.1045 SECONDS.

0.3	0.133	- 0.3	- 0.230	0.182	5.10
0.5	0.231	- 0.5	- 0.408	0.320	5.38
0.7	0.438	- 0.7	- 0.543	0.491	5.90
1.0	0.718	- 1.0	- 0.833	0.826	6.95
2.	1.50	- 2.	- 1.50	1.50	6.30
3.	2.04	- 3.	- 2.09	2.07	5.81
4.	2.18	- 4.	- 2.14	2.16	4.55
5.	2.14	- 5.	- 2.26	2.21	3.71
10.	2.26	-10.	- 2.61	2.43	2.05

AMPLIFIER TIME CONSTANT = 0.1573 SECONDS

0.5	0.120	- 0.5	- 0.485	0.303	5.10
0.7	0.378	- 0.7	- 0.660	0.519	6.23
1.0	0.583	- 1.0	- 0.957	0.770	6.49
2.	1.58	- 2.0	- 1.560	1.57	6.61
3.	1.87	- 3.0	- 1.955	1.91	5.35
4.	2.08	- 4.0	- 2.14	2.11	4.44
5.	2.14	- 5.0	- 2.29	2.22	3.74
10.	2.43	-10.0	- 2.50	2.46	2.07

of the autosyn signal to about 7 deg./sec./deg. at 1
degree and then decreases. No concern need be given
for signals greater than 3 degrees as these do not
occur experimentally in the closed loop experiment.

Even for large signals, a major part of the
signal occurs in the low gain region. Thus a gain of
5.1 was selected for the value of gain for the closed
loop. After this gain was established, the feedback
potentiometer was never readjusted.

6. Selection of the Magnitude of the
Input Signal.

With the experimental value of $\dot{q}_{o\ max}$, the
linear limiting line is drawn on log-log graph paper as
shown in Figure 52. The amplitude curves for $T_i = 1/K$.
and $T_i = 1/4K$ were drawn on similar graph paper as shown
in Figure 51. The amplitude ratio curve data was taken
directly from Figure 6, using $K = 5.1$. With the frequency
scales alined, the graph papers were displaced vertically
until each curve in turn became tangent to the linear
limit line. At each point when tangency occurred, the
input signal corresponding to the unity amplitude ratio
was noted.

The two time constant values selected covers the
range of values used in the experimental work and thus an
input signal less than the maximum indicated by the above
process is allowable. Based on this graphical study, an

input signal of ±3/16 inch was used. The superimposed
amplitude ratio curves when tangent to the linear limit
line are shown in Figure 52.

            7. Experimental Procedure for Determining
the Closed Loop Servomechanism Phase Lag and Amplitude
Ratio.

            The servomechanism components and the
measuring equipment were connected as shown in the schematic
drawing of Figure 47 and the photograph of Figure 48. The
servo amplifier was balanced, the torque motor and transfer
valve were zeroed, and the autosyn pairs were phased as
previously described. The Brush D.C. amplifier and the
two D.C. amplifiers of the phase measuring unit are warmed
up for about one hour prior to conducting the dynamic test
on the servo system. This warm-up period enables a greater
degree of stability to occur in the D.C. amplifiers.

            After allowing an additional five minutes for
the servo amplifier to warm up, the variable speed driving
motor of the signal generating unit is adjusted to its
slowest driving speed. At this low frequency (approxi-
mately 0.1 cycles per second), the amplitude ratio is
assumed to be unity. The attenuator in the signal generat-
ing unit is adjusted so that the stroke of the actuator
becomes equal to 3/8 inches or a total stroke ±3/16 inches.
The above stroke length is of such a magnitude that the
closed loop servo system will operate within the linear

FIG. 51

THEORETICAL
AMPLITUDE RATIO
AS OBTAIN
FROM FIGURE 6 FOR
K=51 DEG./SEC/DEG

$T=\frac{1}{K}$

$T=\frac{1}{4K}$

ous BAERISWYL
APL-JHU-12 APR 5

FREQUENCY IN CYCLES PER SECOND

AMPLITUDE RATIO
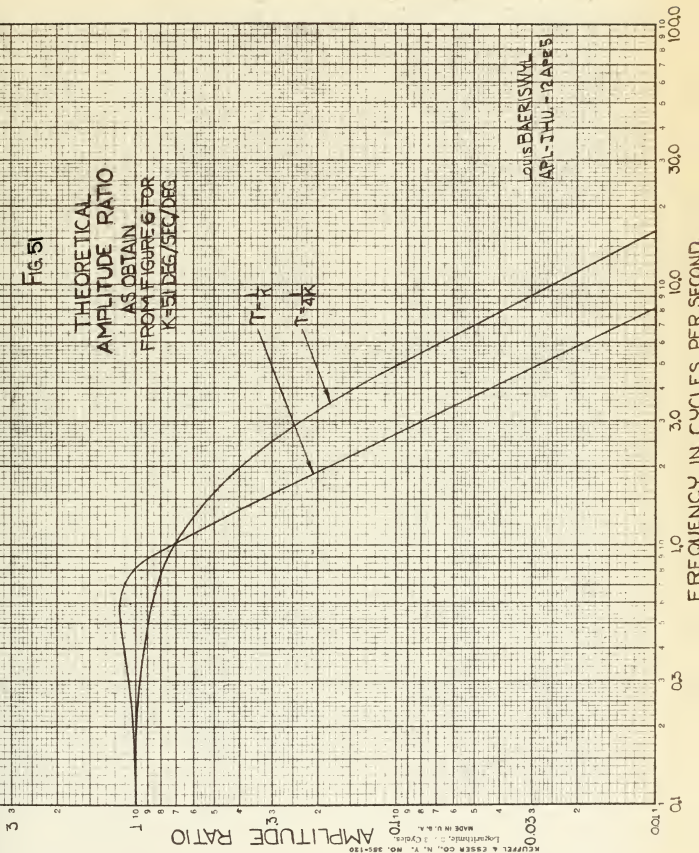
FIG. 52

GRAPHICAL METHOD FOR DETERMINING THE MAXIMUM ALLOWABLE INPUT SIGNAL SO THAT THE SERVO MECHANISM $\dot{\theta}_{o\,MAX} = 1.37$ INCHES/SECONDS OPERATES IN THE LINEAR REGION

LINEAR LIMIT $af = \dot{\theta}_{o\,max}/2\pi$

SATURATION LIMIT $af = \ddot{\theta}_{o\,MAX}/4$

SATURATION REGION

NON-LINEAR REGION

LINEAR REGION

$T = \dfrac{1}{4K}$

$T = \dfrac{1}{K}$

$K = 51$ deg./sec/deg.

INPUT AMPLITUDE IN INCHES

FREQUENCY IN CYCLES PER SECOND

Louis BAERISWYL
APL/JHU-R APR 51

region for all applied input signal frequencies. This conforms with the theory presented in Part 5, Section II, and the practical considerations of Parts 4 and 6, Section III.

The basic procedure of the test was repeated three times. In each of the three series of tests, three different condenser pairs were connected in the filter circuit feeding the 6AQ5 tubes of the servo amplifier. The values of the three condenser pairs used were 4, 8 and 12 μ f.

The signal generating unit is equipped with a tachometer-voltmeter unit, which is connected to the variable speed driving motor and which may be used to obtain a rough setting of the input signal frequency. This tachometer-voltmeter unit was calibrated and the calibration curve is shown in Figure 53.

The signal generating unit was adjusted so that the output signal frequency was approximately the value desired as indicated by the tachometer-voltmeter unit. The accumulators were charged to a pressure above 1000 psi. The accumulator pressure dropped continually as the stored oil was used by the actuator. The phase shift dial was rotated so that Lissajou figure on the cathode ray oscilloscope was closed to a straight line at all times as the pressure dropped. When the pressure gage on the accumulator side of the hydraulic loop read

VOLTMETER READING	FREQUENCY
25	23.80
24	22.95
23	22.00
22	21.20
21	20.25
20	19.45
19	18.35
18	17.50
17	16.50
16	15.60
15	14.50
14	13.55
13	12.67
12	11.70
11	10.70
10	9.90
9	8.73
8	7.90
7	6.86
6	5.92
5	4.97
4	4.06
3	3.01
2	2.17
1	1.31
.0	.0

CALIBRATION OF A TACHOMETER -
VOLTMETER vs FREQUENCY AS
DETERMINED FROM BRUSH RECORDER
DATA.

FIG. 53.

D.C. VOLTMETER READING - VOLTS

FREQUENCY IN CYCLES PER SECOND

LouisEngebourL Jr
APL/JHU-22Feb51.

1000 psi, the phase shift dial reading was recorded
and the Brush recorder was turned on. The measured
phase lag was recorded from the phase shift dial and
the amplitude ratio and input signal frequency were
determined from the data presented on the recorder
tape. The amplitude and phase measuring systems have
been fully described in previous parts of this section.
The input signal frequency was increased until the
output signal had become so small that the Lissajou
figure is no longer sensitive as a phase measuring
method, being a closed line over a wide range of phase
lags. To indicate the sensitivity of the phase measur-
ing system, two photographs of the Lissajou figure were
taken when the output and input signals are inphase and
when five degrees out of phase, as shown in Figures 54
and 55. For these two photographs, the input signal
frequency was approximately 5 cycles per second, with the
cathode ray tube intensity reduced to an extent so that
the Lissajou figure was just visible. It is believed
that at moderated input signal frequencies, the phase
measuring system results are reproduceable to ±1/4 degrees.
This condition of high accuracy degenerates at frequencies
below 0.1 cycles per second, as the persistance of the
cathode ray tube used was low, and at high frequencies
as the output signal of the servomechanism becomes non-
sinusoidal and small.

Fig. 54. Lissajou Figure - Inphase.

Fig. 55. Lissajou Figure - 5° Out of Phase.

.   . The determined frequency, amplitude ratio, and measured and corrected phase lag is tabulated in Tables XII to XVII, for the three selected time constant conditions of the servo amplifier. The corrected phase lag data as a function of frequency is plotted in Figure 56 and the amplitude ratio data as a function of frequency is plotted in Figures 57 and 58.

Calculations of the theoretical phase characteristics for second and third order systems with amplifier time constants of 0.1573, 0.1045, and 0.0526 seconds were made. The loop gain constant was taken as 5.1 degrees/second/degree. The second time constant of assumed third order system was taken as 0.0034 seconds. The calculated values of phase lag are tabulated in Table XVIII. These theoretical curves are plotted on Figure 56.

Calculations of the theoretical amplitude ratio characteristics for the above mentioned conditions of the servomechanism system are tabulated in Table XIX and plotted in Figures 57 and 58.

TABLE XII. AMPLITUDE RATIO AND PHASE LAG DATA FOR THE
EXPERIMENTAL CLOSED LOOP SYSTEM WITH THE SERVO AMPLIFIER
TIME CONSTANT EQUAL TO 52.6 MILLISECONDS.

FREQUENCY IN CYCLES PER SECOND	AMPLITUDE RATIO	MEASURED PHASE LAG IN DEGREES	CORRECTED PHASE LAG IN DEGREES
.1274	1.000	10.5	10.5
.217	.982	15.	15.
.333	.965	21.5	21.5
.400	.950	25.5	25.5
.465	.950	29.	29.
.587	.950	36.	36.
.636	.942	40.	40.
.690	.935	44.5	44.5
.782	.915	48.5	48.5
.894	.910	57.5	57.5
.890	.900	59.5	59.5
1.020	.850	67.5	67.5
1.035	.865	70.5	70.5
1.175	.800	76.5	76.5
1.22	.740	81.	81.
1.35	.683	86.	86.
1.39	.666	90.	90.
1.54	.617	96.	96.
1.64	.550	101.5	101.5
1.77	.500	105.	105.
1.89	.467	111.	111.
2.00	.433	116.	116.
2.22	.366	121.	121.
2.35	.325	125.	125.
2.53	.300	130.	130.
2.78	.266	134.	134.
2.86	.233	138.	138.

TABLE XIII. AMPLITUDE RATIO AND PHASE LAG DATA FOR
THE EXPERIMENTAL CLOSED LOOP SYSTEM WITH THE SERVO
AMPLIFIER TIME CONSTANT EQUAL TO 52.6 MILLISECONDS.

FREQUENCY IN CYCLES PER SECOND	AMPLITUDE RATIO	MEASURED PHASE LAG IN DEGREES	CORRECTED PHASE LAG IN DEGREES
3.17	.192		
3.20		143.	143.
3.60	.140		
4.00	.133		
4.16		154.	154.
4.70	.088		
5.18		160.	159.9
6.00	.058		
6.20		166.5	165.9
6.88	.044		
7.19		171.	170.
7.25		170.	169.
8.10		174.	172.6
8.33	.028		
9.38		177.	175.
10.00	.020		
10.90	.016		
11.20		182.	179.2
11.24	.014		
12.10		183.	179.7
12.13	.012		
13.18		184.	180.2
14.12		188.	183.8
15.15		190.	185.3

TABLE XIV. AMPLITUDE RATIO AND PHAS. LAG DATA FOR THE
EXPERIMENTAL CLOSED LOOP SYSTEM WITH THE SERVO AMPLIFIER
TIME CONSTANT EQUAL TO 104.5 MILLISECONDS.

FREQUENCY IN CYCLES PER SECOND	AMPLITUDE RATIO	MEASURED PHASE LAG IN DEGREES	CORRECTED PHASE LAG IN DEGREES
.1035	1.000	7.5	7.5
.1153	1.000	10.5	10.5
.1515	1.000	13.	13.
.215	1.000	15.	15.
.278	1.000	19.	19.
.400	1.007	26.	26.
.490	1.007	32.	32.
.550	1.015	37.	37.
.625	1.033	41.	41.
.678	1.050	51.	51.
.726	1.033	54.	54.
.778	1.033	60.	60.
.848	1.000	67.	67.
.890	.985	73.5	73.5
.950	.924	82.5	82.5
1.000	.882	89.	89.
1.062	.840	95.	95.
1.100	.767	99.5	99.5
1.183	.708	105.	105.
1.231	.708	108.	108.
1.333	.617	115.	115.
1.400	.551	120.	120.
1.435	.535	125.	125.
1.565	.457	130.	130.
1.692	.373	135.	135.
1.800	.333	140.	140.
1.906	.291	145.	145.
2.07	.250	150.	150.
2.29	.200	155.	155.
2.50	.133	159.	159.

TABLE **XV**   AMPLITUDE RATIO AND PHASE LAG DATA FOR THE
EXPERIMENTAL CLOSED LOOP SYSTEM WITH THE SERVO AMPLIFIER
TIME CONSTANT EQUAL TO 104.5 MILLISECONDS.

FREQUENCY IN CYCLES PER SECOND	AMPLITUDE RATIO	MEASURED PHASE LAG IN DEGREES	CORRECTED PHASE LAG IN DEGREES
2.69		161.	161.
2.85	.109		
3.19		166.	166.
3.55	.0644		
3.75		170.	170.
4.14		172.	172.
4.62		175.5	175.5
4.625	.0356		
5.21		178.5	178.5
5.27	.0282		
6.05		180.	180.5
6.55	.0170		
7.15		184.5	185.5
7.22	.0133		
7.50	.0089		
8.07		189.	190.4
9.32		193.	195.0

TABLE XVI. AMPLITUDE RATIO AND PHASE LAG DATA FOR THE
EXPERIMENTAL CLOSED LOOP SYSTEM WITH THE SERVO AMPLIFIER
TIME CONSTANT EQUAL TO 157.3 MILLISECONDS.

FREQUENCY IN CYCLES PER SECOND	AMPLITUDE RATIO	MEASURED PHASE LAG IN DEGREES	CORRECTED PHASE LAG IN DEGREES
.0975	1.000	9.5	9.5
.257	1.000	15.	15.
.306	1.005	18.	18.
.392	1.072	24.5	24.5
.445	1.092	30.	30.
.500	1.180	37.	37.
.516	1.190	41.	41.
.562	1.206	45.5	45.5
.569	1.225	48.5	48.5
.597	1.227	52.	52.
.647	1.230	62.5	62.5
.674	1.222	70.	70.
.682	1.232	72.5	72.5
.737	1.167	86.	86.
.900		100.	100.
.925		112.	112.
.933	.918	114.	114.
1.000	.800	120.	120.
1.250		132.	132.
1.182	.600	137.5	137.5

TABLE XVII. AMPLITUDE RATIO AND PHASE LAG DATA FOR THE
EXPERIMENTAL CLOSED LOOP SYSTEM WITH THE SERVO AMPLIFIER
TIME CONSTANT EQUAL TO 157.3 MILLISECONDS.

FREQUENCY IN CYCLES PER SECOND	AMPLITUDE RATIO	MEASURED PHASE LAG IN DEGREES	CORRECTED PHASE LAG IN DEGREES
1.272	.500		
1.408	.387		
1.56		148.5	148.5
1.635	.300		
1.715	.233		
1.770	.193		
1.92		161.	161.
1.96	.117		
2.03	.134		
2.21	.107		
2.50	.0467	171.	171.
3.03		174.	174.
3.08	.0386		
3.53		177.5	177.5
3.67	.0219		
4.04	.0180		
4.10		182.	182.
4.58	.0116		
5.00	.0064		
5.10		187.	187.1
5.48		189.	189.2
5.82		192.	192.4

TABLE XVIII.   THEORETICAL PHASE LAG FOR A SECOND AND THIRD ORDER SYSTEM, USING A CLOSED LOOP GAIN CONSTANT OF 5.1 INCHES/SECOND/INCH.

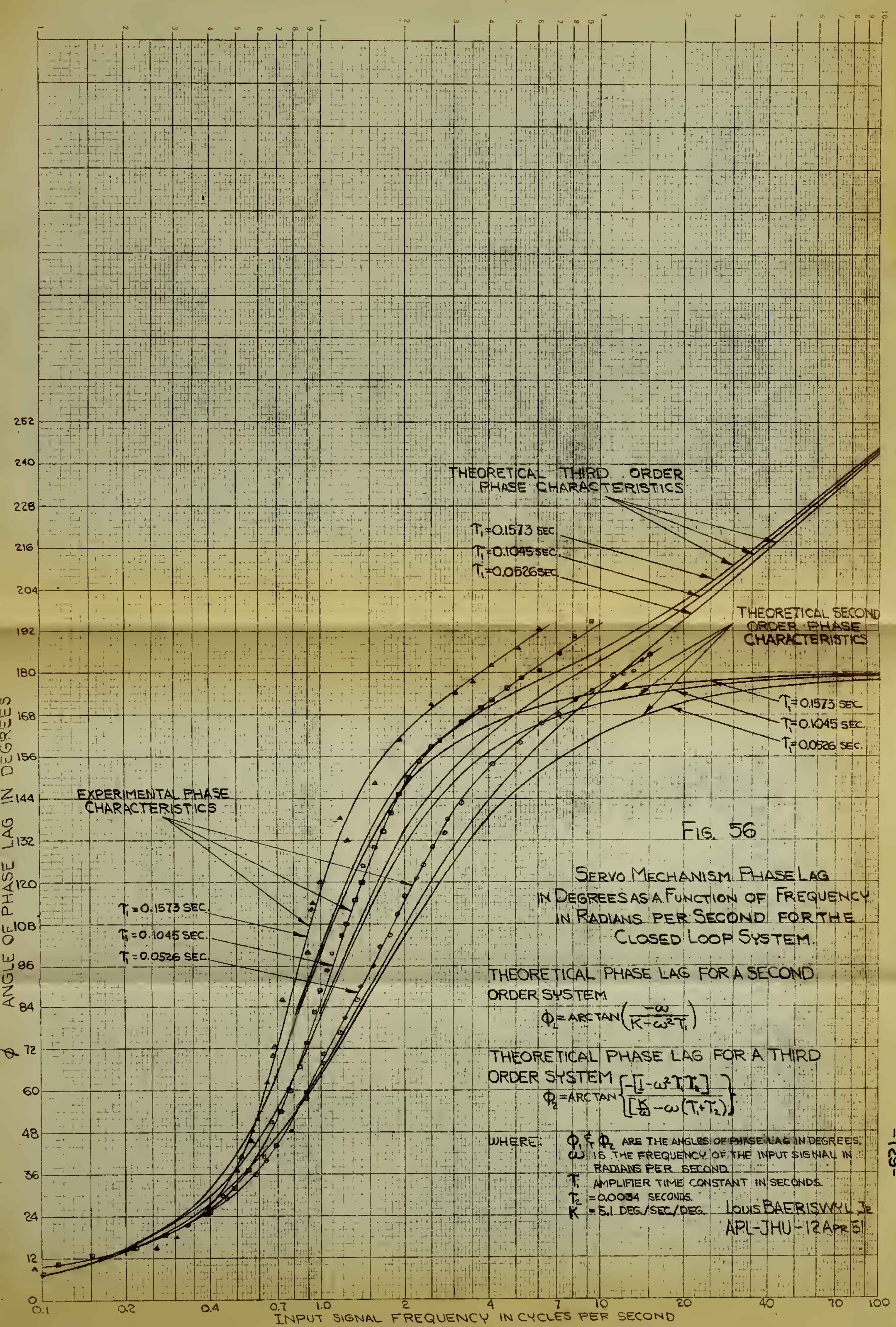| Frequency In Cycles/Sec.	Phase Lag in Degrees For the Second Order System			Phase Lag in Degrees for a Third Order System τ_2 =.0034		
	τ =.0526	τ =.1045	τ =.1573	τ =.0526	τ =.1045	τ =.1573
.1	7.05	7.07	7.10	7.06	7.07	7.10
.2	14.06	14.27	14.53	14.10	14.30	14.53
.4	27.82	29.60	31.50	27.87	29.53	31.3
.7	41.1	55.00	64.80	47.45	55.4	40.6
1.0	62.2	81.22	100.03	65.10	82.26	101.32
2.0	104.22	130.4	147.50	107.22	135.1	150.38
4.0	133.05	157.65	165.05	143.6	162.75	170.07
7.0	155.5	167.39	171.64	164.4	176.14	180.+
10.0	162.7	171.25	174.20	175.09	183.38	186.33
20.0	171.31	175.42	177.09	194.6	198.74	200.7
40.0	175.64	177.84	178.55	216.3	218.	219.1
70.0	177.52	178.75	179.17	233.75	235.	235.3
100.0	179.25	179.13	179.40	243.13	243.97	244.3

All time constants given in seconds.

TABLE XIX. THEORETICAL AMPLITUDE RATIO FOR A SECOND AND THIRD ORDER SYSTEM USING A CLOSED LOOP GAIN CONSTANT OF 5.1 INCHES /SECOND / INCH.

Frequency In Cycles/Sec.	Amplitude Ratio for The Second Order System			Amplitude Ratio for Third Order System		Amplitude Ratio for A
	$\tau=.0526$	$\tau=.1045$	$\tau=.1573$	$\tau=.0526$	$\tau=.1045$	$\tau_2=.0034$ $\tau_1=.1573$
.1	1.000	1.000	1.011	.998	1.000	1.001
.2	0.990	1.000	1.013	.986	1.002	1.019
.4	0.943	1.005	1.060	.958	1.003	1.063
.7	0.336	.950	1.050	.858	.964	1.067
1.0	.732	.803	.804	.743	.816	.813
2.0	.394	.310	.218	.404	.304	.2192
4.0	.1358	.0767	.0526	.129	.0776	.0522
7.0	.04715	.0253	.0169	.0474	.0250	.0167
10.0	.02420	.0124	.00823	.0235	.01211	.00808
20.0	.00612	.0034		.00503	.00284	.00139
40.0	.001515			.001165		

THEORETICAL THIRD ORDER
PHASE CHARACTERISTICS

$T_1 = 0.1573$ SEC
$T_1 = 0.1045$ SEC.
$T_1 = 0.0526$ SEC

THEORETICAL SECOND
ORDER PHASE
CHARACTERISTICS

$T_1 = 0.1573$ SEC.
$T = 0.1045$ SEC.
$T = 0.0526$ SEC.

EXPERIMENTAL PHASE
CHARACTERISTICS

$T_1 = 0.1573$ SEC.
$T_1 = 0.1045$ SEC.
$T_1 = 0.0526$ SEC.

FIG. 56

SERVO MECHANISM PHASE LAG
IN DEGREES AS A FUNCTION OF FREQUENCY
IN RADIANS PER SECOND FOR THE
CLOSED LOOP SYSTEM.

THEORETICAL PHASE LAG FOR A SECOND
ORDER SYSTEM

$$\phi_1 = \text{ARCTAN}\left(\frac{-\omega}{K + \omega^2 T_1}\right)$$

THEORETICAL PHASE LAG FOR A THIRD
ORDER SYSTEM

$$\phi_2 = \text{ARCTAN}\left\{\frac{[1 - \omega^2 T_1 T_2]}{[\frac{K}{\omega} - \omega(T_1 + T_2)]}\right\}$$

WHERE: $\phi_1 \& \phi_2$ ARE THE ANGLES OF PHASE LAG IN DEGREES.
ω IS THE FREQUENCY OF THE INPUT SIGNAL IN
RADIANS PER SECOND.
T_1 AMPLIFIER TIME CONSTANT IN SECONDS.
$T_2 = 0.0054$ SECONDS.
$K = 5.1$ DEG./SEC./DEG.   LOUIS BAERISWYL JR
APL-JHU-12APR 51

ANGLE OF PHASE LAG IN DEGREES

ϕ

252 240 228 216 204 192 180 168 156 144 132 120 108 96 84 72 60 48 36 24 12 0

INPUT SIGNAL FREQUENCY IN CYCLES PER SECOND

0.1   0.2   0.4   0.7 1.0   2   4   7 10   20   40   70 100

THE OUTPUT TO INPUT AMPLITUDE RATIO AS A FUNCTION OF THE INPUT SIGNAL FREQUENCY IN RADIANS PER SECOND FOR A CLOSED LOOP SECOND ORDER SYSTEM.

EXPERIMENTAL AMPLITUDE RATIO CHARACTERISTICS
$T = 0.0526$
$T = 0.1045$
$T = 0.1573$

SYMBOLS
K — CLOSED LOOP GAIN IN DEG./SEC./DEG.
T — AMPLIFIER TIME CONSTANT IN SEC.
ω — INPUT SIGNAL FREQUENCY IN RAD./SEC.

$$|A| = \frac{K}{\sqrt{(K - T\omega^2)^2 + \omega^2}}$$

THEORETICAL AMPLITUDE RATIO CHARACTERISTICS
$T = 0.0526$
$T = 0.1045$
$T = 0.1573$

FIG. 57

Louis BAERISWYL
APL/JHU 13 APR 51.

FREQUENCY IN CYCLES PER SECOND

THE OUTPUT TO INPUT
SIGNAL AMPLITUDE RATIO AS
A FUNCTION OF THE INPUT SIGNAL FREQUENCY
IN RADIANS PER SECOND FOR A CLOSED LOOP
THIRD ORDER SYSTEM

$|A|$ - OUTPUT TO INPUT AMPLITUDE RATIO

EXPERIMENTAL AMPLITUDE
RATIO CHARACTERISTICS

$T_1 = 0.0526$
$T_1 = 0.1045$
$T_1 = 0.1573$

SYMBOLS
K - CLOSED LOOP GAIN IN DEG./SEC./DEG.
T_1 - AMPLIFIER TIME CONSTANT IN SEC.
ω - INPUT SIGNAL FREQUENCY IN RAD/SEC.
$T_2 = 0.0034$ SEC.

THEORETICAL AMPLITUDE
RATIO CHARACTERISTICS

$$|A| = \frac{K}{\sqrt{\left[K - \omega^2(T_1 + T_2)\right]^2 + \left[\omega - \omega^3(T_1 T_2)\right]^2}}$$

FIG. 58

$T_1 = 0.0526$
$T_1 = 0.1045$
$T_1 = 0.1573$

L.BAERTSWIL
APL/JHU
APR-51

FREQUENCY IN CYCLES PER SECOND

IV.   CORRELATION OF THE EXPERIMENTAL AND
THEORETICAL RESULTS.

The experimental phase lag characteristic
curves for the closed loop servomechanism are plotted
in Figure 56, from the tabulated data of Tables XII to
XVII. The phase lag in degrees is plotted as a
function of the input signal frequency in cycles per
second. A set of three experimental curves were obtained
using three different servo amplifier time constants
equal to 0.0526, 0.1045, and 0.1573 seconds. Theoretical
second order system phase lag characteristic curves,
with these same delays, are also plotted on Figure 56
from the tabulated data of Table XVIII.

There is a high degree of correlation between
the experimental and theoretical results at low frequen-
cies. As the frequency increases, the experimental
phase lag increases to a value greater than that pre-
dicted by the second order system theory. An error of
from 10 to 15 percent exists between the theoretical
and experimental phase lag results for the frequency
range from 0.7 to 7.0 cycles per second. If experimental
data could have been obtained for higher frequencies, it
appears from the trend of the slope of the experimental
curve that the percentage error would further increase with
increased frequencies. Up to a frequency of approximately

2 cycles per second the general shape of the theoretical and experimental curves are similar. However, beyond this frequency the shapes of these two sets of curves differ markedly.

Three theoretical third order system phase lag curves are also plotted in Figure 56, from the tabulated data of Table XVIII. The curves are derived using two time delays, one being constant for the set with a time constant of 0.0034 seconds, and the other time delay having time constants of 0.0526, 0.1045, and 0.1573 seconds.

The correlation between the theoretical third order system phase lag and the experimental phase lag, is improved over the second order system correlation for the frequency range employed in this test. The percentage error in the phase angle between 0.7 and 7.0 cycles per second is reduced to a value of from 5 to 10 percent. Further, the shape of the theoretical and experimental phase lag curves are similar and both extend beyond 180 degrees.

The experimental and theoretical second order system amplitude ratio curves are plotted in Figure 57, from the data of Tables XII to XVII, and XIX. The experimental results indicate peak over-shoot values greater than that predicted by the theory. The negative slope

of the experimental results are greater than the
theoretically predicted slopes. The final trend of
the slope of the experimental amplitude ratio appears
to be increasing negatively. The percentage error
between the experimental and theoretical amplitude ratio
varies not only with the frequency, but also with the
servo amplifier time constant.

When the output signal has decreased to one
percent of the input signal, the percentage frequency
error is 23, 33 and 43 percent for the servo amplifier
time delays of 0.0526, 0.1045, and 0.1573 seconds, respect-
ively. While these errors are large, they occur at the
extreme of the obtained experimental results and are the
largest errors recorded in this test.

The experimental and theoretical third order
system amplitude ratios are plotted in Figure 52, from
the tabulated data of Tables XII to XVII and XIX. The
correlation of the experimental amplitude ratio and the
results as predicted by third order system theory are
a slight improvement over those predicted by second
order theory. Since there is practically no difference
between the second and third order system amplitude ratio
curves in the range drawn, other than a slight increase
in the negative slope of the third order system results,
only a little comment need be made. The amount of error

is only slightly reduced in this case and the slope
of the experimental curves continues to be greater
than the theoretical values.

In general the experimental phase lag and
output attenuation are greater than that predicted by
third order system theory. This indicates that the
order of the system is greater than the third. These
additional delays may be due to the torque motor being
an effective second or third order delay, instead of the
assumed first order delay. This is particularly so in
the light of its dynamic phase lag characteristics.
Compressibility of the hydraulic oil in the actuator
may also cause an additional small delay. Lastly there
may be small delays due to the differential transformer
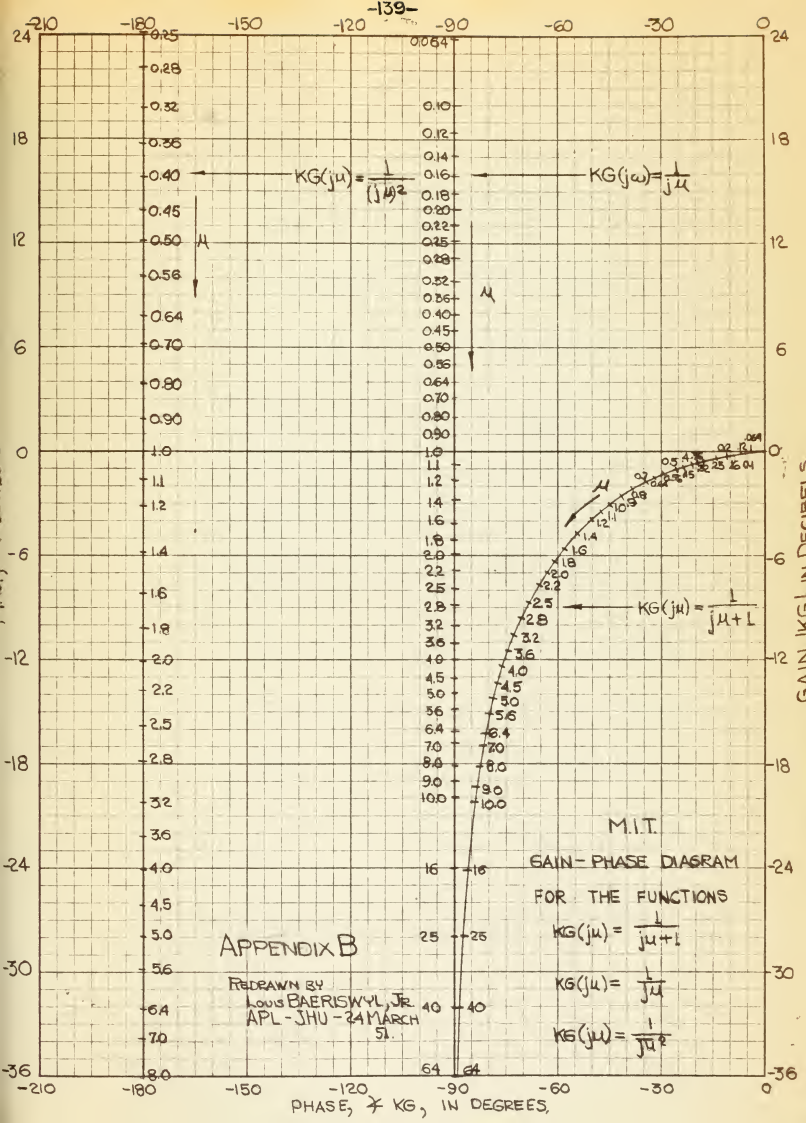and the autosyn pair.

V. CONCLUSIONS.

For the closed loop hydroelectric servo-
mechanism tested, it is concluded that:

1. The phase lag and amplitude ratio
of the servo system is predicted more
accurately by the theoretical results
for the third order system, than those
of the second order system. This is seen
directly from all three figures, (Figures
56, 57 and 58) showing the final closed
loop characteristics.

2. The theoretical third order closed
loop system may be used to predict charac-
teristic results over a frequency range
up to approximately 10 cycles per second,
when engineering accuracy is required.
This is particularly true with regard to
the phase lag characteristics.

3. The order of the closed loop system
is greater than the third, as indicated
by the phase lag and output signal attenua-
tion being greater than that theoretically
predicted for a third order system.

APPENDIX A. SYMBOLS.

A   - Amplitude ratio of the output to input signal, $|\theta_o/\theta_i|$.

e   - Error signal, $(\theta_i - \theta_o)$.

E_m - Amplifier output signal.

f   - Input signal frequency in cycles per second.

j   - Complex operator.

K   - Closed loop gain constant.

K_i - Gain constant of the i th component.

KG(S)   - Closed loop transfer function.

$KG(S)|_\infty$ - Open loop system transfer function.

max   - Maximum.

S   - Laplace operator.

t   - Time.

X   - Torque motor output displacement.

$\dot{X}$ - Transfer valve rate of output oil flow.

Y_i - Transfer function of the i th term.

$\dot{Y}$ - Actuator velocity.

$\dot{z}$ - Mechanical linkage output velocity.

θ_i - Input signal.

θ_o - Output signal.

$\dot{\theta}_o$ - Output signal velocity.

τ - Time constant.

ϕ - Phase angle between input and output signals.

ω - Input signal angular frequency in radians per second.

M.I.T.

GAIN — PHASE DIAGRAM

FOR THE FUNCTIONS

$$KG(j\mu) = \frac{1}{j\mu + 1}$$

$$KG(j\mu) = \frac{1}{j\mu}$$

$$KG(j\mu) = \frac{1}{j\mu^2}$$

APPENDIX B

REDRAWN BY
LOUIS BAERISWYL, JR.
APL - JHU - 24 MARCH
51.

$$KG(j\mu) = \frac{1}{(j\mu)^2}$$

$$KG(j\omega) = \frac{1}{j\mu}$$

$$KG(j\mu) = \frac{1}{j\mu + 1}$$

GAIN |KG| IN DECIBELS

PHASE, ∠ KG, IN DEGREES.

BIBLIOGRAPHY

1. G. S. Brown and D. P. Campbell, Principles of Servomechanisms, John Wiley & Sons, Inc., New York, 1948.

2. M. F. Gardner and J. L. Barnes, Transients in Linear Systems, Vol. 1, John Wiley & Sons, Inc., New York. 1947.

3. F. Paddison & W. Good, High Speed Linear Torque Motor, Published APL letter to D. T. Sigley from F. Paddison & W. Good.

4. Autosyn System File. AY-200-1, Eclipse Pioneer Division, Bendix Aviation Corporation.

5. Autosyn System File, AY-200-2, Eclipse Pioneer Division, Bendix Aviation Corporation.

6. Autosyn System File, AY-220-3, Eclipse Pioneer Division, Bendix Aviation Corporation.

7. Operating Instructions for DuMont Type 185-A Electronic Switch and Square-Wave Generator, Allen B. DuMont Laboratories, Inc., Passaic, N.J.

8. Brush Oscillograph Equipment Operating Information, Section V, Brush Development Co., Cleveland, Ohio.

9. Brush Oscillograph Equipment Operating Information, Section II, Brush Development Co., Cleveland, Ohio.

10. DuMont Instrument and Tube Application Notes, Application Note Number 1, Allen B. DuMont Laboratories, Inc., Passaic, N.J.

11. Reference Data for Radio Engineers, pg. 96, Federal Telephone and Radio Corporation, New York, N.Y., 1949.

12. Dynamic Characteristic Data for the Linear High Speed Torque Motor, Serial Number 15, Curtiss Wright Corporation, Columbus, Ohio.

VITA

Louis Baeriswyl, Jr. was born in Cincinnati, Ohio, July 10, 1925. He attended Withrow High School in Cincinnati and upon graduation in June, 1943, entered the U. S. Naval Reserve and was assigned to the Naval V-12 Unit at Northwestern University, Evanston, Illinois. In February, 1946 he was commissioned a second lieutenant in the U. S. Marine Corps Reserve and awarded the degree of Bachelor of Science in Mechanical Engineering. Following assignments at Parris Island, S.C. and Quantico, Va., and upon completion of the U. S. Marine Corps Basic School, he was commissioned a second lieutenant in the U. S. Marine Corps.

After serving as a tank platoon leader in North China and a reconnaissance platoon leader at Oceanside, California, with the First Marine Division, he was assigned to the U. S. Naval Post Graduate School, Anapolis, Maryland. On completing the two year course under the Ordnance Department, he was awarded the degree of Bachelor of Science in Electrical Engineering.